Instituto Tecnológico y de Estudios Superiores de Monterrey

Campus Monterrey

School of Engineering and Sciences

Controlled drug delivery strategies: Advances on the synthesis and molecular dynamics of dendrimers, and optimization of liposomes preparation by Dual Asymmetric Centrifugation

A dissertation presented by

Diana Sampogna Mireles

Submitted to the
School of Engineering and Sciences
in partial fulfillment of the requirements for the degree of

Doctor

in

Biotechnology

Monterrey Nuevo León, December 1st, 2017

Instituto Tecnológico y de Estudios Superiores de Monterrey

Campus Monterrey

School of Engineering and Sciences

The committee members, hereby, certify that have read the dissertation presented by Diana Sampogna Mireles and that it is fully adequate in scope and quality as a partial requirement for the degree of Doctor in Biotechnology,

Dr. Jesús Ángel Valencia Gallegos
Tecnológico de Monterrey, School of Engineering and Sciences
Principal Advisor

Dr. Janet Alejandra Gutiérrez Uribe
Tecnológico de Monterrey
School of Engineering and Sciences
Committee Member

Dr. José Ascención Hernández Hernández
Tecnológico de Monterrey
School of Medicine
Committee Member

Dr. Oscar Alejandro Aguilar Jiménez
Tecnológico de Monterrey
School of Engineering and Sciences
Committee Member

Dr. Perla Elizondo Martínez
Universidad Autónoma de Nuevo León,
Faculty of Chemical Sciences
Committee Member

Dr. Rubén Morales Menéndez
Dean of Graduate Studies
School of Engineering and Sciences

Tecnológico de Monterrey
01 DIC 2017
Dirección Nacional de Posgrado
Dr. Rubén Morales Menéndez

Monterrey Nuevo León, December 1st, 2017

Declaration of Authorship

I, Diana Sampogna Mireles, declare that this dissertation titled, "Controlled drug delivery strategies: Advances on the synthesis and molecular dynamics of dendrimers, and optimization of liposomes preparation by Dual Asymmetric Centrifugation" and the work presented in it are my own. I confirm that:

- This work was done wholly or mainly while in candidature for a research degree at this University.
- Where any part of this thesis has previously been submitted for a degree or any other qualification at this University or any other institution, this has been clearly stated.
- Where I have consulted the published work of others, this is always clearly attributed.
- Where I have quoted from the work of others, the source is always given. With the exception of such quotations, this thesis is entirely my own work.
- I have acknowledged all main sources of help.
- Where the thesis is based on work done by myself jointly with others, I have made clear exactly what was done by others and what I have contributed myself.

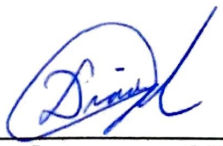

Diana Sampogna Mireles
Monterrey Nuevo León, December 1st, 2017

Dedication

To my dear parents Emma and René:

Thanks for all your unconditional confidence, support, patience, and encouragement.
You were my main motivation for pushing through this work.

Acknowledgements

I would like to express my deepest gratitude to my family and friends, for their unconditional support along this whole journey.

This work was possible thanks to the following collaborations and institutions:

Tecnológico de Monterrey for tuition and funding the project and CONACyT for maintenance support.

To my mentor Dr. Jesús. A. Valencia-Gallegos for his consulting and support.

To Dr. Sergio R. O. Serna-Saldívar and Nutriomics group for their financial support by PBI (Programa de Becarios de Investigación, Tecnológico de Monterrey) program.

For the characterization of dendrons and dendrimers we would like to acknowledge MSc. Elda G. Gómez López from Tecnológico de Monterrey for the acquisition of FT-IR spectra; Dr. Luis E. Elizalde-Herrera from Centro de Investigación en Química Aplicada (CIQA), located in Saltillo (Mexico), for his help running the NMR spectra, MSc. Gloria Macedo-Raygoza and Dr. Miguel J. Beltrán-García from Universidad Autónoma de Guadalajara (Mexico) for their help in the measuring of MALDI-TOF mass spectra.

The molecular dynamics study of structural analysis of binding functionality of folic acid-PEG dendrimers against folate receptor (Chapter 2) was done in the Center for Bioinformatics and Integrative Biology (CBIB), Facultad de Ciencias Biológicas of Universidad Andrés Bello (Santiago, Chile) in collaboration with Dr. Fernando Danilo González Nilo, director of the center. This work was also possible thanks to the support of Ingrid Daniela Araya Durán and Valeria Márquez Miranda.

The DAC optimization for liposomes production was completely supported by the Global Scientific Capabilities Centre of Excellence in Global Drug Development, Novartis Pharma and the Global Health Office in Novartis Institutes for BioMedical Research, Basel, Switzerland. The work was done by the guidance of Dr. Andreas Fisch and Dr. Farshad Ramazani at the department of Technical Research and Development.

Controlled drug delivery strategies: Advances on the synthesis and molecular dynamics of dendrimers, and optimization of liposomes preparation by Dual Asymmetric Centrifugation

by

Diana Sampogna Mireles

Abstract

In early phase of drug development, New Chemical Entities (NCEs) are used as highly active drugs, with limited availability, and high cost. This study presents two alternatives of drug delivery systems, site-specific dendrimers and liposomes, with potential use as carriers of highly active drugs like pristimerin. Advances in the synthesis of site-specific dendrimers with bis-MPA as branching precursor and three key building blocks are reported, including compounds with folic acid (FA) to provide selectivity to folate receptors of cancer cells, pristimerin as cancer drug model, and fluorescein isothiocyanate (FITC) as fluorescent dye for future evaluation as cancer treatment. Five different dendrimer syntheses were reported, differing on their nucleus (bis-MPA or ethylene glycol) and the linker of folic acid (PEG 3350 and triethylene glycol TEG). Different purification techniques, such as normal-phase and reverse-phase column chromatography, size exclusion chromaography, dialysis and ultrafiltration, were probed according to their chemical characteristics and solubility. Characterization was carried out by FT-IR, MALDI-TOF-MS and/or NMR. Theoretical evidence generated in this work supports that FA-PEG750 and FA-PEG3350 dendrimers can be applied to selectively carry drugs and interact with cancer cell receptors (FR-α).

Another drug delivery carrier, and a viable alternative to the use of dendrimers is liposomes. Liposomes are the most mature drug carriers for passive and active targeting commercially available in oncology and other disease treatments. Dual Asymmetric Centrifugation (DAC) is a novel, fast, simple, and reproducible method for liposomal formulation screening, it facilitates liposomes preparation, and favors small diameters (<120 nm) in a small scale, with high drug encapsulation (EE). An optimization of DAC parameters (type and volume of buffer, beads size, centrifugation speed and time) was done to obtain liposomes of 70-80 nm with high encapsulation efficiency (71%). Also, dialysis was the best method for liposomes purification in comparison to Zeba-Spin and Micro-Spin size-exclusion columns, and can be applied to other drug delivery systems, like dendrimers.

Over all, site-specific dendrimers demand a meticulous control on their structure during synthesis. Their preparation is time consuming and analytically complex. Meanwhile, theoretical evidence supports their potential to selectively carry drugs and interact with cancer cell receptors. Meanwhile, liposomes are a faster, easier and versatile alternative as drug delivery carriers of highly toxic drugs.

Keywords: Dendrimers – Drug Delivery Systems – Folic Acid – Pristimerin – Selectivity – Molecular Dynamics – Liposomes – Dual Asymmetric Centrifugation

CONTENTS

List of Figures

CHAPTER 1 – Advances on the synthesis of dendrimers for controlled drug delivery

CHAPTER 2 – Structural analysis of binding functionality of folic acid-PEG dendrimers against folate receptor

CHAPTER 3 - Optimization of Dual Asymmetric Centrifugation for liposomes preparation

List of Tables

CHAPTER 1 – Advances on the synthesis of dendrimers for controlled drug delivery

CHAPTER 3 - Optimization of Dual Asymmetric Centrifugation for liposomes preparation

CHAPTER 1

Advances on the synthesis of dendrimers for controlled drug delivery

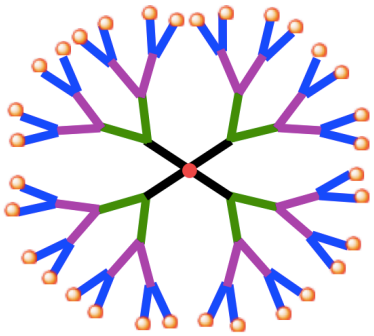

CHAPTER 1. Advances on the synthesis of dendrimers for controlled drug delivery

Abstract

In early phase of drug development, New Chemical Entities (NCEs) are used as highly active drugs, with limited availability, and high cost. This section focus on site-specific dendrimers as an alternative of drug delivery systems, with potential use as carriers of highly active drugs like pristimerin. Advances in the synthesis of site-specific dendrimers with bis-MPA as branching precursor and three key building blocks are reported, including compounds with folic acid (FA) to provide selectivity to folate receptors of cancer cells, pristimerin as cancer drug model, and fluorescein isothiocyanate (FITC) as fluorescent dye for future evaluation as cancer treatment. Five different dendrimer syntheses were reported, differing on their nucleus (bis-MPA or ethylene glycol) and the linker of folic acid (PEG 3350 and triethylene glycol TEG). Different purification techniques, such as normal-phase and reverse-phase column chromatography, size exclusion chromatography, dialysis and ultrafiltration, were probed according to the chemical characteristics and solubility of each compound. Characterization was carried out by FT-IR, MALDI-TOF-MS and/or NMR.

1. Introduction

1.1 Cancer and its treatment

Cancer is the second leading cause of death globally, and was responsible for 8.8 million deaths in 2015 according to WHO (World Health Organization, 2017). Globally, nearly 1 in 6 deaths is due to cancer. Approximately 70% of deaths from cancer occur in low- and middle-income countries. In Mexico (2014), including data of hospitalary morbidity by malign tumors, cancer in hematopoietic organs is the most frequent type of cancer in men (59.2%) and women (61.1%) under 20 years old. In men, the second place corresponds to malignant tumors from the lymphatic system (8.6%), followed by bone and articular cartilage (6.8%). The last one occupies the second place in women (6%), and the third place for women is occupied by lymphatic system and encephalo neoplasia and other parts of the central nervous system (5.9%).[1]

Cancer is a disease caused by mutations in the genes that control cell division, cell death (apoptosis) and cell-cell interactions (like cell adhesion). Tumor cells proliferate rapidly and uncontrollably. This is a problem since its genetic content is damaged. When cell division occurs, they transmit an erroneous genetic message to the other new cells that also become damaged. Normal cells stop dividing when they enter in contact with similar cells (contact inhibition). However, cancer cells lose control over their inhibition capacity and continue dividing uncontrollably, invade local tissues and distribute to other parts of the body (metastasis).

Chemotherapy is a treatment that consists in introducing chemicals through the body to eradicate damaged cells. In the bloodstream, the drug distributes through the organism until it reaches the cancer cells. Then, it surpasses the cell membrane and reaches the nucleus, where the cell stores the genetic information. The ability of chemotherapy to destroy cancer cells depends on its capacity to stop cell division, damaging the RNA or DNA. The faster the cells divide, the greater the probabilities that chemotherapy destroys them and the tumor gets smaller. There are a wide variety of drugs that restrain the development of tumoral cells. A disadvantage of using this kind of treatment is that it does not differentiate between healthy cells and cancer cells. Therefore, they present secondary effects that not only affect the life quality of the patients, but also imply an additional expense for their treatment.[2]

1.2 Drug Delivery Systems

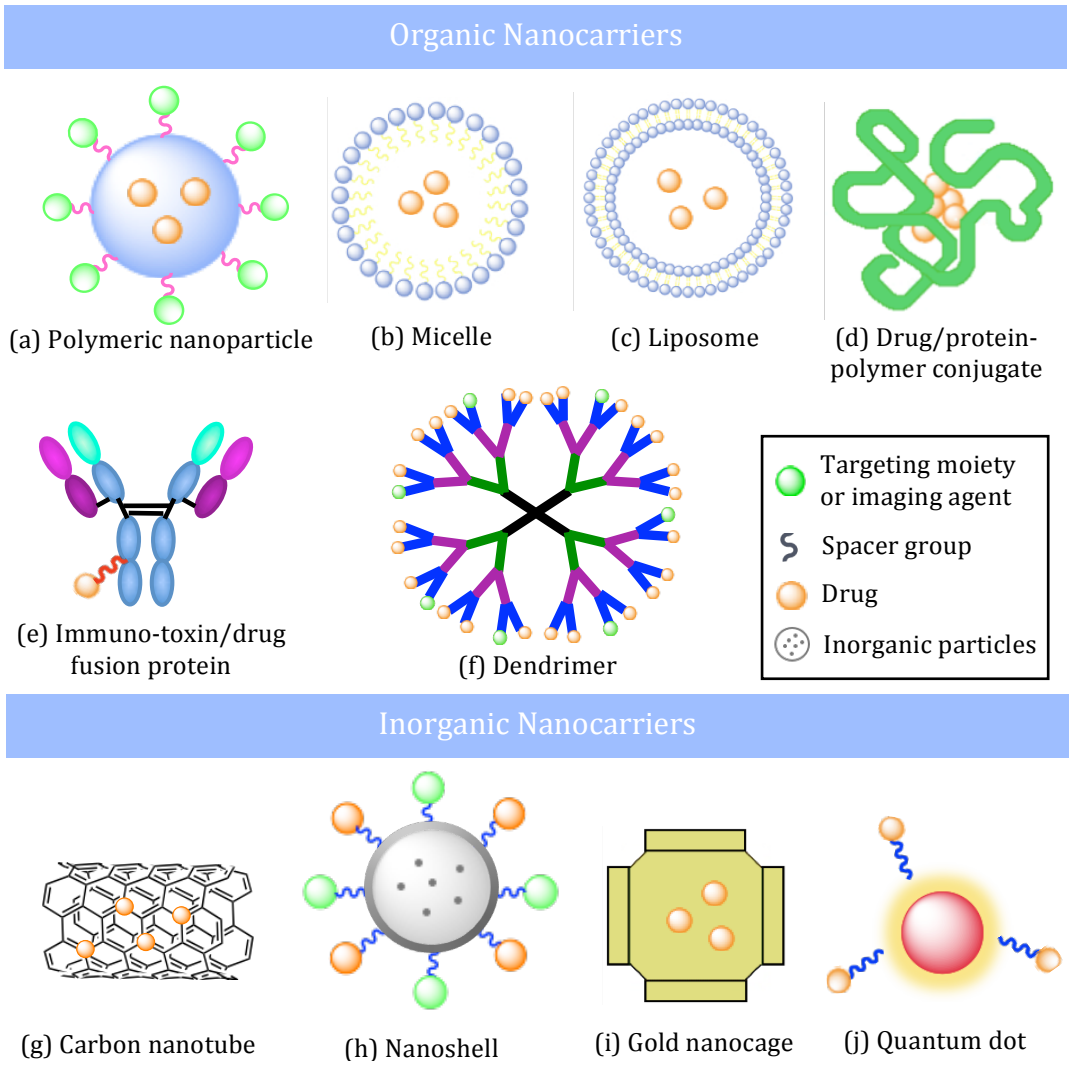

Figure 1. Drug delivery systems classification.

One of the most recent technologies that has been studied in order to avoid secondary effects of cancer therapies are drug delivery systems. They have the potential to improve drug's viability and releasing time, which allows obtain less aggressive therapies than those in the market.

There is a wide classification of drug delivery systems (Figure 1). Nanoparticles used as drug delivery systems have a size of 3-200 nm approximately. These systems can be formed using polymers to obtain polymeric nanoparticles, micelles or dendrimers; lipids can be used to form liposomes; virus to obtain viral nanoparticles and organometallic compounds to form carbon nanotubes.

Polymeric nanocarriers transport the drug that is physically or covalently trapped inside of their matrix. They can also be encapsulated, in the case of polymeric nanoparticles, they can have a nucleus or amphiphilic layers, like in the case of polymeric micelles, or highly ramified molecules, like dendrimers.[3] Abraxane is an example of polymeric nanocarrier, a commercial treatment FDA-approved, used against metastatic breast cancer. Its formulation consists in albumin nanoparticles with paclitaxel (taxol).[4]

Liposomes are self-assembled structures consisting of lipidic bilayers. They have a spherical structure with a hydrophilic center surrounded by a lipidic bilayer. Nowadays, we can find several FDA-approved formulations, like Doxil, Myocet and DaunoXome.[4] Table 1 shows some examples of drug delivery systems that have been used in cancer therapies.[5]

Table 1. Drug delivery systems used in cancer therapies

Drug delivery systems	Formulation	Characteristics
Nanoparticles	Gel nanoparticles modified with PEG, loaded with DNA	Intracellular delivery to tumors and into the nucleus.
	Nanoparticles with dextrane-drug conjugate incorporated in chitosan.	Efficient vehicles for the suppression of tumor volume.
Liposomes	Liposomes modified with FA-PEG-DOPE and DNA	Efficient delivery of endosomal DNA pH-sensitive.
	Folate-conjugated liposomes	Efficient delivery of cytotoxic drug to tumors.

Based on the search for publications in the last 20 years, liposomes conform around 96% of delivery systems used in clinical trials for cancer applications (Figure 2). They became a potential drug delivery system since the 1970s, giving almost five decades of improvement in the pharmacological field due their high versatility of administration and chemical modification.

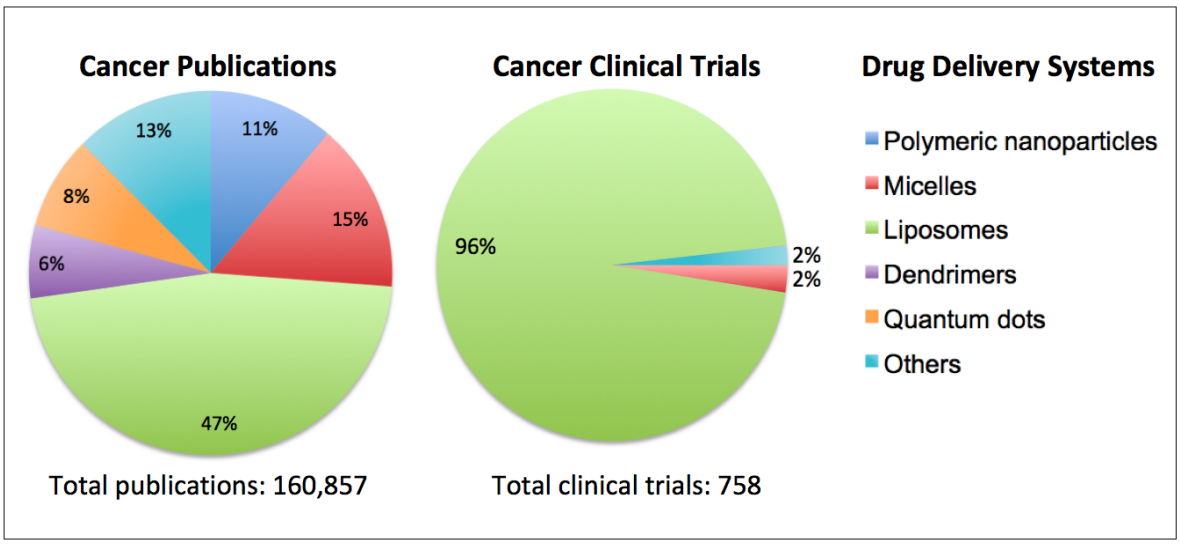

Figure 2. Comparison of publications and clinical trials reported for drug delivery systems with cancer applications.

Search terms – Cancer drug delivery systems: "cancer" and "drug delivery"; polymeric nanoparticles: "cancer" and " polymeric nanoparticles"; micelles: "cancer" and "micelle"; liposomes: "cancer" and "liposome"; carbon nanotubes: "cancer" and "carbon nanotube"; immunotoxin: "cancer" and "immunotoxin"; drug fusion protein: "cancer" and "drug fusion protein"; dendrimers: "cancer" and "dendrimer"; polymer-conjugate drugs: "cancer" and "polymer conjugate drug"; polymer-conjugate protein: "cancer" and "polymer conjugate protein"; nanoshells: "cancer" and "nanoshell"; quantum dots: "cancer" and "quantum dot"; gold nanocages: "cancer" and "gold nanocage". Publications: identified using the above search strings in SciFinder including journal and patents selections activated. Clinical trials: identified using the above search strings and the clinical trial selection activated using SciFinder. The search data was limited between 1996-2016.

1.3 Nanomedicine and formulations against cancer

Ideally, drugs for cancer treatment should first, after administration, be able to reach the desired tumor tissues through the penetration of barriers in the body with minimal loss of their volume or activity in the blood circulation. Second, after reaching the tumor tissue, drugs should have the ability to selectively kill tumor cells without affecting normal cells with a controlled release mechanism of the active form. These two basic strategies are also associated with improvements in patient survival and quality of life by increasing the intracellular concentration of drugs and reducing dose-limiting toxicities simultaneously.[3]

1.3.1 Passive selectivity

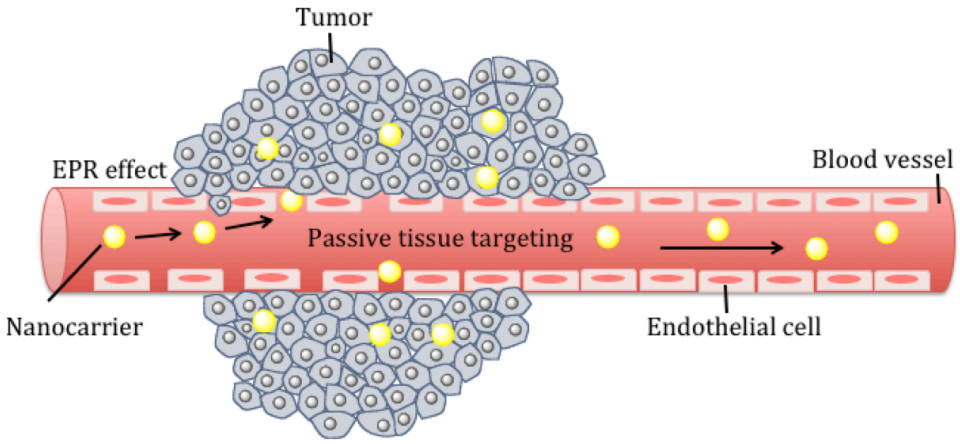

Figure 3. Passive tumoral nanocarriers selectivity by EPR. Long circulation therapeutic nanoparticles accumulate in a passive way on the solid tumor tissue by EPR.[3]

The unique pathophysiologic characteristics of tumor vessels enable macromolecules, including nanoparticles, to selectively accumulate in tumor tissues. Fast-growing cancer cells demand the recruitment of new vessels (neovascularization) or rerouting of existing vessels near the tumor mass to supply them with oxygen and nutrients. The enhanced permeability and retention effect (EPR) constitutes an important mechanism by which macromolecules, including nanoparticles above 50 kDa, can selectively accumulate in the tumor interstitium (Figure 3).[3]

Another contributor to passive targeting is the unique microenvironment surrounding tumor cells, which is different from that of normal cells. Fast-growing cancer cells show a high metabolic rate, and the supply of oxygen and nutrients is usually not sufficient for them to maintain this. Therefore, tumor cells use glycolysis to obtain extra energy, resulting in an acidic environment. Additionally, cancer cells express and release unique enzymes such as matrix metalloproteinases, which are implicated in their movement and survival mechanisms.[3]

1.3.2 Active selectivity

A drug delivery system comprising a binary conjugate (polymer-drug conjugate) that depends only on passive targeting mechanisms inevitably faces intrinsic limitations to its specificity. One approach suggested to overcome these limitations is the inclusion of a targeting ligand or antibody in polymer-drug conjugates.[3]

Internalization usually occurs via receptor-mediated endocytosis. Tumor-specific ligands on the nanoparticles bind to cell-surface receptors, which trigger internalization of the nanoparticles into the cell through endosome. As a pH value in the interior of the endosome becomes acidic, the drug is released from the nanoparticles and enters to the cytoplasm. The drug-loaded nanoparticles bypass the

P-glycoprotein efflux pump not being recognized when the drug enters cells, leading to high intracellular concentration.[3]

1.3.3 Antigen or receptor expression

In order that antigens or receptors function as tumor targets, they should be expressed exclusively on tumor cells, they must be expressed homogeneously on all target tumor cells, and cell-surface antigens and receptors should not be shed into bloodstream.[3]

1.3.4 Folate receptors

Folate receptors (FRα, FRβ y FRγ) are cysteine-rich cell-surface glycoproteins that bind folate with great affinity to mediate cellular uptake of folate. Although expressed at very low levels in most tissues, FR-α receptors are expressed at high levels in numerous cancers to meet the folate demand of rapidly dividing cells under low folate conditions. The folate dependency of many tumors has been therapeutically and diagnostically exploited by administration of anti-FRα antibodies, high affinity antifolates, folate based imaging agents and folate conjugated drugs and toxins. Chen et al. (2013) determined the crystal structure of human FR-α in complex with folic acid at a 2.8 Å resolution in order to understand how folate binds its receptors.[6] FR-α receptor has a globular structure stabilized by eight disulphide bonds and contains a deep open folate-binding pocket comprised of residues that are conserved in all receptor subtypes.[6] The folate pteroate moiety is buried inside the receptor, whereas its glutamate moiety is solvent-exposed and sticks out of the pocket entrance, allowing it to be conjugated to drugs without adversely affecting FR-α binding. The extensive interactions between the receptor and ligand readily explain the high folate-binding affinity of folate receptors and provide a template for designing more specific drugs targeting the folate receptor system.

Folate (vitamin B_9) is an important one-carbon donor for the synthesis of purines and thymidine -essential component of nucleic acids- and indirectly, via S-adenosyl methionine, for methylation of DNA, proteins and lipids. Folate deficiency is therefore associated with many diseases, including fetal neural tube defects, cardiovascular disease and cancers. In adult tissues, folate is mainly taken up by reduced folate carrier, an ubiquitously expressed anion channel that has relatively low folate binding affinity. In contrast, high affinity uptake of the food supplement folic acid and the physiologically prevalent folate N^5-methyltetrahydrofolate (5-mTHF) requires the function of three subtypes of folate receptor (FRα, FRβ y FRγ), which are cysteine-rich glycoproteins that mediate folate uptake through endocytosis. Inside of the cell, the acidic environment of the endosome promotes the release of folate from receptors, which is then transported into the cytoplasm by proton-coupled folate transporter. The expression of folate receptors is largely restricted to cells important for embryonic development (for example, placenta and neural tubes) and folate resorption (kidney). Among the three FR isoforms, FR-α is the most widely expressed, with very low levels in normal tissues, but high expression levels in many tumors. Despite intense research on the folate structure-activity relationship, the molecular

basis for the high-affinity recognition of folates by FR-α remains elusive owing to the technical difficulties in expression, purification and crystallization of FR-α for structural studies.

Folate and folate-conjugated drugs binding to FR remains unknown. The FRα-folic acid complex structure illustrates how the receptor assumes a deep folate-binding pocket that is formed by conserved residues across all receptor subtypes and provides detailed insights into how folic acid interacts with its receptors.

1.3.5 Internalization of selective conjugates

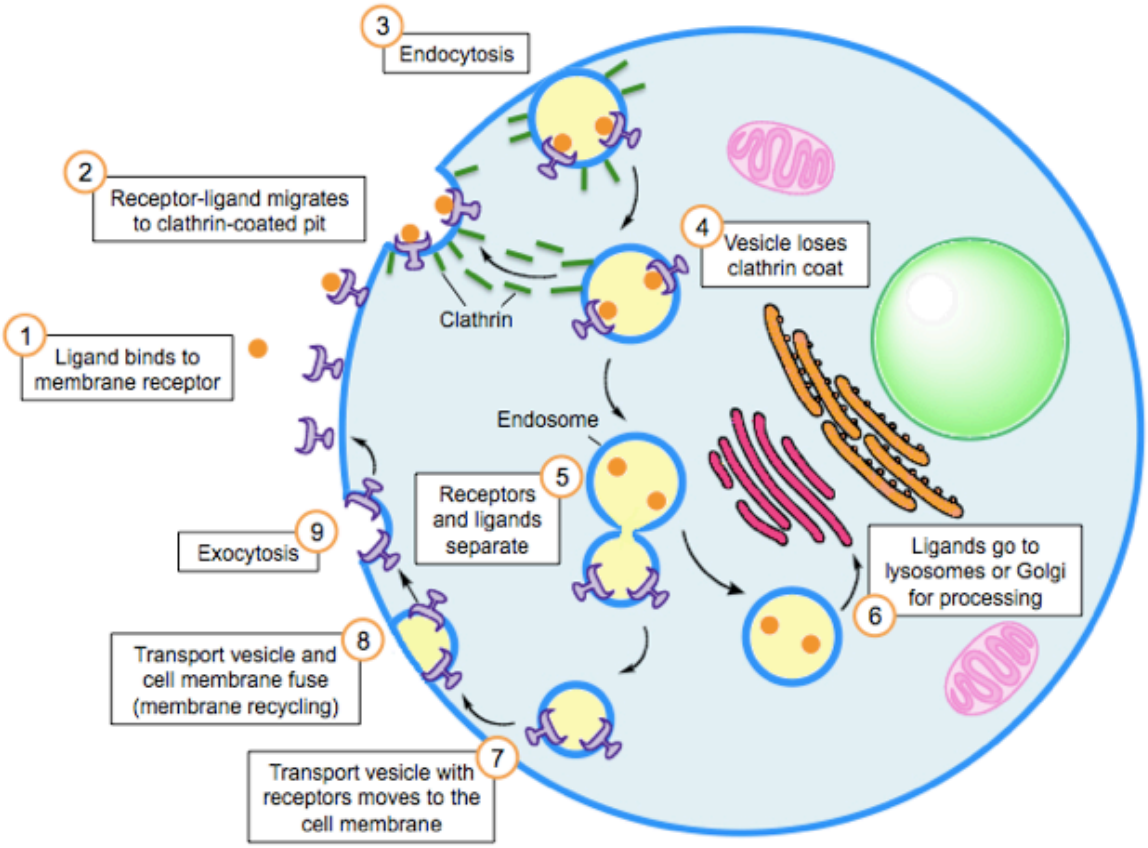

Figure 4. Nanoparticles internalization by receptor-mediated endocytosis

Once folate conjugates are bound to a FR cell surface, they are transported into the cell through a process called receptor-mediated endocytosis (Figure 4). After binding, the cell membrane invaginates the ligand-receptor complex and pinches off to form an endosome that is transferred to the target organelle. As the endosomal compartment acidifies to pH~5, the folate conjugate and its drug may be released from the receptor into the cytosol. Trafficking of the acidic endosome to a recycling center then allows separation of membrane-bound FR from released conjugates/free drug. Released folate conjugates are seen to escape the endosome through an unknown mechanism, resulting in drug deposition in the cytoplasm, providing the drug the appropriate physicochemical properties to cross the endosomal membrane. Once they are released, they can be directed to the target organelle depending of the drug.

Meanwhile, membrane bound FR largely recycles back to the cell surface, allowing for delivery of additional folate-linked drugs into the cell and repeating the process.[3,7,8]

In cancer cells, the recycling rate *in vivo* varies from one cycle every four hours to one cycle every twelve hours. Also, it has been observed relatively few folate conjugates destroyed inside lysosomes, allowing as a result the delivery of hydrolytically sensitive materials, such as genes and ribozymes, towards cells.

On the other hand, folate receptors exhibit limited expression in healthy cells, but frequently are present in a great variety of cancer cells. For example, they are overexpressed in ovary epithelial cancer, mammary glands, colon, lung, prostate, nose, throat, brain, etc. Also, a strong correlation has been found between folate receptors expression and the grade and histological stage of the tumor. Cancers on highly not-differentiated metastasis considerably express more folate receptors than their low degree located counterparts. They are also overexpressed in activated macrophages. Since, macrophages cause or perpetuate a wide variety of inflammatory and autoimmune diseases, their elimination or selective suppression with drugs directed to folate receptors may improve or stop the progression of those diseases without damaging normal tissues.[8] Folate receptors on normal cells are largely inaccessible to folate conjugates in the blood, and consequently, toxicity to healthy tissues that express folate receptors has not been observed.

Other features that render folic acid an attractive ligand for use in drug targeting include its low molecular weight (MW 441), water solubility, stability to diverse solvents, pH, and heat, facile conjugation chemistry, lack of immunogenicity, and high affinity for its receptor. The small size of the folate ligand also allows for good tissue penetration and rapid clearance from receptor negative tissues.[8]

1.4 Dendrimers

1.4.1 Generalities

Dendrimers are polymeric synthetic macromolecules with repeated ramifications that grow from a nucleus to form a tree-like structure. They also have functional groups on their periphery that can be manipulated according to the desired applications (Figure 5).

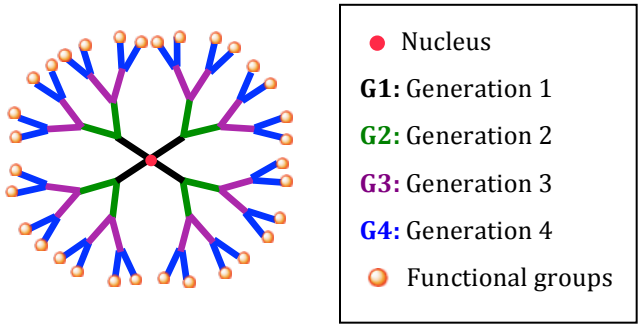

Figure 5. Dendrimer structure.

Dendrimers can be synthesized by divergent and convergent methods, or a combination of both for asymmetrical dendrimers. Divergent method consists in the synthesis of a dendrimer whose ramifications (generations) grow from the nucleus to the periphery. In the other hand, convergent method consists in the construction of dendrons from the periphery to end with the union of the focal point or nucleus. This last method present less risk of defects in the final structure. It is worthy to specify that there can be a synergy between both methods as synthesis strategies. The number of repetitions or ramifications corresponds to the number of generations that each dendrimer possess.[9,10]

The advantage of dendrimers is that they can be synthesized and designed for specific applications. They are physiologically ideal drug delivery systems due to their feasible topology, functionality and dimensions; and also, their size is very close to various important biological polymers and assemblies such as DNA and proteins. Many of their properties include: nanoscale sizes that have similar dimensions to important bio-building blocks, such as DNA and proteins. Numbers of terminal surface groups suitable for bioconjugation of drugs, signaling groups, targeting moieties or biocompatibility groups. Surfaces may be designed with functional groups to augment or resist trans-cellular, epithelial or vascular permeability. An interior void space may be used to encapsulate small molecule drugs, metals, or imaging moieties. Encapsulating in that void space reduces the drug toxicity and facilitates controlled release. Surface groups that can be modified to optimize biodistribution; receptor mediated targeting, therapy dosage or controlled release of drug from the interior space. They also have the ability to arrange excretion mode from body, as a function of nanoscale diameter.[11]

There are diverse publications about the use of dendrimers of different compounds against diverse cancer cell lines which even if it has been proven that they reduce toxicity, they continue to have secondary effects.[12] Some of these dendrimers include polyamidoamine (PAMAM) conjugated with cisplatin;[13] 2,2-bis (hydroxymethyl) propanoic acid (bis-MPA) as doxorubicin (DOX) carrier vehicle, and PEGylated dendrimers. Functional dendrimers[14] have also been studied for imaging, directionality and target cells selectivity studies,[15] and also for chemotherapeutic purposes.

Nowadays, there are multiple advances in drug delivery systems, including polymeric microcapsules and microarrangements spheres, liposomes, polymeric conjugates and nanoparticles approved by the FDA or that are currently in pre-clinic or clinic stage for cancer treatments (Table 2).[16,17] The success of these strategies for cancer therapies is strongly related with the development of delivery systems capable of improving therapeutic index of biologically active molecules.[18]

Table 2. Drug delivery systems and their clinical stage of development for cancer therapies.

Drug	Commercial name	Drug delivery system	Cancer applications	Clinical stage
Cis-platin	SPI-077	Liposomes	Solid tumors	Phase II
Cytarabine daunorubicin	CPX-351	Liposomes	Acute myeloid leukemia	Phase II
Irinotecan HCl:floxuridine	CPX-1	Liposomes	Colorectal	Phase II
CPT-11	MM-398	Liposomes	Gastric and pancreas Colon	Phase II, Phase I
ErbB2/ErbB3-targeted doxorubicin	MM-302	Liposomes	Breast	Phase I
Transferrin-targeted oxaliplatin	MBP-435	Liposomes	Gastric	Phase II
Transferrin-targeted oxaliplatin	MBP-426	Liposome with human transferrin protein targeting agent	Solid tumors, pancreas	Phase I
Topotecan	Brakiva	Liposomes	Relapsed solid tumors	Phase I
Vinorelbine	Alocrest	Liposomes	Solid tumors	Phase I
Cisplatin	Lipoplatin	Liposomes	Lung	Phase III
Annamycin	L-annamycin	Liposomes	Acute lymphoblastic leukemia (ALL) and acute myelogenous leukemia, doxorubicin-resistant breast cancer	Phase I, Phase II
Thermosensitive-doxorubicin	ThermoDox	Liposomes	Hepatocellular; Breast, colorectal, pancreas	Phase III; Phase II
Cationic liposomal paclitaxel	Endo-Tag-1	Liposomes	Pancreas and breast	Phase II
siRNA targeting PCSK9 RNAi targeting liver cancer	ALN-VSP	Liposomes	Liver	Phase I
RNAi targeting polo-like kinase 1 (POLO)	TKM-PLK1 TKM-ApoB	Liposomes	Liver	Phase I
Anti-MUCI cancer vaccine	Stimwax	Liposomes	Lung	Phase III
$F(ab')_2$ fragment of human antibody GAH conjugated with doxorubicin	MCC-465	Liposome with antibody	Stomach	Phase I
Antibody fragment to transferrin receptor conjugated to plasmid DNA with p53 gene	SGT-53	Liposome with antibody fragment targeting agent	Solid tumors	Phase I
Transferrin conjugated to small interfering RNA	CALAA-01	Polymeric nanoparticle	Solid tumors	Phase I

1.4.2 Site-specific dendrimers

A few years ago, it began to grow interest the use of dendrimers as specific site controlled delivery systems in order to increase their selectivity, especially in cancer therapies. Their multifunctional conformation makes them ideal models for the incorporation of drug and a molecule capable of providing selectivity and as a result it can be used as an active controlled delivery system.

Diverse cancer cells have an overexpression of folate receptors on their surface. Folate modified dendrimers, covalently bound with a molecule with anticancer properties, specifically kill cells with those receptors overexpression once they make the intracellular drug delivery by receptor mediated endocytosis.

There are several publications related with the use of folates conjugated to dendrimers to increase their selectivity in cancer therapies. Some of their applications consist in the improvement of synthesis methods[19–22] to increase dendrimers selectivity and as a tool in imaging for tumor identification and diagnosis.[23,24]

Dendrimer molecules with several generations of amine have been used as small organic molecule carriers, chemotherapeutic agents, small ligands or compounds selective to cells, like folic acid. The presence of folic acid on dendrimer surface allows the complex with the chemopreventive agent to bind to folate receptors overexpressed in certain tumor cells. Adding a chemotherapeutic agent to the folate conjugated dendrimer, allows selectivity and direction to cancer cells.[25]

Quintana et al. synthesized a 5 generations PAMAM dendrimer with an ethylenediamine nucleus, covalently bound to folic acid, fluorescein and methotrexate. The study showed a considerable decrease of cytotoxicity in comparison with free methotrexate. In some cases, glycidol was used to block some amino groups and form hydrophilic hydroxylated regions on dendrimer surface to promote its water solubility.[26] Majoros et al., then probed the same kind of dendrimer, but instead of using methotrexate as chemotherapeutic agent they used paclitaxel (taxol), which is a natural compound, in contrast to synthetic methotrexate.[27]

Hong et al. investigated the binding affinity of those dendrimer-folate derivates with respect to folate binding protein (FBP), which is typically overexpressed in cancer cells. They measured the binding constants of a series of dendrimeric folate conjugates with different levels of folate modification (dendrimers with 2 to 14 folates). The results indicated that the combination of multiple folates in only one dendrimer increased the FBP protein binding up to 5 magnitude orders.[28]

Kukowska-Latallo applied that discovery in controlled drug delivery using a PAMAM dendrimer of 5 nm of diameter as a carrier. Acetylated dendrimers were conjugated with folic acid and methotrexate and fluorescein. The conjugates were injected to immunodeficient mice with human KB (epithelial human cancer) tumors that overexpress folic acid receptor. Folate conjugated nanoparticles were concentrated in the tumor and liver tissue for more than 4 days after their administration, in contrast to non folate polymers. Folate polymer tumor tissue localization could be attenuated

by a previous free folic acid injection *in vivo*. Confocal microscopy confirmed the conjugates internalization with the anticancer active in tumoral cells. Using a controlled delivery system with methotrexate increased antitumoral activity and significantly decreased its toxicity, obtaining therapeutic responses impossible to be obtained using free drug.[29] Other advantages of using drug-conjugated dendrimers in comparison with free drug are: the increment in plasma half life, decrease of drug resistance, and its controlled release.

1.4.3 PEGylated dendrimers

PEGylated dendrimers are a class of nanocarriers capable of doing an effective delivery of a high drug load to attack cancer relatively in an inoffensive way. These dendrimers not only drastically increment drug load and solubility, but also dendrimer residues without drug can be easily eliminated, controlled release, their half life time is short, etc. They also improve their kinetic stability making them useful for delivery, carrying and extended delivery of bioactive species. PEGylation also can improve directionality to active sites with immunogenicity, antigenicity, and reduced toxicity, because it protects the dendrimers against destructive mechanisms in the body.[15] It has been found that using PEG in nanoparticles improves absorption in BT20 cells, while it reduces its absorption by macrophage cells. Also, it has been probed that surfaces covered with PEG prevent plasma proteins absorption incrementing, as a result, the time in blood circulation of the particles, allowing them to reach target tissues.[30]

Also, dendrimeric conjugates have been designed using borum neutron capture therapy (BNCT) for cancer treatment. Shukla et al. used a G-3 PAMAM dendrimer modified with folate and polyedric decaborate clusters with an average of 1 to 1.5 PEG_{2000} units in order to make a therapeutic conjugate. The folate component was not conjugated with surface amines, but in the extreme of an additional unit of amino-PEG_{800}. The use of PEG groups facilitated the increment in half life in *in vivo* studies and prevented the complex immediate absorption in the liver.[31]

1.5 Pristimerin

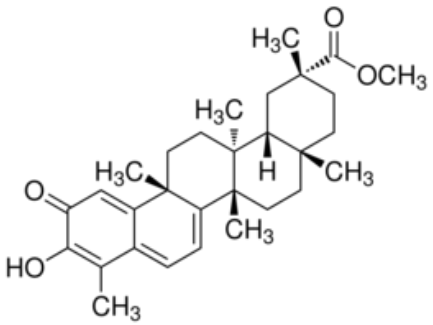

Figure 6. Pristimerin molecular structure

Natural compounds have become more important in anticancer drug development since they are more tolerable in human body. Celastraceae family has been studied for

these purposes.[32] *Mortonia greggii* Gray is a specie that lives under certain conditions of constant stress and, as a result, stores cytotoxical compounds, such as pristimerin (Figure 6). Pristimerin is a natural triterpenoid quinone methide, the methyl ester of celastrol, with chromophore properties. It is of great interest due to its antimicrobial and anti-inflammatory properties, as well as antitumoral effects in diverse cancer cell lines.[33] The orange pristimerin crystals are mainly stored on the cell wall of the plants radicular system, in the root cortex or periderm; but it can also be found (in a significantly less proportion) in the aerial system, especially leaves.[34,35] The main reason why the plant stores pristimerin is due to its cytotoxic properties and defense mechanisms typical of triterpenoids. *Mortonia greggii* synthesizes pristimerin since it is a plant that is usually under high stress levels, typical of phase II enzymes and other compounds with cytotoxic properties. In addition, it is also favored by the frequent climatic and environmental changes, typical from its habitat, in this case located in the north of Mexico and Texas.[7,36] The plant also synthesizes pristimerin to defend against stress agents and for cells survivance.[37] Human breast cancer cells MDA-MB-231 treated with pristimerin, have shown a fast apoptosis induction and therefore, can be evaluated as a chemopreventive agent against breast cancer.[38–40]

The cytotoxic activity of pristimerin has been widely studied.[39–47] It induces apoptotic cell death in some cancer cell lines including breast cancer, lung[39], prostate[40] and acute myeloid leukemia.[48] Also, it has shown a synergic activity with taxol (anticancer drug) to induce death in cervical cancer cells[44] and inhibits growth of chronic myeloid leukemia cells resistant to imatinib (anticancer drug).[45] Pristimerin has shown several mechanisms of cell death induction: proteosome inhibition,[40] suppression of activity of nuclear factor NF -Kβ, cyclin D1 expression[49] and caspases activation.[39,40]

Several studies have reported that pristimerin has a promising clinical potential as a therapeutic agent against cancer.[34,45–47] However, its use as free drug would lead to multiple secondary effects since it does not distinguish between cancer and non-cancerous cells. Lu et al. reported cytotoxicity of the molecule against healthy bone marrow cells[45] and proposed to use protective bone marrow agents to help decrease the secondary effects or structural modification of pristimerin. Lopez-Barrios reported that pristimerin is not a chemopreventive agent due its high cytotoxicity.[50] In this work, chemical modifications of pristimerin were also analyzed, finding a reduction of cytotoxicity by the interference of reactivity of the methylene-quinonic group.

In 2011, Gomes et al. reported IC_{50} values of several natural products, including pristimerin and the positive control paclitaxel (taxol), probed in breast (LM3) and lung cancer (LP07) cell lines.[18] The results demonstrated a significant difference between pristimerin (IC_{50} 5 μM in both LP07 and LM3) and paclitaxel (IC_{50} 74 μM in LP07 and 191 μM in LM3). Therefore, a dosage of pristimerin 15 times lower than paclitaxel can kill 50% of LM3 cells, and a dosage 38 times lower than paclitaxel for LP07 cells. As a result, pristimerin presents great potential for anticancer therapies development. However, it is necessary to develop strategies to reduce secondary effects and provide direction and selectivity to cancer cells.

1.6 Imagenology applied to dendrimers with folate

The use of dyes as fluorescent labels has been considered as a simple and useful tool for the identification of drugs or polymers due to the high sensibility, proper of fluorescent pigments. There are multiple publications in the medical field where drugs and proteins are labeled with dyes to facilitate screening and diagnosis.[51]

Fluorescein isothiocyanate (FITC) is one of the fluorescent dyes more frequently used (Figure 7), which has a wide range of applications in biochemistry. For example, it is used for peptides and protein labeling[52] and in drug screening by fluorescence microscopy studies,[53] flow cytometry[54] and immunofluorescence essays.[55]

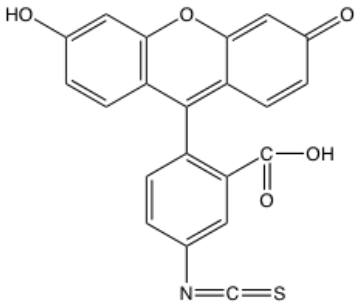

Figure 7. Molecular structure of FITC

1.6.1 Cell culture and treatment

It is important to start *in vitro* tests with cells that overexpress folate receptors. Human epidermoid carcinoma (KB) cells overexpress folate receptors, especially when they grow in a medium with low levels of folic acid.

1.6.2 Cytotoxicity essay

MTT essay is used to quantify cell viability by the enzymatic conversion of MTT to formazan by the active mitochondrion of living cells.

1.6.3 Fluorescence microscopy

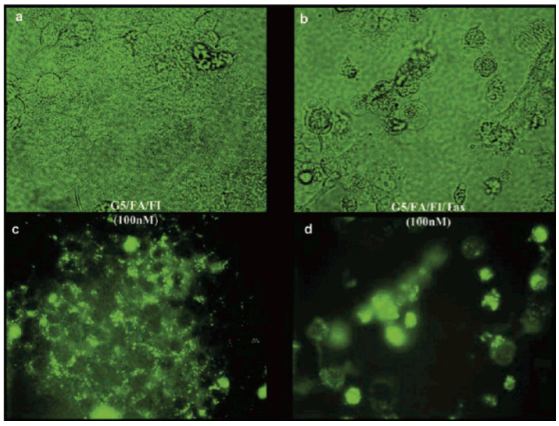

Figure 8. Fluorescence microscopy of KB (FR+) cells with folate receptor overexpression, treated with either 100 nM G5-Ac^3-FITC-FA (a and c) or 100 nM G5-Ac^3-FITC-FA-OH-Taxol (b and d). Panels a and b show the visible light image of panels c and d, respectively. The cells treated with the drug-free G5-Ac^3-FITC-FA bind to the KB cells but are nontoxic (panel c). The cells treated with the drug containing G5-Ac^3-FITC-FA-OH-Taxol bind to the KB cells and kill them (panel d).[27]

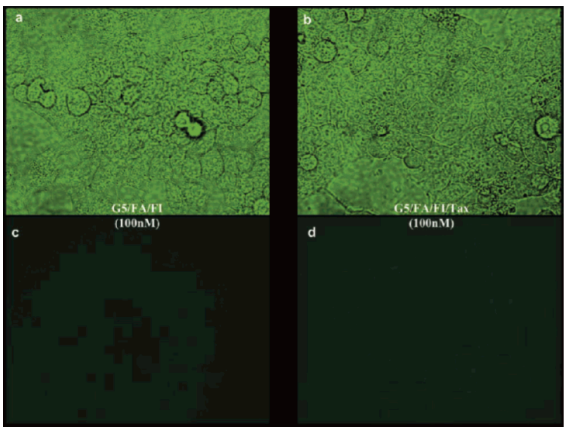

Figure 9. Fluorescence microscopy of KB (FR-) cells without folate receptors overexpression, treated with either 100 nM G5-Ac^3-FITC-FA (a and c) or 100 nM G5-Ac^3-FITC-FA-OH-Taxol (b and d). Panels a and b show the visible light image, while panels c and d show the fluorescent image. Panels a and c show the same view, as do panels b and d. Neither the G5-Ac^3-FITC-FA nor G5-Ac^3-FITC-FAOH-Taxol binds to the KB cells or shows any toxic effects.[27]

1.6.4 Flow cytometry

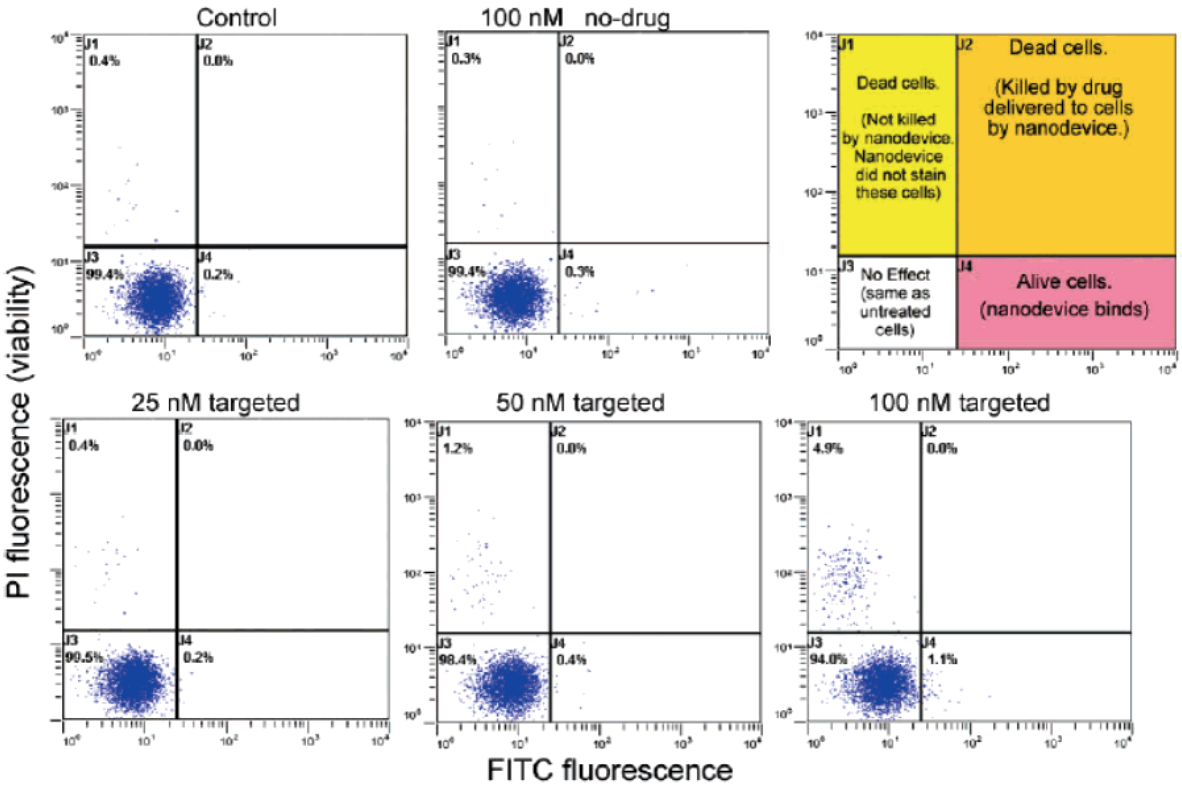

Figure 10. Flow cytometry of KB cells without folate receptors overexpression (negative folic acid receptor) analyzed after flow cytometry treatment. Non-significant cytotoxicity was observed. Before de analysis by flow cytometry, the cells were tinted with propidium iodide to identify dead or dying cells.[27]

Flow cytometry is a technique that simultaneously measures and analyzes multiple physical characteristics of singular particles, like cells, while they flow through a beam of light. The properties that can be measured include relative particle size, granularity or intern complexity and fluorescence intensity. Those characteristics are determined using an optic-electronic system that registers the way in which the cell disperses the light from the incident laser and emits fluorescence.[56]

Flow cytometry is also a very useful tool to visually probe the cytotoxicity of dendrimers. The cells are incubated with a dye, such as propidium iodide (1.25 μg/mL) or FITC for 5 minutes at room temperature, in order to estimate cell death. Dead cells are not able to exclude the propidium iodide dye, therefore, the dye binds to nucleic acids of the cell causing a red fluorescence in cells. Meanwhile, living cells exclude the propidium iodide and remain without fluorescence. After the incubation with propidium iodide, the data analysis by flow cytometry can be done.[27]

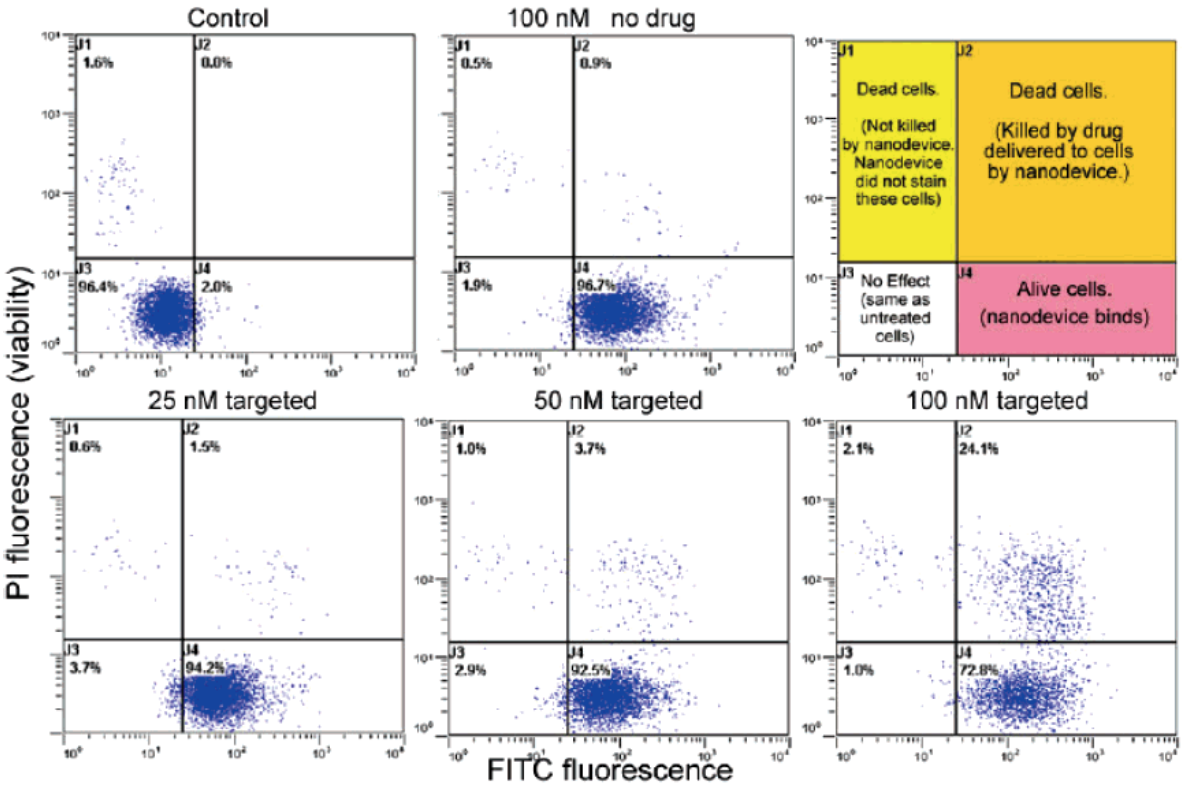

Figure 11. Flow cytometry of KB cells with folate receptors overexpression, analyzed after flow cytometry treatment. Non-significant cytotoxicity was observed. More than 24% of the cells died due to treatment with 100 nM of the targeting G5-Ac3-FITC-FA-OH-Taxol dendrimer conjugate. Before flow cytometry analysis, cells were stained with propidium iodide to identify dead or dying cells.[27]

Majoros et al. (2006) reported some interesting results of a multifunctional dendrimer in contact to cancer cells without and with folate receptors overexpression (Figure 10 and Figure 11 respectively).

2. Objectives

2.1 General objective

To perform the synthesis of building blocks for site-specific dendrimers, including folic acid (FA) to provide selectivity to folate receptors of cancer cells, pristimerin as

cancer drug model, and fluorescein isothiocyanate (FITC) as fluorescent dye, using bis-MPA as branching precursor.

2.2 Specific objectives

- To perform the synthesis of dendrons and compounds that can be used as building blocks in multiple syntheses of dendrimers, and their characterization by FT-IR, MALDI-TOF-MS or NMR.
- To compare the synthesis and purification of compounds with triethylene glycol (TEG) and polyethylene glycol (PEG 3350) as linkers of folic acid.
- To evaluate different methods for dendrons purification, such as column chromatography with silica gel of normal and reverse phase (C18), Sephadex for size exclusion chromatography, dialysis, and ultrafiltration.

3. Materials and Methodology

3.1 Materials

3.1.1. Synthesis of dendrons and dendrimers

All of the material and reagents were purchased from Sigma-Aldrich (St. Louis, MO) with the following exceptions. 2,2,5-trimethyl-1,3-dioxane-5-carboxylic acid (**BMPAP**) and 1,4-Dimethylpyridinium *p*-toluenesulfonate (**DPTS**) were synthesized by the method described by Valencia, 2010.[41] The reactions were followed by thin layer chromatography (TLC) of normal phase, by TLC silica gel 60 F_{254} (20 x 20 cm) sheets and for reverse phase using TLC Silica gel 60 RP-18 $F_{254}S$ (20 x 20cm), both from Merck (Darmstadt, Germany). The detection of TLC spots was accomplished either by UV at 254 and 365 nm, vapors of iodine crystals, or bromocresol green indicator to verify the presence of carboxylic acid. A hydrogenator, Parr (Moline, IL), was used for the hydrogenation of compounds. A rotavapor Hei-Vap value HB/G3, Heidolph (Schwabach, Germany) was used to remove the solvents.

3.1.2. Purification

Different purification systems were probed according to the compounds properties, such as their solubility, molecular weight and polarity. Column chromatography was manually prepared either with silica gel of normal phase mesh 200-425, Sigma-Aldrich (St. Louis, MO) or by reverse phase C18. Flash chromatography Rf 200 Teledyne was used for a fast purification using RediSep Gold Teledyne Isco columns, normal and reverse phase (C18). Size exclusion chromatography (SEC) with Sephadex G-15 (<1.5 kDa) or Sephadex G-50 (1.5-30 kDa), Sigma-Aldrich (St. Louis, MO), manually packed column. Different dialysis systems were tested including PlusONE Mini Dialysis Kit (GE Healthcare), 1 kDa, 2 mL and Thermo Scientific Slide-A-Lyzer G2 Dialysis cassettes 7 kDa, 3 mL. A Sartoflow Slice 200 Benchtop with membranes of 5 kDa was used for ultrafiltration.

3.1.3. Characterization

The analysis and characterization of dendrons and dendrimers was performed with the following techniques and instruments. Infrared spectroscopy (FT-IR): spectrometer FT-IR (ATR) Spectrum 400, Perkin Elmer (Waltham, MA).
Proton and Carbon-13 Nuclear Magnetic Resonance Spectroscopy (^{1}H NMR and ^{13}C NMR): For quick and simple characterization, a Mercury 60 (60 MHz), Varian (Palo Alto, CA) instrument, located at Tecnológico de Monterrey, (Monterrey, Mexico) was used. The characterization of every compound was done with a NMR spectrometer Bruker Avance III, 600 MHz, located in Centro de Química Pura y Aplicada, CIQA (Saltillo, Coahuila). Tetramethylsilane (TMS) was used as reference and the samples were prepared with deuterated chloroform ($CDCl_3$), deuterated dimethylformamide (DMF-*d7*) for samples with FITC and/or folic acid, all of them acquired by Sigma-Aldrich. Prediction spectra were calculated with ChemDraw Ultra 12.0 Suite, Perkin Elmer software.
MALDI-TOF-MS Spectrometry: The characterization of high molecular weight polymers and dendrimers was done by mass analysis using an Autoflex II MALDI-TOF mass spectrometer (Bruker Daltonics, Bremen, Germany). The measurements were performed in linear positive mode, using a nitrogen laser (337 μm) at 50 Hz frequency. The acceleration voltage was 19.50 kV, with delay time acquisition. The analytical samples were obtained by the dried-droplet method. Briefly, 1 μL of an analyte solution in methanol (1 mg/mL) was loaded on the MALDI plate (MTP 384 target plate polished steel BC) and allowed to dry at 23°C. Each sample was covered with 2 mL of matrix (α-Cyano-4-hydroxycinnamic acid) solution (10 mg/mL, 50% acetonitrile, water 47.5% and 2.5% trifluoroacetic acid) and allowed to dry at 23°C before the plate was inserted into the vacuum chamber of the MALDI instrument. Data analysis was carried in FlexAnalysis 3.0 software (Bruker Daltonics).

3.2 Methodology

Most of the syntheses and purification methods found in this work have been completely developed according to structural chemistry principles applied for each compound, and in some cases synthesis or purification methods were adapted from published material. The main components of the synthesis of dendrimers (for this work) were folic acid (FA) to provide selectivity of the carrier to folate receptor (FR-α) overexpressed in cancer cells (e.g. KB), pristimerin as a cancer drug model, and FITC as fluorescent dye for future *in vitro* and *in vivo* tests.

PEG3350 was chosen as a linker of folic acid, mainly to enhance solubility of the dendrimers, which otherwise would be affected due the limited and varied solubility characteristic of the main components FA, FITC and pristimerin.

In addition, triethylene glycol (TEG) was also used as linker of folic acid as an alternative of PEG3350 to reduce molecular weight of dendrons and dendrimers and facilitate their characterization.

The dendrimer structure was based on polyester using bis-MPA (BMPA) as a precursor for the synthesis of branching molecules, like EB and EB-AS, which function as the "arms" or linkers of FA and pristimerin, and forming their corresponding dendrons of folic acid and of pristimerin, respectively.

Thereby, five different dendrimer syntheses are reported in this work, as alternatives for site-specific dendrimers. The difference between them relies mainly in the dendrimer nucleus and linker of folic acid:

- First, a bifunctional dendrimer with a nucleus of BMPA, and PEG3350 as linker of FA (Figure 12A).
- Second, a trifunctional dendrimer, with the same structure as the first one except for the addition of FITC with an hexamethylene diamine (HMDA) linker, for a future evaluation in cells (KB) and *in vivo* tests (Figure 12B).
- Third, a bifunctional dendrimer with folic acid and pristimerin, like the one from Figure 12A, with a nucleus modification, using ethylene glycol instead of BMPA. The use of ethylene glycol could be preferable, since BMPA in combination with the branching molecules with carboxylic groups (EB-AS), form an anhydride that can potentially be unstable. Meanwhile, BMPA was still used as a precursor for branching purpose, and PEG3350 remained as a linker for folic acid (Figure 13). This dendrimer was also applied in a molecular dynamics study, about the binding functionality of FA-PEG, by comparing the use of two different PEG's (PEG750 and PEG3350) and evaluating their effect over FA linker. This theoretical evidence is explained in detail in Chapter 2.
- Fourth, the synthesis of a trifunctional dendrimer was adapted according to the one with ethylene glycol nucleus and PEG3350 linker (Figure 13), adding FITC to the structure (Figure 14).
- Fifth, a trifunctional dendrimer with TEG, instead of PEG3350, as a low-molecular weight linker of folic acid, pristimerin succinate, and FITC with HMDA linker, parting from BMPA nucleus (Figure 15).

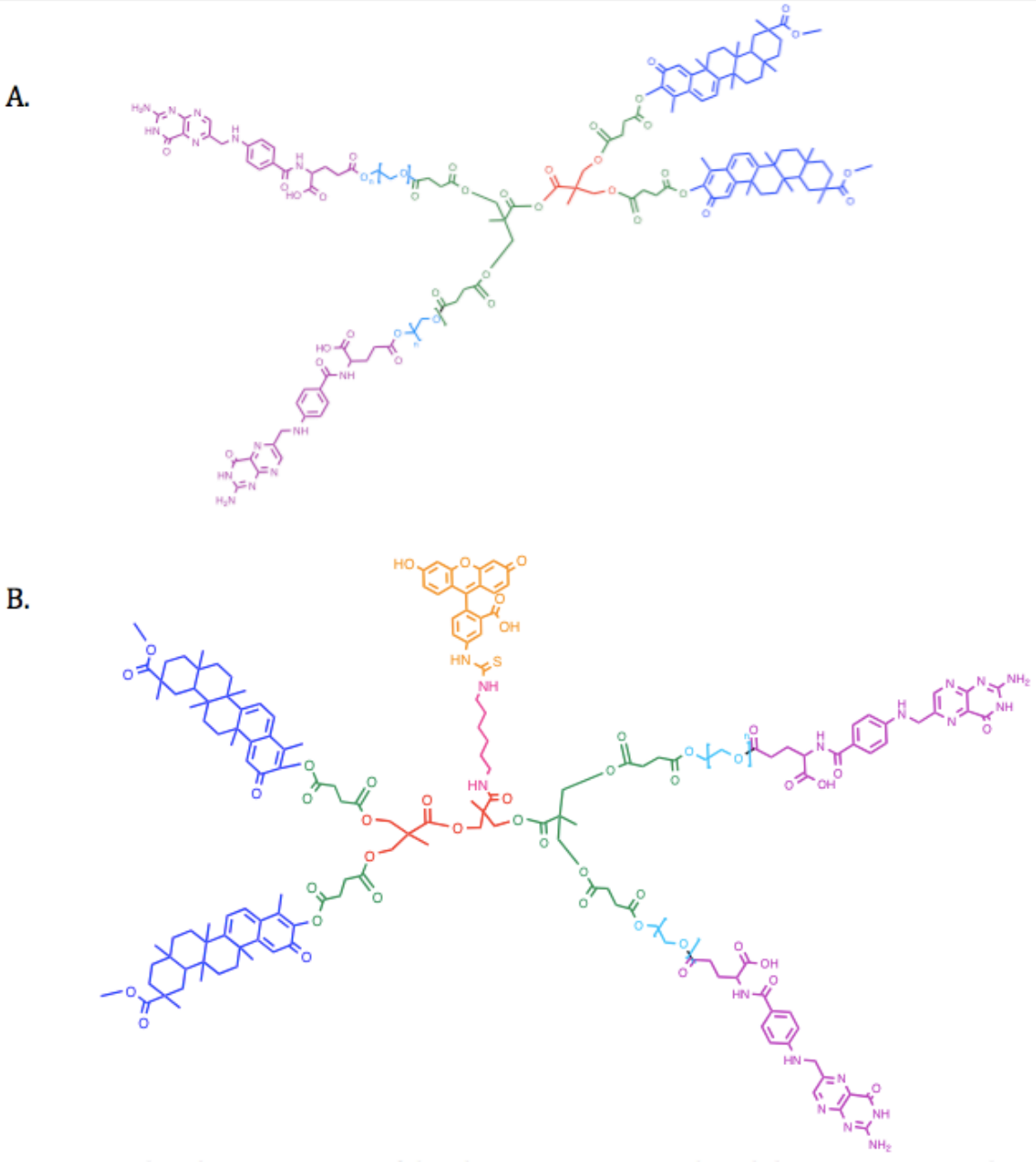

Figure 12. Molecular structures of dendrimers conjugated with bis-MPA as a nucleus (red), polyester ramifications (green), PEG 3350 as linker (teal), folic acid as ligand (purple), and pristimerin drug (blue). A. Bifunctional dendrimer for therapeutic purposes. B. Trifunctional dendrimer conjugated with FITC (orange) for *in vitro* studies and HMDA as linker (pink).

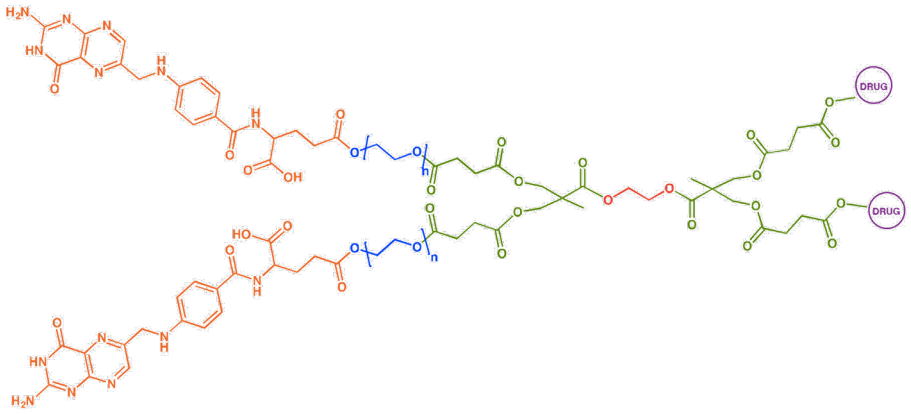

Figure 13. Molecular structure of bifunctional dendrimer conjugated with ethylene glycol as a nucleus (red), polyester ramifications (green), PEG 750 or PEG 3350 as linker (teal), folic acid as ligand (purple), and pristimerin drug (blue).

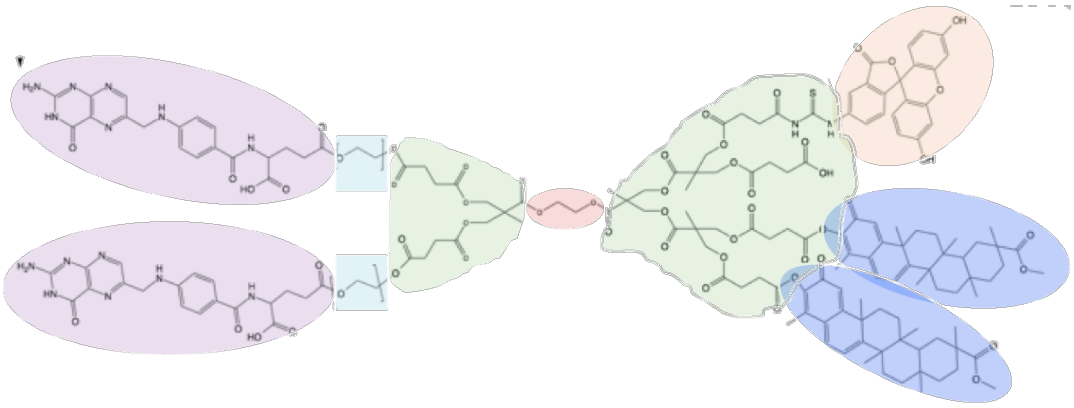

Figure 14. Molecular structure of trifunctional dendrimer conjugated with ethylene glycol as a nucleus (red), polyester ramifications (green), PEG 3350 as linker (teal), folic acid as ligand (purple), and pristimerin drug (blue).

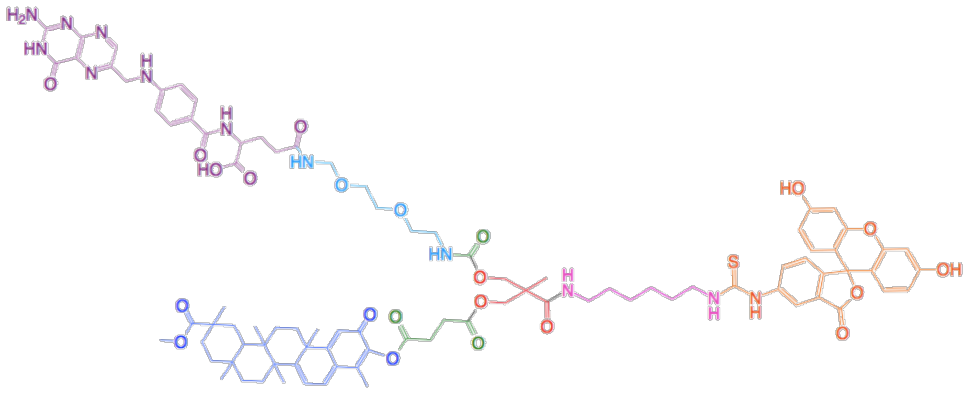

Figure 15. Molecular structure of trifunctional conjugate with polyester ramifications (green), TEG as linker (teal), folic acid as ligand (purple), and pristimerin as drug (blue).

3.2.1 Chemical synthesis

A complete methodology for the five dendrimers syntheses is reported in this section. However, they have several compounds in common; for example, the branching molecules with BMPA (EB-AS), C1-PEG3350, FITC-HMDA, etc. Therefore, the syntheses of some key building blocks with FA, FITC, and pristimerin were carried out.

The dendrimers were obtained by synthesis of one generation (G1) of BMPA. Their structure was built based on polyester ramifications such as bis-(2,2-hydroxymethyl)propanoic acid (**BMPA**) and benzyl-2,2-bis(methylol)propionate and succinic anhydride (**EB-AS**) as branching molecules. The dendrimers were functionalized in their periphery with pristimerin for chemotherapeutical effects; folic acid (**FA**), to selectively direct the dendrimer to folate receptors overexpressed in cancer cells; and fluorescein isothiocyanate (**FITC**) as a fluorescent dye for *in vitro* evaluation as a cancer treatment. 1,6-hexamethylenediamine (**HMDA**), PEG_{3350}, and TEG were used as spacers for the reactions with FITC and FA.

A. General synthesis.

BMPAP, EB, and DPTS were synthesized and used as initial compounds for their use in further synthesis.[41] Their synthesis reactions are shown in Figure 16.

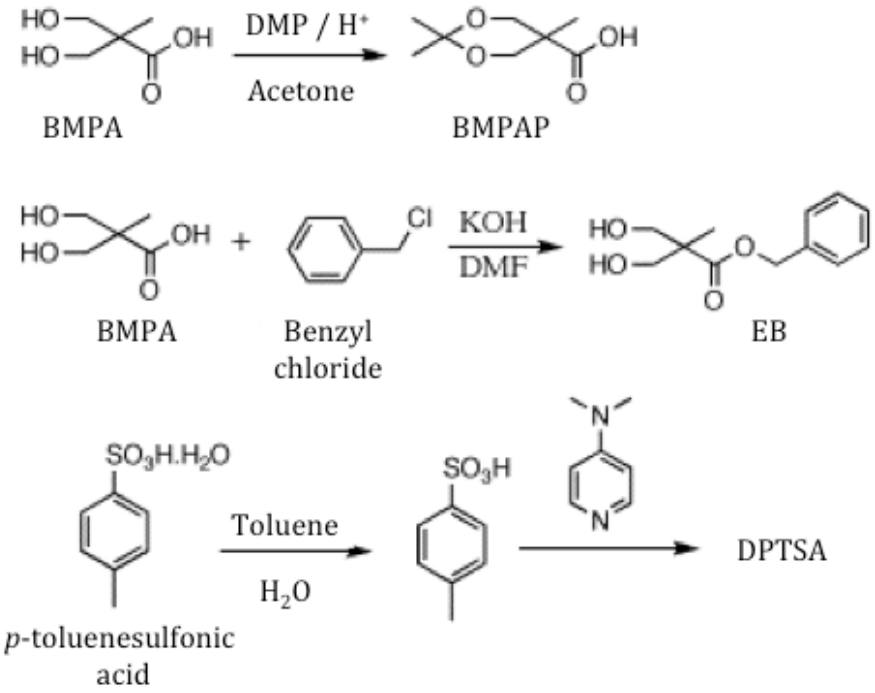

Figure 16: Synthesis of general compounds.

Multiple protection and deprotection of functional groups, were necessary along the synthesis, to control the specific site of binding for each compound. A detailed methodology is described next.

Protection of acetonide group of 2,2-bis(hydroxymethyl) propanoic acid (BMPAP)

A mixture of 16 g BMPA, 1.4 g *p*-toluene-sulfonic acid, 28 mL dimethoxypropane (DMP) and 100 mL of acetone, was prepared in a flask. The reaction remained under stirring for 2 hours at room temperature (30°C). 12 mL of Na_2CO_3 10% solution was added and the solvent was removed. The obtained solid was dissolved in DCM and washed in a separation funnel with water. The DCM was removed by rotavapor. The fusion point of the product (115-117°C) was determined to verify its purity. [41,42]

Benzyl 3-hydroxy-2-(hydroxymethyl)-2-methylpropanoate (benzyl ester of BMPAP, EB)

BMPA (9 g, 67 mmol) and KOH (4.3 g, 78 mmol) were dissolved in 50 mL of DMF. The reaction remained under stirring at 340 rpm at 100°C during 1 hour. Once the reaction was completed, the mixture was cooled at room temperature in order to add benzyl chloride (10.22 g, 80.787 mmol). The KCl salt was filtered by vacuum with filter #41 and the solvent was removed by rotavapor. Next, the product was washed with DCM and water. The rest of humidity was removed with NaCl and the solvent was evaporated by rotavapor. The product was purified by recrystallization with Hexane:DCM 1:1, it was stored in the freezer at 2°C for 18 hours, and then filtered by vacuum with paper #41 to obtain white crystals (87%). The purity of the product was verified by determining its fusion point (PF theo: 75°C); ^{1}H NMR ($CDCl_3$) δ 1.08 (s, 3H, -CH_3), 3.74 (d, 2H, -CH_2OH), 3.95 (d, 2H,-CH_2OH), 5.22 (s, 2H, -CH_2Ar), 7.36 (m, 5H, ArH); ^{13}C NMR($CDCl_3$) δ 17.16, 49.35, 66.64, 67.49, 127.84, 128.28, 128.63, 175.69.[42]

1,4-Dimethylpyridinium *p*-toluenesulfonate (DPTS)

p-toluenesulfonic acid (14.4 g, 83.62 mmol) was added to a baker with 150 mL of toluene. The baker was placed over a heating mantle. A Stark & Dean trap and a condenser were adapted to the baker and the trap was filled with toluene. The reaction was stirred and heated until the *p*-toluenesulfonic acid was completely dehydrated. The expected volume of water from the trap was calculated. Once the acid was dehydrated, dimethylaminopyridine (DMAP) (9.3 g) was added to 120 mL of toluene and slowly added (20-30 min) to the stirring solution of dehydrated acid. Then, the suspension was filtered under vacuum and washed with toluene. The solvent was evaporated by rotavapor and the product dried. The fusion point of the product (PF theo: 161-162°C) was determined to verify its purity. A recrystallization with DCM can be done if necessary.[41,42]

B. Protecting groups removal

Benzyl group removal

A catalytic hydrogenation reaction at low pressure was done to recover the carboxylic function. The compound was dissolved in methanol in the hydrogenation reactor. The catalyzer, 10% Pd/C suspended either in methanol or DMF, according to the sample solubility and it was added to the sample solution. The recipient was placed in the

hydrogenator, which was purged 3 times with 30 psi of hydrogen. The reaction occurred at 50 psi of hydrogen and stirred until the reaction was completed. The suspension was filtered with a filter #5 to remove the catalyzer. The solvent was removed by rotavapor. [42]

Another method to remove benzyl group consists in the addition of triethylsilane (TES), using 20% Pd/C as catalyzer for the liberation of hydrogen *in situ*. However, this method is more sensitive and must be done under inert atmosphere with argon.[57]

Deprotection of acetonide group

Deprotection reactions of acetonide group was done by adding ion exchange resin DowexTM 50WÅ~8 hydrogen form, 1:1 against grams of sample and using methanol as solvent. The mixture remained under stirring until the reaction was completed. The reaction was followed by TLC. Samples with folic acid and FITC taked more time to finish, about 24 hours at room temperature (30°C). The resin was separated from the sample through a filter #41 and the solvent was removed with a rotavapor.[41,42]

C. Synthesis of bifunctional and trifunctional dendrimers with bis-MPA core and PEG 3350 linker.

A synthesis pathway was designed for the obtention of a bifunctional polyester dendrimer, conjugated with folic acid and pristimerin drug, with bis-MPA as core and PEG as linker, for therapeutical use (Figure 17). Also, a synthesis route of a trifunctional dendrimer was designed, similar from the one in Figure 18, with FITC dye as an additional conjugate for *in vitro* tests only **(**Figure 18). The synthesis of compound 4 involved two carboxylic groups (one from the folate ester dendron and another from BMPA as nucleus), to the formation of a highly unstable acid anhydride. Therefore, ethylene glycol nucleus was proposed and a new synthesis route was designed (Figure 19).

1. BMPAP benzyl ester succinylate (EB-AS)

A mixture of AS (1.511 g, 15.099 mmol), EB (1.122 g, 5.003 mmol), and DMAP (0.511 g, 4.183 mmol) was dissolved in 20 mL of DCM. The mixture remained under stirring during 18 hours at 240 rpm and room temperature (30°C). The product was washed in a separation funnel two times using DCM and water, adding HCl 0.5 N until pH 1 was reached. The solvent was removed from the organic phase by rotavapor. The product was purified by column chromatography with silica gel (normal phase) mesh 230-400, using Hexane:EA 1:5 as the eluent.[42]

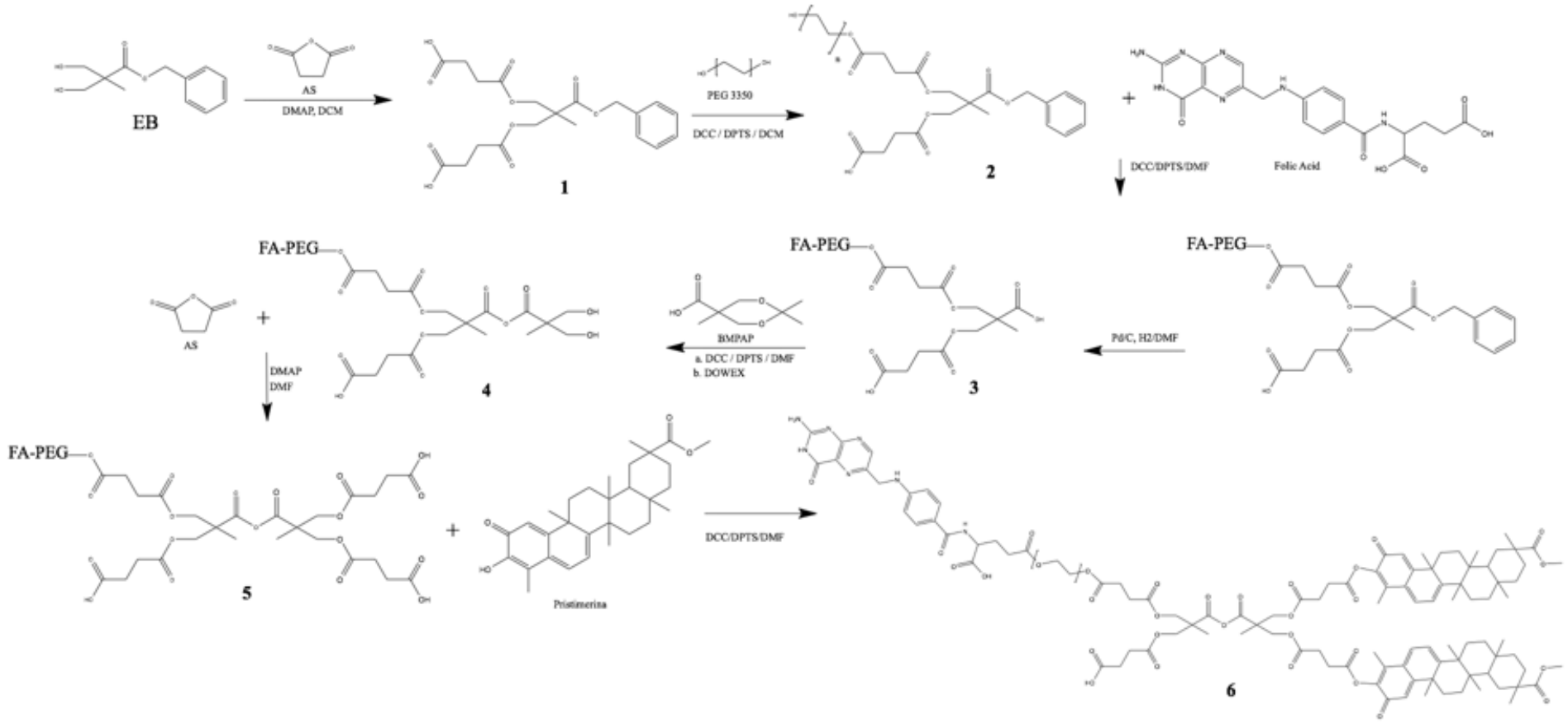

Figure 17. Synthesis of bifunctional dendrimer conjugated with bis-MPA core, PEG_{3350}, FA and pristimerin. Numbers and abbreviations are according to the nomenclature used in the thesis.

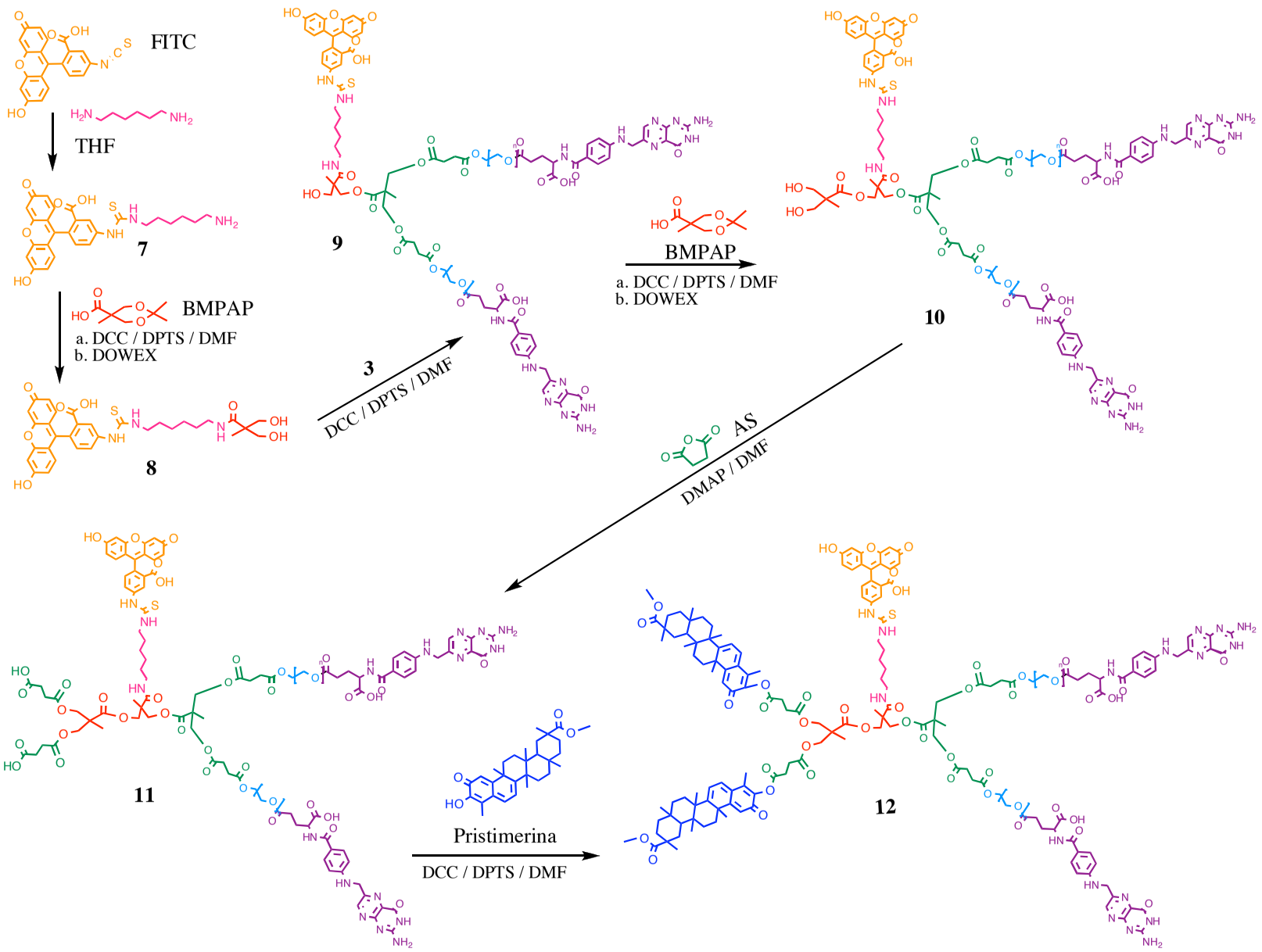

Figure 18. Synthesis of trifunctional dendrimer conjugated with bis-MPA core, PEG_{3350}, FITC, FA and pristimerin. Numbers and abbreviations are according to the nomenclature used in the thesis.

2. EB-AS + PEG3350

Compound 1 (0.194 g, 0.457 mmol) and PEG_{3350} (2.042 g, 0.609 mmol) were separately dissolved in 28 mL of DCM. A solution of DCC (0.093 g, 0.457 mmol) and DPTS (0.054g, 0.183 mmol) in 2 mL of DCM was added dropwise to the previous solution. The reaction remained under stirring at 320 rpm and room temperature (30°C) for 48 hours. Once the reaction was completed, DCU was filtered using filter #41 and the solvent was removed. The product was purified by several methods including Flash chromatography with a reverse phase column C18, using ethanol as the eluent; size exclusion chromatography by column preparation with water as eluent or buffer pH 7 as eluent; ultrafiltration with 5 kDa column and water as eluent, and dialysis cassette 7 kDa and water or buffer as eluent.

3. EB-AS-PEG3350 + folic acid (FA)

FA (0.0503 g, 0.114 mmol) was dissolved in 10 mL of DMF. Then, a solution of compound 2 (0.6g, 0.076 mmol) and DPTS (0.009 g, 0.0304 mmol) in 10 mL of DMF was added to the previous solution. Next, DCC (0.02 g, 0.076 mmol) in 2 mL of DMF was added dropwise to the mixture. The reaction remained under stirring at 500 rpm and 50°C in the dark for 72 hours. Once the reaction was finished, the solvent was removed by rotavapor and the product was purified by two methods, in order to determine the best one for future synthesis. First the product was purified by ultrafiltration (7 kDa, water eluent). The product of a second reaction was purified by dialysis cassette (7 kDa, buffer pH 7.4, 3 days. The benzyl group was removed by hydrogenation. An additional trial was done to remove the benzyl group using TES, Pd/C 20%; the reaction was monitored by TLC starting at 5 min and ending at 26 hours. Both methods were done with methanol as eluent. Purification was done by dialysis cassette 7 kDa during 48 hours.

4. EB-AS-PEG3350-FA + BMPA

Compound 3 (0.664 g, 0.084 mmol) was dissolved in 30 mL of DMF. Then, a solution of BMPAP (0.015g, 0.084 mmol) and DPTS (0.010g, 0.034 mmol) in 10 mL of DMF was added to the previous solution. Next, a solution of DCC (0.021 g, 0.101 mmol) in 2 mL of DMF was added dropwise. The reaction remained under stirring at 500 rpm and 50°C in the dark for 72 hours. Once the reaction was completed, the solvent was removed by rotavapor and the product was purified by column chromatography using Sephadex G-50 as stationary phase 1:20 (grams of silica against grams of Sephadex) and DMF as the elution solvent. The deprotection reaction of the acetonide group was done with ion exchange DOWEX resin.

5. EB-AS-PEG3350-FA-BMPA (compound 4) + AS

A solution of compound 4 (0.691 g, 0.087 mmol), AS (0.026 g, 0.261 mmol) and DMAP (0.032 g, 0.261 mmol) was prepared in 50 mL of DMF. The reaction remained under stirring at 500 rpm and 30°C in the dark during 48 hours. Then, the solvent was removed by rotavapor. Finally, the product was purified by column chromatography

using Sephadex G-50 as stationary phase 1:20 (grams of sample per grams of Sephadex) and DMF as eluent.

6. EB-AS-PEG3350-FA-BMPA-AS (compound 5) + Pristimerin

A mixture of compound 5 (0.220 g, 0.027 mmol), pristimerin (0.025 g, 0.054 mmol) and DPTS (0.007 g, 0.032 mmol) is dissolved in 18 mL of DMF. Then, a DCC (0.003 g, 0.011 mmol) solution in 2 mL of DMF is added dropwise. The reaction remains under stirring for 72 hours at 500 rpm and 30°C in the dark. The solvent is removed by rotavapor and the product is purified by column chromatography using Sephadex G-50 as stationary phase 1:20 (grams of sample per grams of Sephadex) and DMF as eluent.

7. Non-activated FITC-HMDA

First, 0.2 g of FITC (0.514 mmol) was dissolved in 40 mL of THF. Then a solution of HMDA (0.18 g, 1.549 mmol) was added to the FITC solution. The reaction remained under stirring at 200 rpm and room temperature, in the dark, for 48 hours. Once the reaction was completed, the solvent was removed by rotavapor and the product was purified by column chromatography with silica gel (normal phase) and ethanol as eluent.

8. FITC-HMDA-BMPA

This synthesis occurred in two steps. First, the reaction between FITC-HMDA (0.260 g, 0.514 mmol) and bis-MPA with the hydroxyls protected with an acetonide group (BMPAP) (0.358 g, 2.056 mmol) was dissolved in 40 mL of DMF. A solution of DCC (0.116 g, 0.566 mmol) and DPTS (0.066 g, 0.226 mmol) was added dropwise and the reaction remained under stirring at room temperature, in the dark, for 3 days. The solution was vacuum-filtered to remove DCU, and the solvent was removed by rotavapor. The product was purified by column chromatography with silica gel (normal phase) and ethanol as eluent, to obtain FITC-HMDA-BMPAP.
The second step consisted in the deprotection of the hydroxyl groups by a reaction with ion exchange DOWEX resin.

D. Synthesis of trifunctional dendrimer with ethylene glycol core and PEG 3350 linker.

The synthesis procedure to obtain a trifunctional dendrimer with FA, pristimerin, and FITC is described next, but now using an ethylene glycol nucleus and some adaptations in the synthesis steps (Figure 19). The preparation methods for each synthesis are not described in this section, since we observed multiple challenges related to the stability of several compounds and characterization. Therefore, a fourth triconjugated structure and synthesis was proposed.

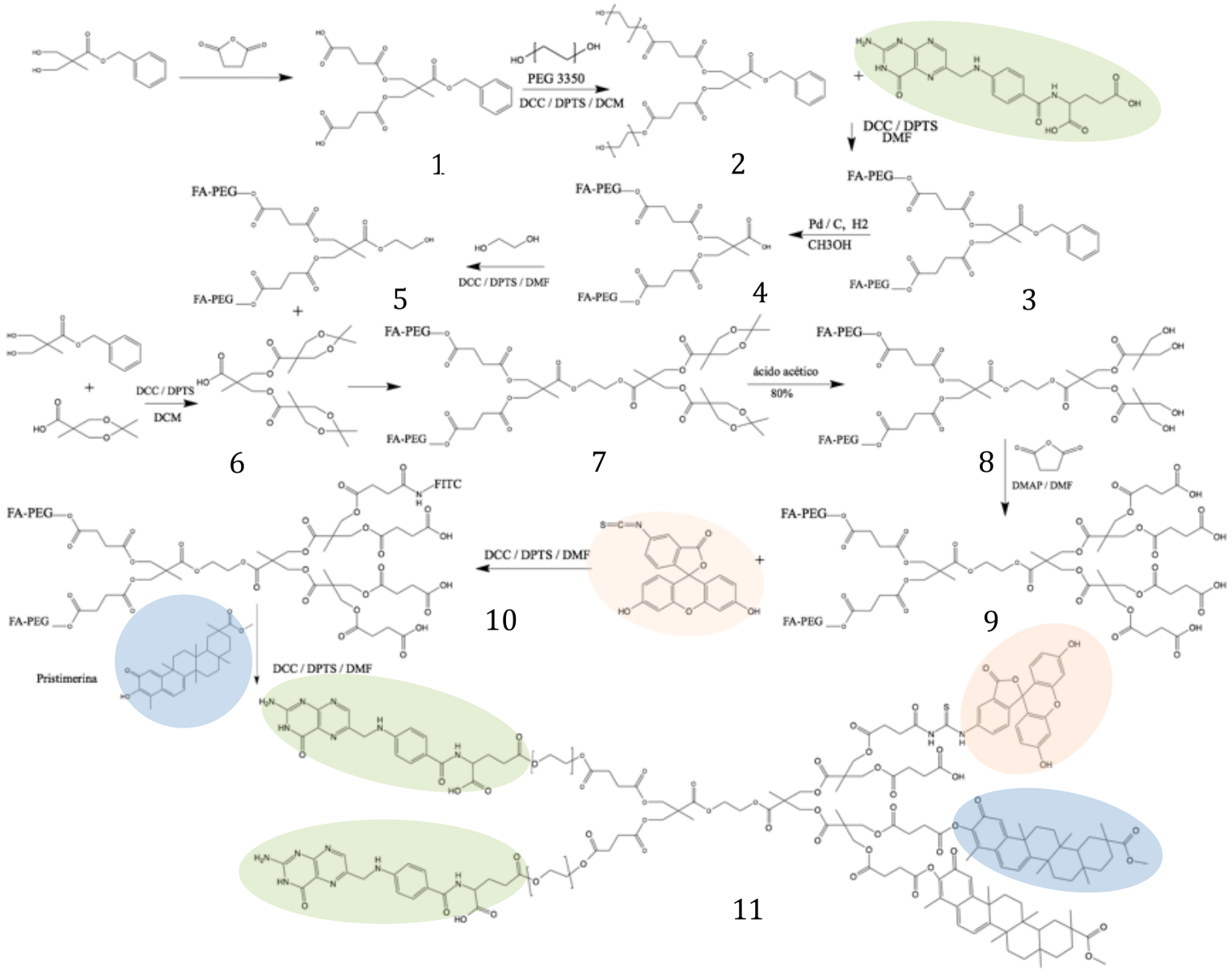

Figure 19. Synthesis of trifunctional dendrimer conjugated with ethylene glycol core, PEG_{3350}, FITC, FA and pristimerin. Numbers and abbreviations are according to the nomenclature used in the thesis.

E. Synthesis of trifunctional conjugate with FA, FITC, and pristimerin, using TEG linker.

An alternative and simpler synthesis of a trifunctional conjugate with FA, Pristimerin, and FITC was proposed using triethylene glycol (TEG) instead of PEG 3350 as linker of FA to the rest of the dendrimer to facilitate purification and characterization (Figure 21).

1. FITC-HMDA

A solution of HMDA (1.0 g, 2.568 mmol) in 400 mL of buffer $NaHCO_3$-Na_2CO_3 pH 9, 0.1 M was prepared. Meanwhile, a solution of FITC (0.5 g, 4.302 mmol) in 100 mL of the same buffer was separately prepared. FITC solution was slowly added to the amine solution. The reaction remained under stirring during 24 hours in the dark.[58] The solvent was removed by rotavapor. The product was dissolved in ethanol and centrifuged during 15 min at 5,000 rpm, and 4°C. The solution was decanted and purified by Phenomenex C18-E cartridges. The pellet obtained from decantation was washed again with ethanol and the purification step was repeated.

2. BMPAP-Oxalyl chloride

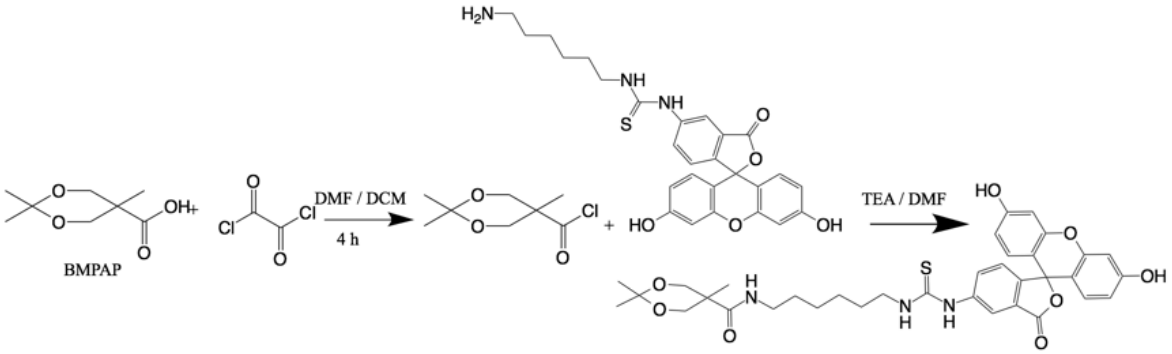

Figure 20. Synthesis of FITC-HMDA-BMPAP.

The synthesis of FITC-HMDA-BMPAP was done in two steps (Figure 20). First, the formation of acyl chloride was done by the following procedure. BMPAP (0.083 g, 0.477 mmol) was dissolved in 10 mL of DCM, adding one drop of DMF. The solution remained under stirring at 0°C. A solution of oxalyl chloride (0.06 g, 0.477 mmol) dissolved in 3 mL of DCM was added dropwise to the BMPAP solution. The reaction remained under stirring for 4 hours at room temperature and completely covered. Once the reaction was completed, FITC-HMDA was immediately added to the solution.

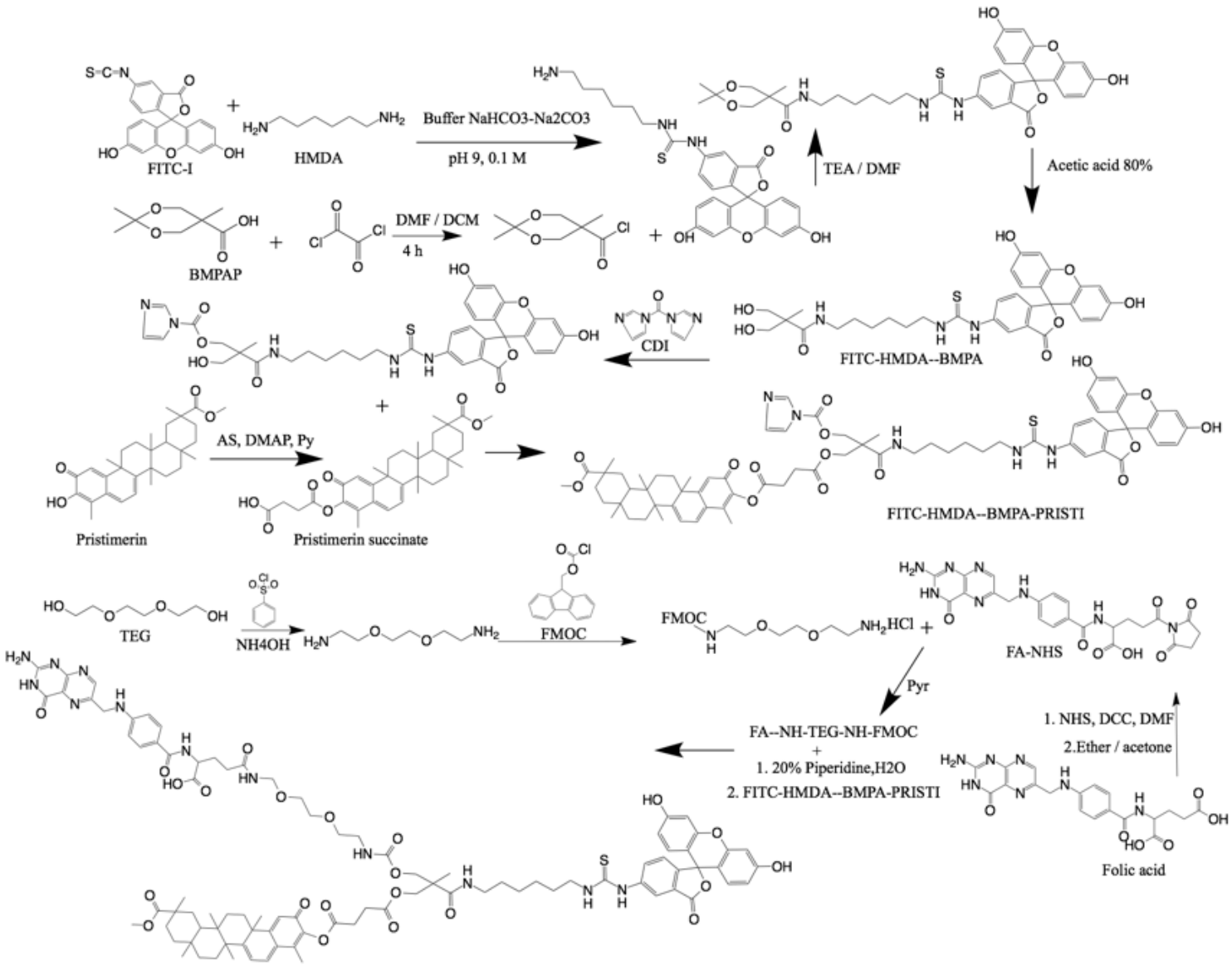

Figure 21. Synthesis of trifunctional dendrimer conjugated with triethylene glycol linker, FA, FITC, and pristimerin. Numbers and abbreviations are according to the nomenclature used in the thesis.

3. FITC-HMDA-BMPAP

FITC-HMDA (0.35 g, 0.529 mmol) was previously dissolved in DMF, and 112 μL of TEA was added (0.8 mmol). It is important to consider that this solubilization taked time, and the solution had a high viscosity. Therefore, it is recommended to do it overnight in order to proceed with the reaction with acyl chloride. The acyl chloride of BMPAP was immediately added and the reaction was stirred in the dark at 40°C for 4 days. The solution was filtered by vacuum and the solvent was removed by rotavapor. The filtration liquid was purified by column chromatography with silica gel (normal phase) with hexane:ethanol 1:1 as eluent. The precipitate was purified by Phenomenex C18-E cartridge, using $NaHCO_3$.Na_2CO_3 buffer pH 9, 0.1 M, since ethanol favors precipitation increasing the sample turbidity, and with buffer an orange clear solution was obtained.

Note: The preparation of amides is not easily to occur directly with the addition of a carboxylic acid. The acid protonates the amine preventing the next reaction to occur because the carboxylate is a poor electrophile and the ammonium ion is not nucleophilic. It is simpler to firstly convert the carboxylic acid to acyl chloride (which is more reactive). Therefore, acyl chloride was prepared and later used immediately with FITC-HMDA.

4. FITC-HMDA-BMPA

The deprotection of FITC-HMDA-BMPAP was done with acetic acid 80%. The reaction remained under stirring during 12 hours at room temperature, in the dark.
Another option that can be used to deprotect the acetonide group is with ion exchange resin DOWEX. However, it is not recommended to use it with compounds with FITC and FA, since it gets more difficult to separate the resin from the product.

5. Carbonyl imidazole of FITC-HMDA-BMPA

First, dissolve the FITC-HMDA-BMPA in THF. The protection of one hydroxyl group from FITC-HMDA-BMPA is done with carbonyldiimidazole (CDI) 2:1. The reaction remains in THF at room temperature, in reflux during 1 hour. In this case the protection of only one hydroxyl group is desired for a subsequent reaction (7). Also, we suggest to begin with only half of CDI equivalents, relative to FITC-HMDA-BMPA, to be assured that it binds only to one hydroxyl group.[59]

6. Pristimerin succinate

The hydroxyl group of pristimerin was modified with succinic anhydride to a mono ester in order to have a terminal carboxylic group for further syntheses. This method has not been reported in literature but was based in the oleanolic acid modification reported by Bertha de la Re[60] (Figure 22).

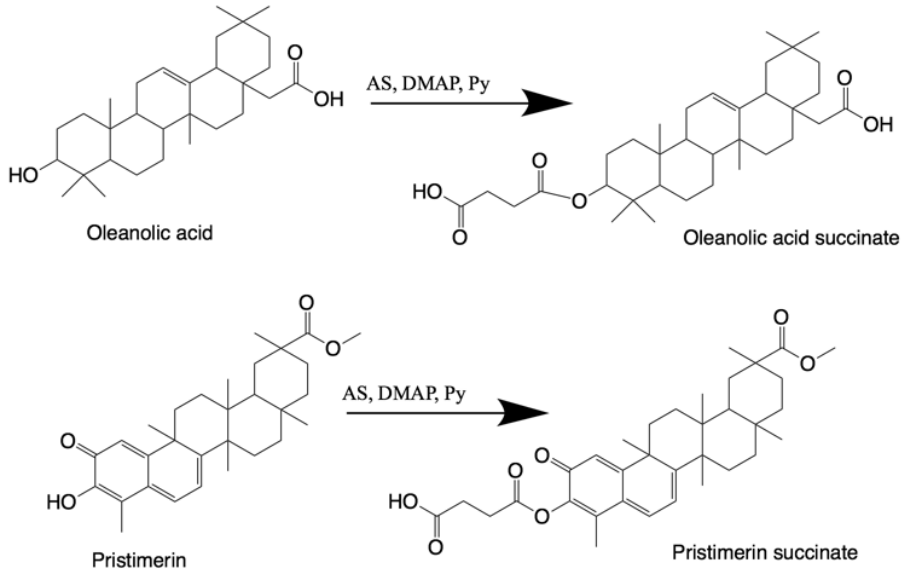

Figure 22. Modification of hydroxyl group of oleanolic acid vs pristimerin.

Pristimerin (0.031 g, 0.065 mmol) and AS (0.098 g, 0.975 mmol) 1:15 were stirred together in 2 mL of TEA. DMAP 5% relative to pristimerin was added to the mixture, and remained under stirring for 24 hours in the dark at room temperature. Then, cold water was added for precipitation. The precipitate was washed in a separation funnel with DCM and water, adding HCl until pH 7 was reached. The solvent was removed by rotavapor, and the product was dried overnight under vacuum. The product was purified by column chromatography using hexane:acetone 7:3 (normal phase). Methanol can be used for crystallization.

7. FITC-HMDA-BMPA-Pristi

Carbonyl imidazole of FITC-HMDA-BMPA (5) and Pristimerin succinate (6) 2:1 are dissolved in DMF. DCC (1.1 eq.) and DPTS (0.4 eq.) are added to favor the reaction. The solution is stirred for 48 hours at room temperature in the dark. DCU is filtered and the solvent is removed by rotavapor.

8. TEG-Diamine

This procedure was adapted from literature, where they used PEG-diamine instead of TEG-diamine.[8] 0.5 g of TEG (3.329 mmol) were dissolved in 10 mL of DCM. Then, 0.35 mL of triethyl amine (TEA) was added and the flask was placed in an ice bath. 2.539 g of benzenesulfonyl chloride was separetely dissolved in 13 mL of DCM. Note that it takes time to completely dissolve this solution. Once dissolved, the solution with benzenesulfonyl chloride was slowly added with a dropping funnel (covered) to the stirring solution with TEG, leading to the formation of white vapors inside the flask. Then, the reaction was stirred for 12 h at room temperature. Finally, a slightly yellow and transparent solution was obtained. The product was washed with $NaHCO_3$ 50 mM and the organic phase was filtered through $MgSO_4$ anhydrous. The solvent was removed by rotavapor and the yellow oil was immediately dissolved in an excess of

ammonium, leading to the formation of a white precipitate. The reaction remained under stirring during 48 hours, and a clear solution was obtained. The product was extracted with DCM and filtered with $MgSO_4$ to remove humidity. The solvent was removed in the rotavapor. The product crystallization can be done with ethyl ether if necessary, obtaining as a final product a white solid (Rf: 0.4, hexane:EA 1:1, iodine vapors). The yield was 88%.

9. TEG-diamine monoprotected with FMOC

This procedure was adapted from literature, where they used PEG-diamine instead of TEG-diamine.[8] Therefore it can also be used in the other synthesis where PEG3350 is used. TEG-diamine (0.15 g, 1 mmol) is dissolved in 10 mL of a 10 mM $NaHCO_3$ solution and diluted with an additional 10 mL of acetonitrile, and 260 mg (1 mmol) of 9-fluorenyl- methyloxycarbonyl (FMOC) is dissolved in 50 mL of acetonitrile and added dropwise under stirring. The mixture is left to react for an additional 1 h at room temperature, and then the mixture is acidified with HCl. The acetonitrile is evaporated by rotavapor, and the water is lyophilized. The product is desalted by dissolving the lyophilized sample in DCM followed by filtering out the NaCl. The DCM is removed by rotavapor, and the mixture of products is dissolved in water and separated by a cation exchange column (Sephadex CM-25). The monoprotected fraction is eluted with a 25 mM NaCl solution, collected, acidified with HCl, and lyophilized. The final product is desalted again by dissolving it in DCM, filtering out the solids, and evaporating the solvent. The product can be crystallized with ethyl ether. The yield from literature is 30%.[61]

10. Folic acid activation (FA-NHS)

Folic acid (0.492 g, 1.146 mmol) was dissolved in 15 mL of DMF. A solution of DCC (0.154 g, 0.7486 mmol) in DMF was added dropwise to the previous solution. NHS (0.128 g, 1.1146 mmol) was added dropwise to the solution, and the reaction remained under stirring overnight at room temperature in the dark. Once the reaction was completed, DCU was filtered at 10,000 rpm, 30 min. The product was immediately used for the next step.

11. Trifunctional dendrimer (FITC-HMDA-BMPA-FA-Pristimerin)

This reaction occurred in 3 steps. First, the reaction of activated folate (FA-NHS) with TEG-diamine monoprotected to obtain FMOC-TEG-FA. Second, a deprotection reaction of the FMOC protecting group was carried out. Third, a reaction with NH_2-TEG-FMOC and FITC-HMDA-BMPA-PRISTI dendron was done to obtain the final trifunctional dendrimer proposed. A more detailed procedure for each step is described next.

a. NH_2-TEG-FMOC (0.15 mmol) was coevaporated with three 50 mL portions of dry pyridine and finally dissolved in 100 mL of dry pyridine. Then, FA-NHS ester (0.67 mmol) was added to the solution and the reaction was left overnight under stirring in the dark. Upon completion of the reaction (confirmed by the ninhydrine test) the pyridine was evaporated and the remaining solid was dissolved in 20 mL of 100 mM $NaHCO_3$. The reaction

mixture was purified by column chromatography using Sephadex 25 and the solvent was removed by rotavapor. The yield reported in literature is 80%.[61]

b. The FMOC protecting group was removed from FA-TEG-FMOC by piperidine treatment. FA-TEG-FMOC was dissolved in 25% aqueous piperidine. Then, the precipitate was removed by filtration, and solvents are evaporated by rotavapor. All traces of piperidine were removed by dissolving the product in water and evaporating the solvent. FA-TEG-NH_2 is obtained.
c. According to literature (**Figure 23**) a carbonyl imidazole in presence of amine allowed to remove the protecting group leading to a carbamate linkage.[59] Therefore, FITC-HMDA-BMPA-PRISTI and FA-TEG-NH_2 1:1.5, in reflux for 30 min, at room temperature, led to the formation of the trifunctional dendrimer proposed.

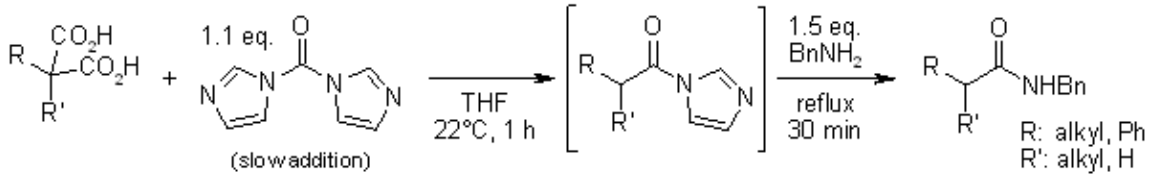

Figure 23. Reaction between a carbonyl imidazole and an amine to obtain an amide.[59]

4. Results and discussion

According to the different dendrimers proposed in this work, we were able to do the synthesis of BMPAP, EB, and EB-AS as alternatives for branching molecules. As PEGylated compounds we obtained C1-PEG3350, C1-PEG3350 with its carboxylic group deprotected by benzyl group removal, and FA-PEG3350-C1 that can be used as a site-specific dendron. Synthesis with TEG included C1-TEG, diamino-TEG, and FA-TEG-NH2. Synthesis of compounds with FITC dye with hexamethylene diamine (HMDA) and BMPAP to obtain FITC-HMDA, FITC-HMDA-BMPAP and its deprotection to obtain FITC-HMDA-BMPA. Also, the hydroxyl group of pristimerin was modified through its hydroxyl group to obtain pristimerin succinate.

Different synthesis approaches and/or purification methods were applied to these compounds according to the complexity of their structure and solubility (Table 3). The compounds of general use and branching molecules like BMPAP and EB, because of their structure simplicity, can be purified with 2 or 3 extractions with DCM-H_2O. The reactions were followed by TLC and their fusion point was determined.

Ultrafiltration (5 kDa) was the best purification method for PEGylated compounds (C1-PEG3350, deprotected C1-PEG3350 and FA-PEG3350-C1) in comparison to column chromatography with silica gel, normal phase. Ultrafiltration was a faster method and there was a higher yield of pure compounds.

Meanwhile, folic acid compounds, such as FA-PEG3350-C1 and FA-TEG-NH_2, showed a higher purification yield when using dialysis cassettes (7 kDa) and PBS buffer, in comparison to SEC with Sephadex. In addition, dialysis could also be used to purify other PEGylated compounds like CI-PEG3350, but this method was only applied to

compounds with lower solubility in organic compounds and with low amount of sample to purify.

Column chromatography with silica gel was a good alternative for simple purifications of low molecular weight compounds, such as EB-AS, CI-TEG and pristimerin succinate, that were soluble in inorganic compounds (hexane: ethyl acetate 1:5, ethanol:DCM 1:2, and hexane:acetone 7:3, respectively), without the risk of damaging a dialysis membrane and in a cost-effective way.

In the other hand, FITC compounds such as FITC-HMDA, FITC-HMDA-BMPAP, and FITC-HMDA-BMPA were more soluble in a buffer solution $NaHCO_3$-Na_2CO_3 (0.1 M, pH 9) and Phenomenex C18-E cartridge was the best purification method.

Table 3. Summary of synthesized compounds with application in site-specific dendrimers.

Nucleus and branching molecules			
Compound	**Application**	**Purification**	**Observations**
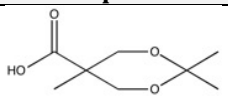 BMPAP	Nucleus and branching molecule	Not necessary further purification than extraction with DCM:H_2O.	Fast and simple synthesis (2 h). Great for branching. Yield: 74%, FP_{exp}: 116°C, FP_{theo}: 115-117°C
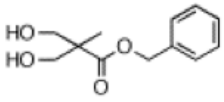 EB	Branching molecule	Wash with DCM:H_2O. Filtration with DCM, high solubility.	Fast and simple synthesis (4h). Recrystallization favored with hexane:DCM 1:1. Yield: 95%, FP_{exp}: 72°C, FP_{theo}: 70-72 °C
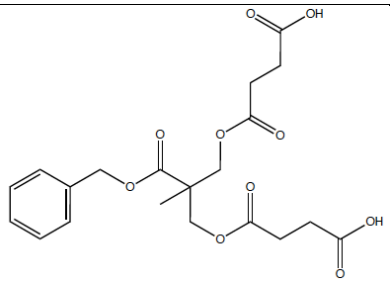 EB-AS or C1	Branching molecule. Dendron	Silica gel column (normal phase), hexane:ethyl acetate 1:5.	Easy synthesis. High product solubility en DCM. Yield: 80% Reaction in DMAP and DCM, 18 h.
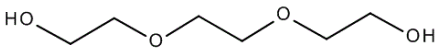 Ethylene glycol	Nucleus	NA	Commercially acquired.

PEGylated compounds			
Compound	**Application**	**Purification**	**Observations**
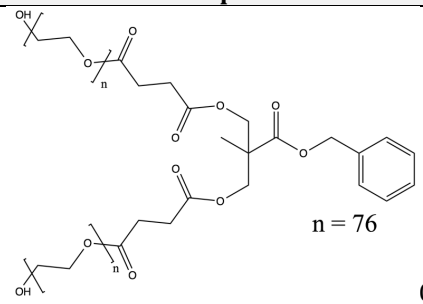 C1-PEG3350	Branching molecule with linker to enhance solubility. Dendron.	1. Column chromatography, silica gel normal phase, ethanol:DCM 1:2 2. Sephadex G-50 column (1.5-30 kDa), ethanol:DCM 1:2 3. Ultrafiltration, 5 kDa, water.	Reaction of 48 h. The product showed a better purification and higher yield (82%) by ultrafiltration against the other methods. Higher product solubility in water. Sephadex purification was slower.
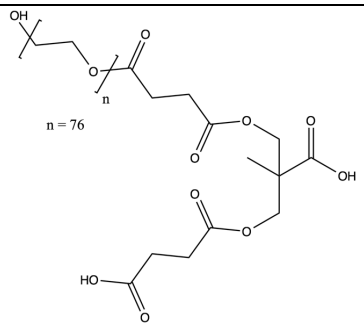 Deprotected C1-PEG3350	Branching molecule with linker to enhance solubility. Dendron.	Filtration with acetone. Ultrafiltration, 5 kDa, water.	Slow deprotection of carboxyl group by benzyl removal with hydrogenator, 37 h in time intervals, methanol. Yield: 50%
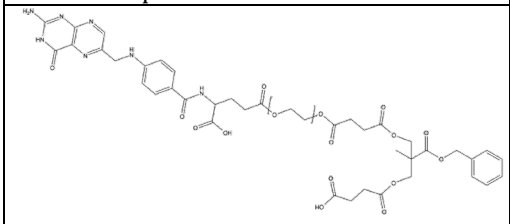 FA-PEG3350-C1	Site-specific dendron.	Ultrafiltration, normal phase, 5 kDa, water	Reaction time: 48 h. Yield: 62%. Product soluble in water and methanol.
		Dialysis cassette 7 kDa, PBS buffer 3x, water 3x.[62]	Best option. 3 days in dialysis, moderately soluble. 35 mg of sample per dialysis. Yield: 72%
TEG compounds			
Compound	**Application**	**Purification**	**Observations**
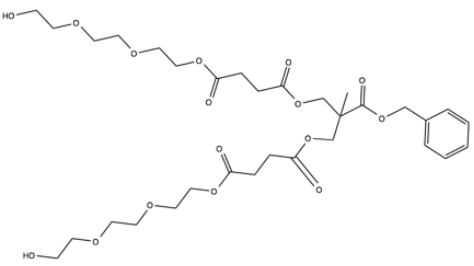 CI-TEG	Branching molecule. Dendron.	Column chromatography, silica gel normal phase, ethanol:DCM 1:2	Reaction time: 24 h Simple synthesis . Yield: 72%
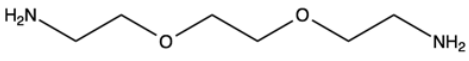 Diamino TEG	Nucleus and linker.	Extraction with $NaHCO_3$ and DCM. Rf: 0.4	The reaction is followed by TLC (hexane:ethyl acetate 1:!), silica gel. Reaction of 48 h. Yield: 95%
	Site-specific compound.	Centrifugation 8,000 rpm, 20°C,	Folic acid should be activated (FA-NHS)

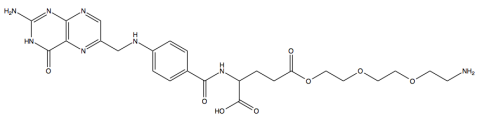 FA-TEG-NH_2		20 min. Then, Sephadex G-15, $NaHCO_3$ 100 mM.	for 12 h before reaction with diamino TEG 12 h.. Yield: 78 %.
		Dialysis cassette 7 kDa, PBS buffer 3x, water 3x.	Best option. 3 days in dialysis, moderately soluble. 40 mg of sample per dialysis. Yield: 85%
FITC compounds			
Compound	**Application**	**Purification**	**Observations**
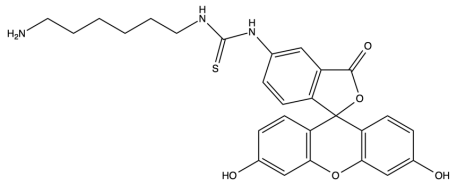 FITC-HMDA	Dye for *in vitro* and in *vivo* tests with linker (HMDA) for further synthesis.	Silica gel column (normal phase), ethanol.	Reaction in THF, 48h, 30°C. Yield: 48%.
		C18-E Phenomenex cartridge (500 mg/6 mL), ethanol.	Reaction in $NaHCO_3$-Na_2CO_3 buffer 0.1 M, pH 9, 24h, 30°C.[58] Yield: 72% (Best alternative, higher solubility). Photosensitive, thermosensitive. Precipitates at T<20°C with ethanol.
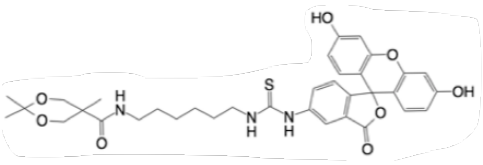 FITC-HMDA-BMPAP	Dendron for *in vitro* and *in vivo* tests with linker (HMDA) for further synthesis.	Normal phase silica gel column, hexane: ethanol 1:1	Slow reaction in DMF (72 h). Yield: 42 %
		Phenomenex C18-E cartridge, Sephadex, $NaHCO_3$-Na_2CO_3 buffer 0.1 M, pH 9	The reaction was favored and completed by doing a previous synthesis of BMPA with oxalyl chloride and an immediate addition of FITC-HMDA. High viscosity of product.
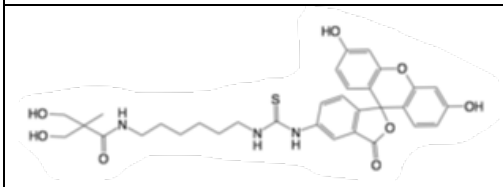 FITC-HMDA-BMPA (Deprotection of OH)	Dendron for *in vitro* and *in vivo* tests with linker (HMDA) for further synthesis.	Filtration of DOWEX resin, methanol.	Best yield with DOWEX resin 82%. 24 h, 30°C.
Pristimerin succinate modification (drug)			
Compound	**Application**	**Purification**	**Observations**
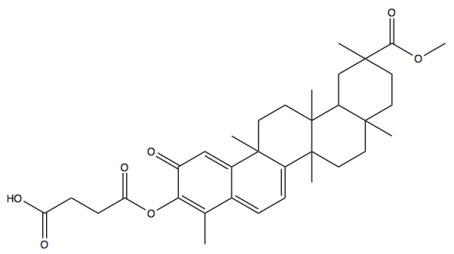 Pristimerin succinate	Cancer drug model.	Normal phase silica gel column, hexane:acetone 7:3. Rf: 0.4	Photosensitive, thermosensitive, hydrophobic. 24 h reaction Yield: 75%

4.1 General synthesis products

In this section, we discuss the results of the synthesis of common compounds used in multiple syntheses, for their application as branching molecules or nucleus.

Characterization of compound 1: EB-AS

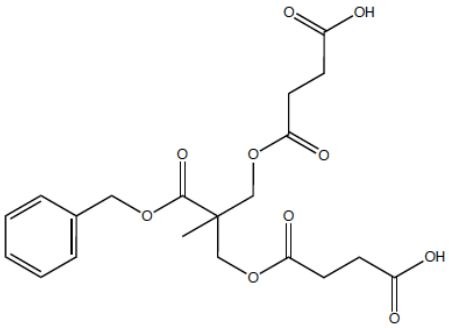

Figure 24. Molecular structure of EB-AS.
Molecular formula: $C_{20}H_{24}O_{10}$ Exact mass: 424.137

EB-AS (Figure 24), also identified as compound 1 in Figures 18 and 20, is commonly used as a branching molecule. It was obtained as clear oil, with high viscosity (yield 90%). Bromocresol green test was positive for carboxylic acids, giving us a general idea that the change in functional groups from terminal hydroxyl to carboxyl, occurred. The structure was confirmed by the analysis of functional groups by FT-IR (Figure 25). The spectrum shows a band of methylene and a carbonyl group, corresponding to esters.

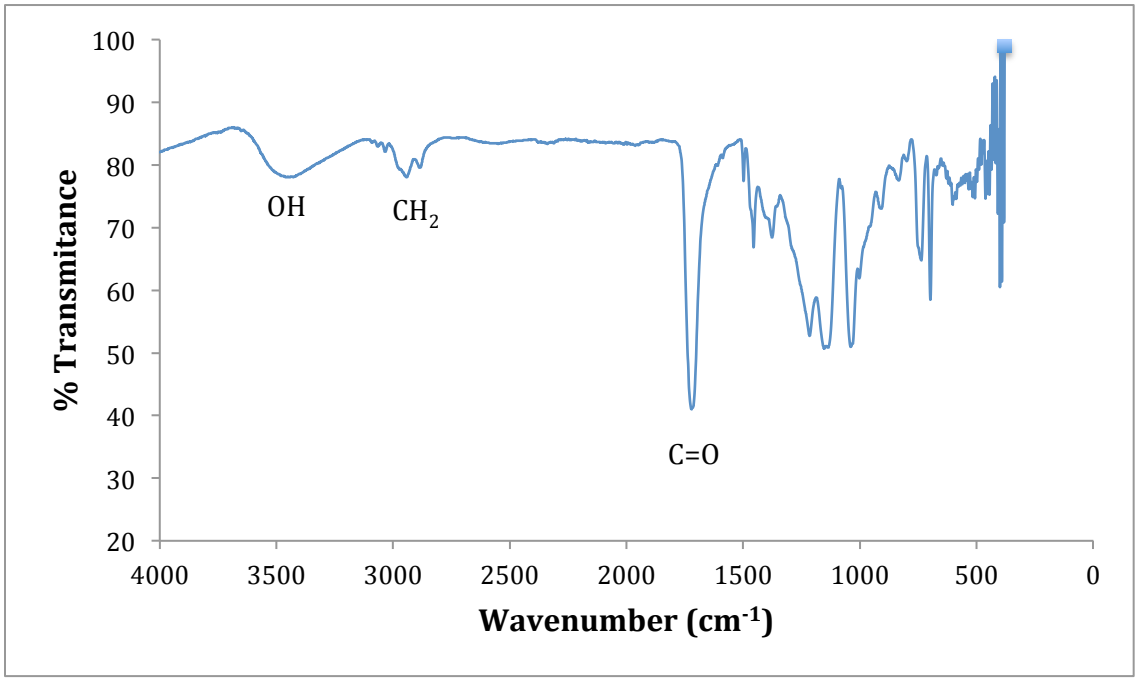

Figure 25. FT-IR of benzyl ester of bis-MPA succinylate (EB-AS).

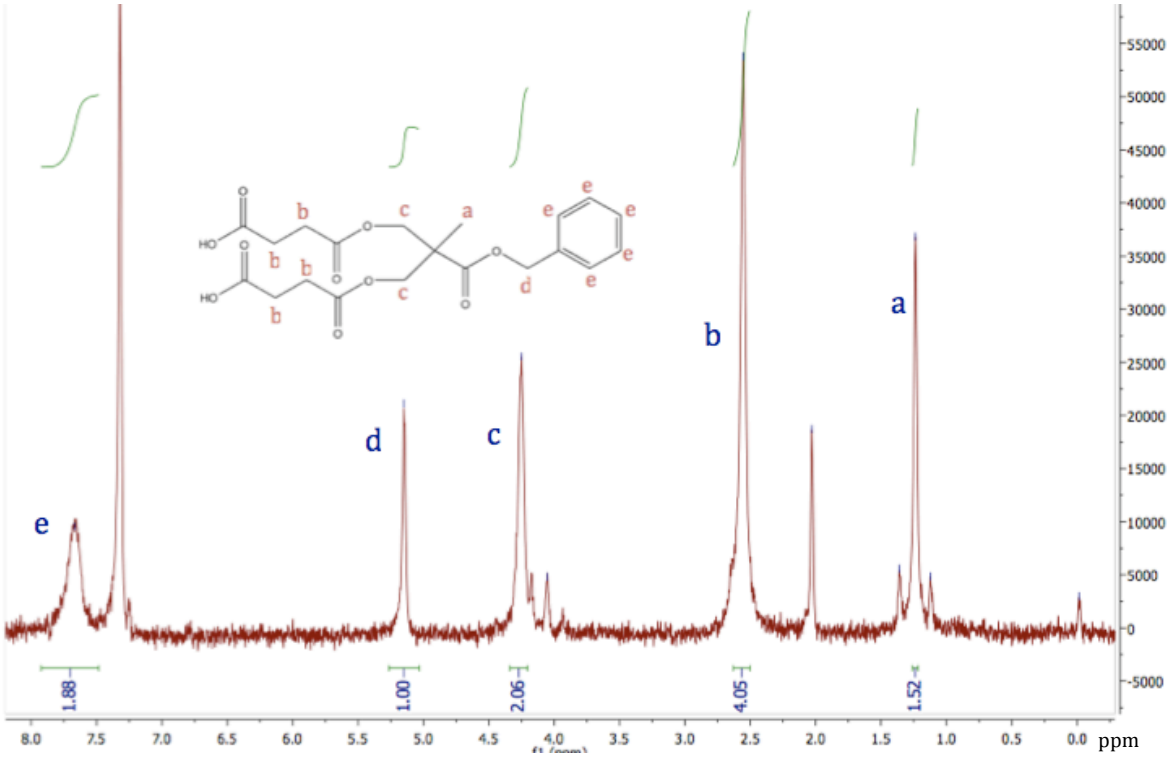

Figure 26. ^{1}H NMR of benzyl ester of bis-MPA succinylate (EB-AS).

Also, the chemical structure was confirmed by ^{1}H NMR. Figure 26 shows the characteristic signals for the compound, the benzyl part always appear as a set of two signals, one in the aromatics region (7-8 ppm) and the benzylic methylene at 5.2 ppm. All benzyl ester show this set of signals as a fingerprint. The methyl protons from the bis-MPA part of the molecule appear at 1.25 ppm as a singlet, and integrates for the corresponding 3 protons. This signal and the singlet at 4.5 ppm are characteristic of the bis-MPA part of the structure integrating for 4 protons. Finally, the signal at 2.6 ppm integrates for all protons of the succinic part of the molecule.

4.2 PEGylated compounds

This section describes the characterization and results from the synthesis of PEGylated compounds, such as C1-PEG3350, its deprotection, and its synthesis with folic acid (FA-PEG3350-C1).

A dendron with EB-AS and two arms with PEG 3350 (C1-PEG 3350), also named as “Compound 2” in the synthesis from Figure 17 and Figure 19, was verified by MALDI-TOF-MS. Since PEG 3350 presents polydispersity, the mass was reported as an average.

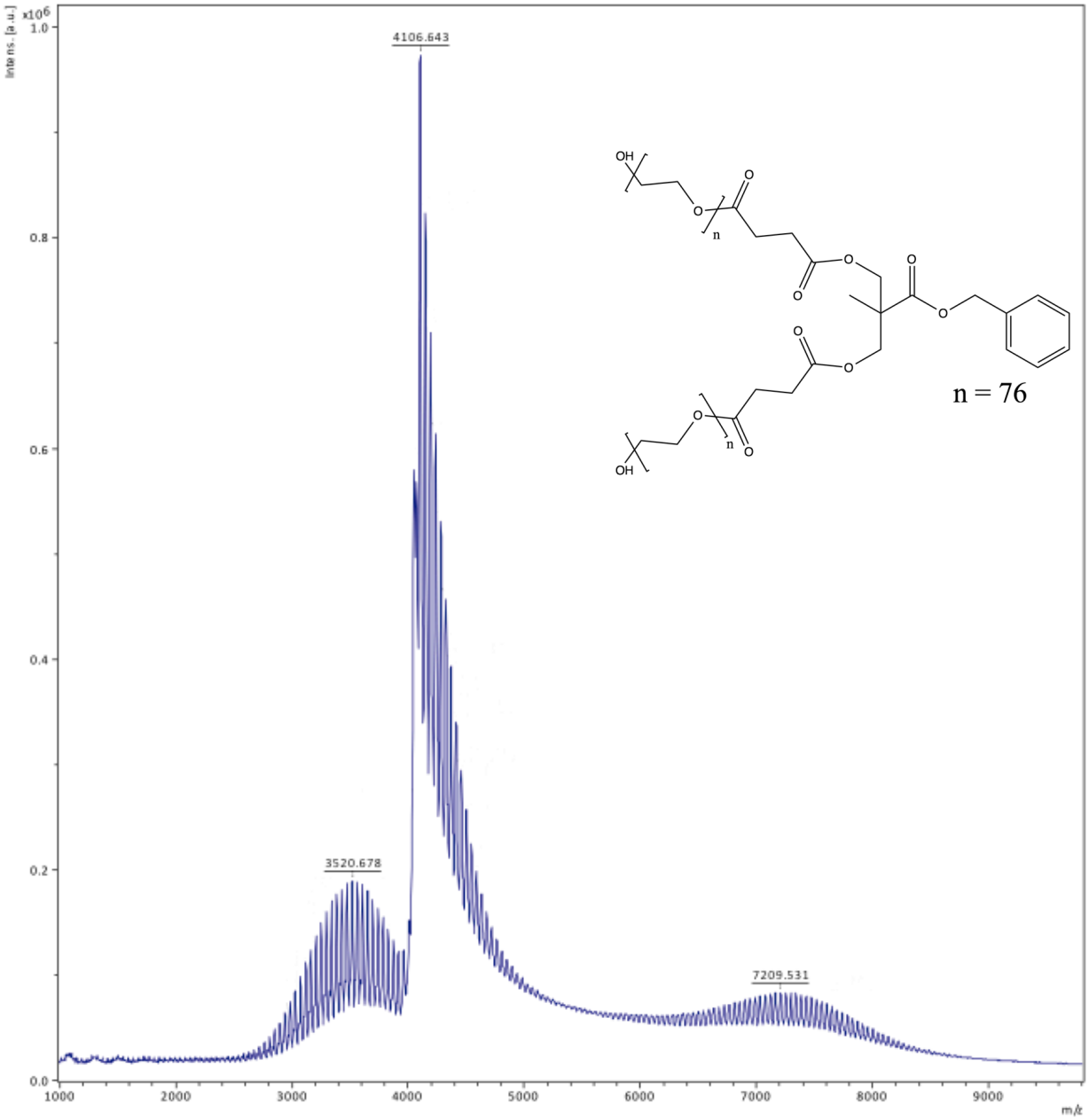

Figure 27. MALDI-TOF-MS of C1-PEG 3350. Purified by Flash chromatography, silica gel. Average MF: $HO(C_2H_4O)nC_{20}H_{23}O_9$. Mn: 6,573 – 7,423 Average Mn: 7,092.40

According to the provider (Sigma-Aldrich), PEG 3350 mass is in a range of 3,421 – 4,091. The spectrum (Figure 27) shows the presence of free PEG 3350 as a typical bell-shaped distribution for polymers centered around 3500-3600 m/z showing a difference of approximately 200 mass units form the nominal value of 3350. If we consider such difference value for the mass quantification of the complete dendron, then we would have a theoretical value of average Mn of 7300 m/z, which is the approximate average of the right distribution in the graph confirming the structure. Also we detected a mass of 4,106 m/z that corresponds to the dendron with only one PEGylated arm with its average molecular weight determination affected by the

overlapping with the free PEG distribution. The addition of free PEG and the other product of ionization give the complete mass of the desired dendron. This behavior is proper of PEGylated compounds. The presence of the corresponding fragments from the whole dendron in the MALDI-TOF experiment is possible because of the breakdown of the molecule due to the laser energy used as an ionization promoter.

An additional synthesis approach was done, considering a relation 1:1 of PEG and compound 1. Also, according to literature, one unit of folic acid is enough to allow dendrimer-receptor binding.[63] Therefore, we considered that PEG would bind to one dendron arm. This case applies to deprotected C1-PEG 3350 and FA-PEG3350-C1 (Figure 28).

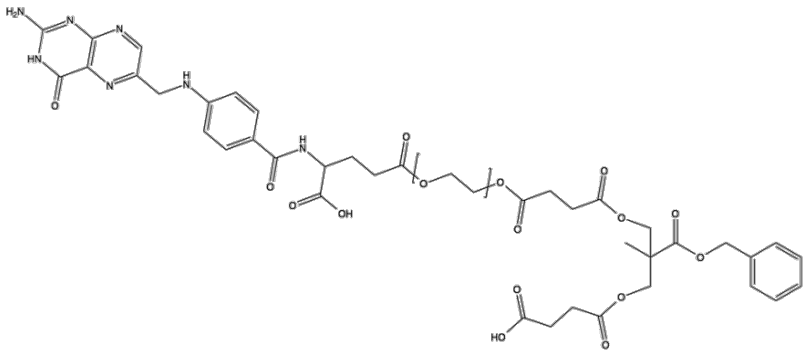

Figure 28. Molecular structure of FA-PEG 3350-C1.

Interpretation of the MALDI mass spectra was again complicated by the polydisperse nature of PEG. The structural difference between each PEGylated compounds reported in this work was very small. Therefore, it is difficult to determine the purity of the compounds. Compound C1-PEG 3350 (Figure 27) was purified by Flash chromatography (silica gel, normal phase); deprotected-C1-PEG 3350 was purified by ultrafiltration; and FA-PEG3350-C1 (Figure 28) by dialysis cassettes. The purification of these compounds by ultrafiltration and dialysis cassettes, apparently led to the removal of free PEG. Meanwhile, using Flash chromatography or manual column chromatography (silica gel) allows us to observe the presence of free PEG in the sample (Figure 27). Additional measurements are recommended; a comparison with a MALDI spectrum of PEG 3350, experimentally used in our synthesis, would be useful as starting point for the elucidation of the other PEGylated structures.

In addition, even though multiple attempts were made for the characterization of PEGylated dendrons by NMR, this method provide vague data regarding their purity. For example, if flaws exist that truncate one or more of the expected branching points, this will yield a polymer with a different number of attachment points and, therefore, different biophysical properties. Additionally, in NMR, the multiplicity makes it difficult to confirm the structural purity. Neither GPC nor NMR provide enough structural information to determine the purity of the compounds due to the methods lack of sensitivity to the subtle changes in overall molecular structure, and the possibility of a low percentage of incomplete reactions or byproducts.[64]

4.3 Compounds with TEG

In order to have a good control over all the synthetic pathway of the dendrons and dendrimers proposed, we evaluated the use of TEG instead of PEG 3350 in the synthesis.

C1-TEG was confirmed by MALDI-TOF-MS (Figure 29).

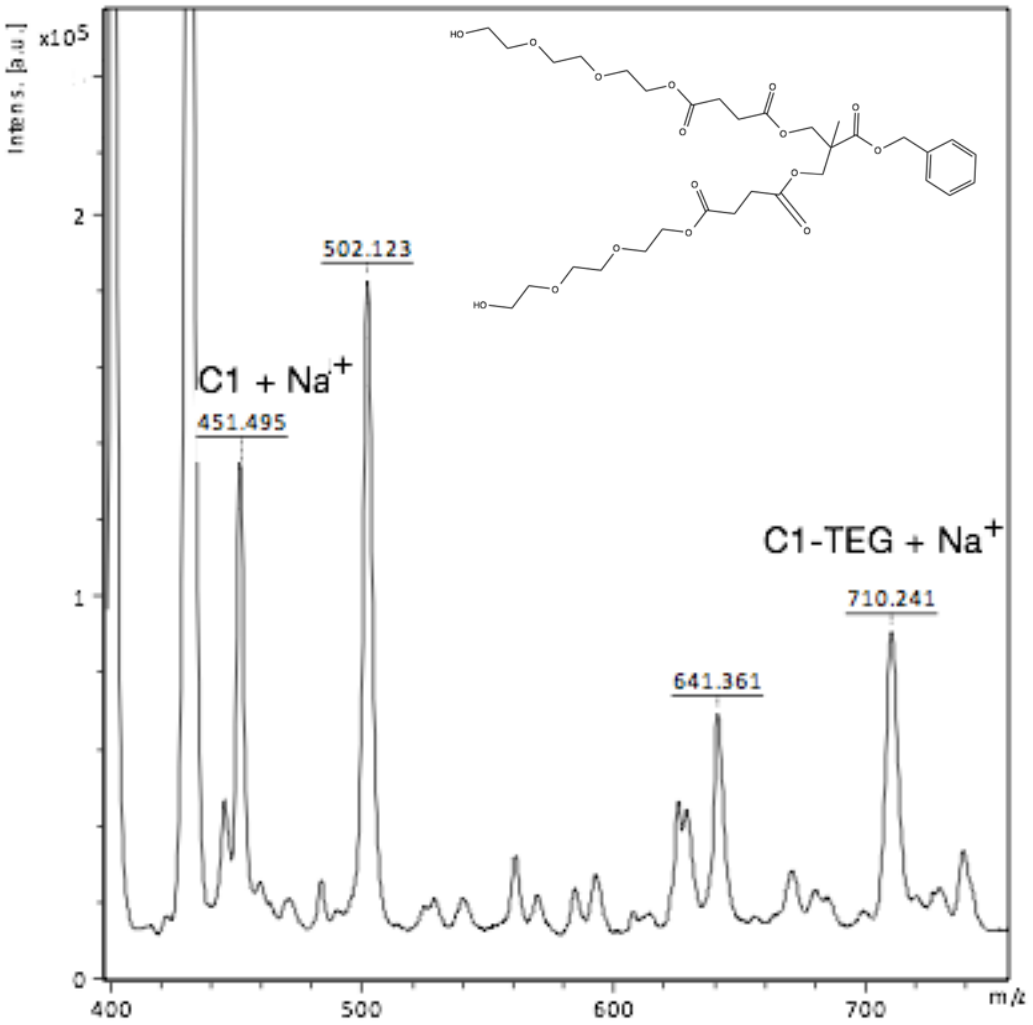

Figure 29. MALDI-TOF-MS of C1-TEG. MF: $C_{32}H_{48}O_{16}$. Exact mass: 688.294

Several modifications of triethylene glycol were done for linking purposes: NH_2-TEG-NH_2, NH_2-TEG-OH, and NH_2-TEG-DHP (dihydropyran) (Figure 30), all of them using benzyl sulfonyl chloride and ammonium. Over all, the most suitable linker was TEG-diamine, due to its simple preparation and characterization.

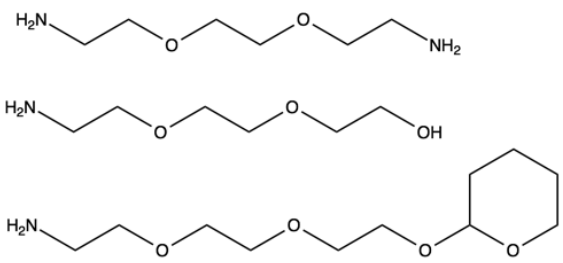

Figure 30. TEG modifications: NH_2-TEG-NH_2, NH_2-TEG-OH , and NH_2-TEG-DHP, respectively.

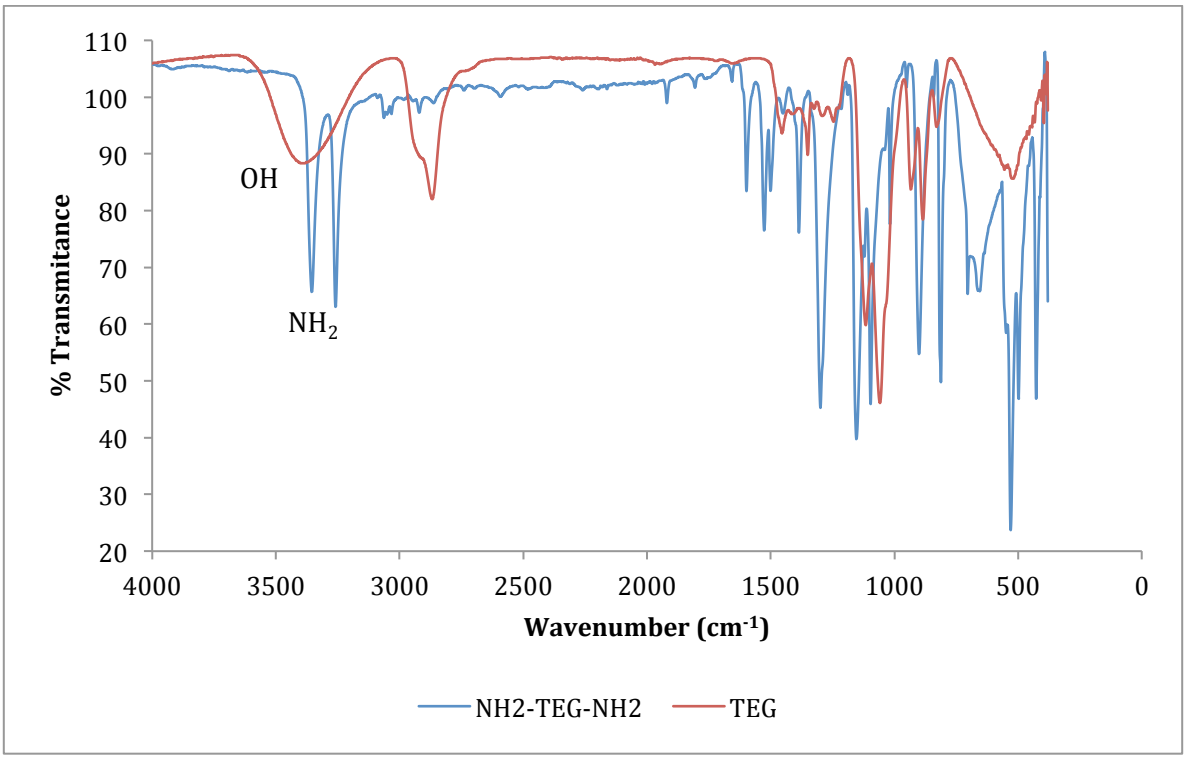

Figure 31. Comparison between FT-IR spectra of diamino triethylene glycol (NH_2-TEG-NH_2) and triethylene glycol (TEG).

Diamino triethylene glycol characterization was done by FT-IR (Figure 31). A comparison between NH_2-TEG-NH_2 and TEG spectra shows the presence of the amine group (sharp signals around 3300 cm^{-1}) characteristic of NH_2-TEG-NH_2, instead of the wide band on the same region, characteristic of hydroxyl groups from TEG. This compound is frequently used as a linker on dendrimers. One of the amino groups from Diamino-TEG can be protected with FMOC (as explained in methodology, section E.9).

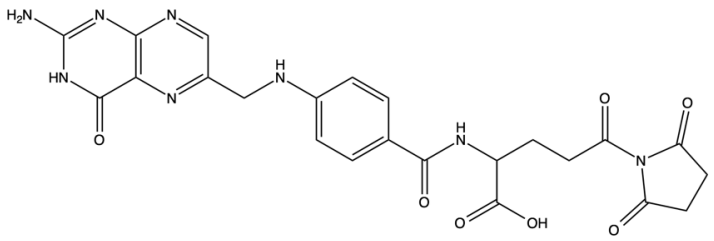

Figure 32. Molecular structure of FA-NHS
Molecular formula: $C_{23}H_{22}N_8O_7$. Exact mass: 522.161

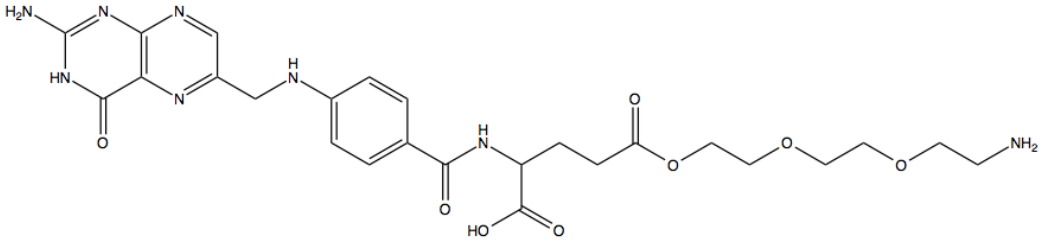

Figure 33. Molecular structure of FA-TEG-NH_2.
Molecular formula: $C_{25}H_{32}N_8O_8$. Exact mass: 572.234

Several attempts were done for the conjugation of folic acid. At first, folic acid was directly conjugated through its carboxyl group to PEG 3350 (e.g. FA-PEG 3350-C1). However, since folic acid has two carboxyl groups, in order to couple only one molecule either of PEG-NH_2 or TEG-NH_2 to one folic acid, care must be taken to activate only one ester group per folic acid molecule prior to coupling. Thus, complete solubilization of the folic acid was imperative prior to the addition of 1 eq. of the coupling reagents (NHS and DCC). Also, folic acid suffers from low solubility in most organic solvents, being only completely soluble in DMSO, followed by DMF. It was decided to work with DMF, since it was more easily removed from the product than DMSO. Unfortunately, when the coupling reaction was carried out either in DMSO and even in DMF, it was very difficult to isolate the product from the reaction mixture. Thus, we decided to separate the ester activation and the coupling step, and we first prepared and isolated the N-hydroxysuccinimide activated FA derivative (Figure 32), which precipitated readily from DMSO and DMF solvents, when a mixture of acetone/ether mixture was added. The activated ester was immediately reacted with a pyridine solution of the amine (TEG-diamine, PEG-diamine, monoprotected PEG-diamine, or monoprotected TEG-diamine).[61] In this case, we did a synthesis of FA-NHS and TEG-diamine (unprotected) 1:1 to directly obtain the FA-TEG-NH_2 (Figure 33), without the protection and deprotection steps with FMOC. The excess of unreacted FA was removed by column chromatography with Sephadex G-15 or Sephadex G-50, according to the molecular weight of the linker. An alternative for purification is gel permeation chromatography (GPC).

In general, the purification of compounds with TEG is complicated. TEG does not favor solubility of the compounds like PEG 3350, especially when it was linked to folic acid.

For example, FA-TEG-NH_2 was purified by Sephadex G-15 and 100 mM $NaHCO_3$ as eluent.[61] However, the product (originally solid) was retained inside of the column, making its purification more difficult. Therefore, a previous centrifugation step (8,000 rpm, 20°C, 20 min) was carried out to separate the solution from the precipitated product. This process was repeated until no visual coloration was observed in the solution. The decanted sample was then added to the column, facilitating the purification, although, this was a time-consuming process. Once the solvent was removed, the product was obtained as yellow leaflets. The sample preparation for NMR analysis was complicated due to its poor solubility even in DMSO-d6.

4.4 Compounds with FITC

The synthesis of FITC-HMDA, its synthesis with BMPAP (FITC-HMDA-BMPAP) and its deprotection (FITC-HMDA-BMPA), are discussed in this section.

The best method to obtain FITC-HMDA (Figure 34) was by using $NaHCO_3$-Na_2CO_3 buffer 0.1 M, pH 9, as reported in another publication[58], instead of using THF as we used to. The product was obtained from the reaction of FITC dye and HMDA linker, as an orange waxy solid. Also, buffer pH 9 decreased by half the time of reaction (24 h) increasing the solubility of the product. Even though we based the synthesis in a published work, this was the first time to report the characterization of FITC-HMDA by FT-IR. A comparison between FT-IR spectra of FITC against FITC-HMDA (Figure 35) showed the presence of the primary amine group (3250 cm^{-1}) of FITC-HMDA, which was not present in the spectrum of free FITC; and the absence of thiocarbonyl group from FITC structure (Table 4). Which indicates that the HMDA was successfully bound to FITC.

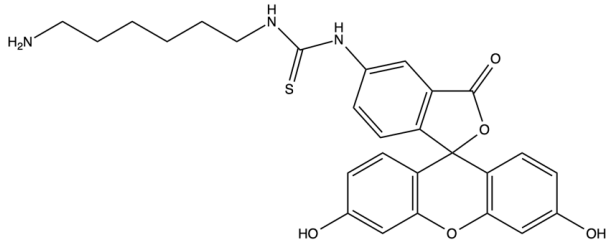

Figure 34. Molecular structure of Compound 5: FITC-HMDA
Molecular formula: $C_{27}H_{27}N_3O_5S$. Exact mass: 505.167

Table 4. Comparison of main signals from FT-IR of FITC and FITC-HMDA.

Compound	*v* (cm^{-1})	Functional group
FITC	1106	C=S
FITC-HMDA	2850-2940 3250	CH_2 NH_2 (amina)

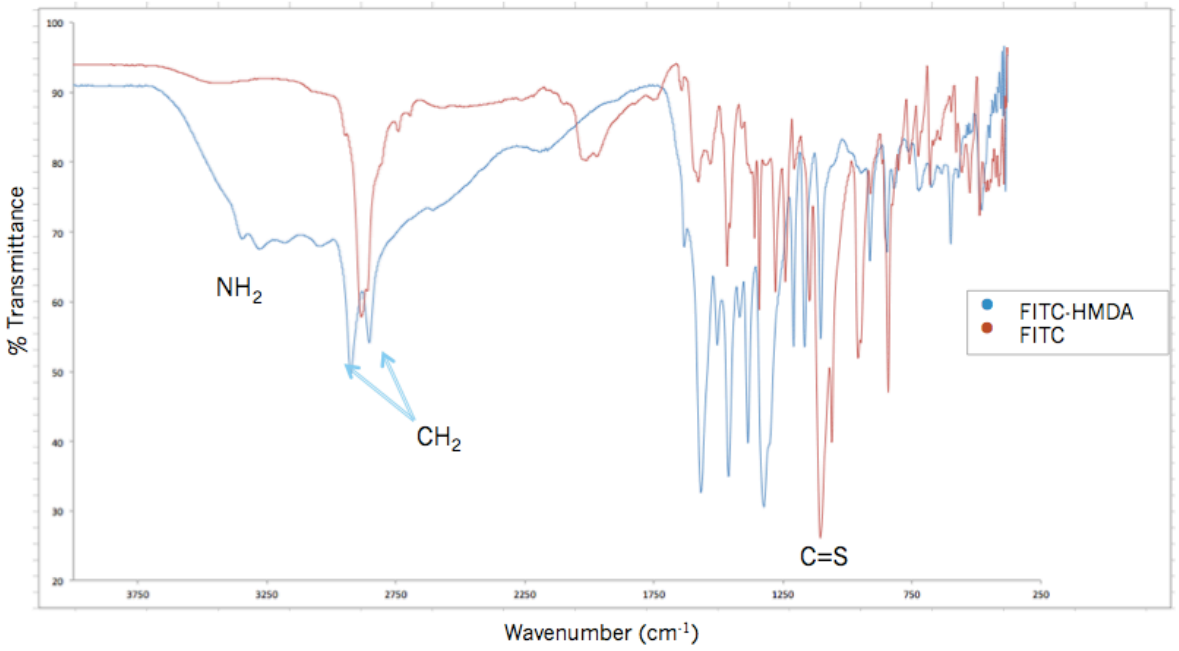

Figure 35. FT-IR of FITC-HMDA. Comparison between free FITC and the compound.

Two methods were used to obtain FITC-HMDA-BMPAP. The first one consists in the reaction of FITC-HMDA with bis-MPA with the hydroxyls protected with an acetonide (BMPAP).[42] However, the NMR spectrum was very different to the prediction. Therefore, a second method was proposed consisting in two immediate reactions: a) the formation of oxalyl chloride (instead of using BMPAP directly), and b) its coupling with FITC-HMDA. The second method is more recommended.

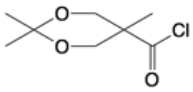

Figure 36. Molecular structure of BMPAP-Oxalyl chloride

The oxalyl chloride of bis-MPA with hydroxyl groups protected with an acetonide (Figure 36) was immediately used in the next reaction with FITC-HMDA due its high reactivity with humidity. Hence, no characterization was necessary.

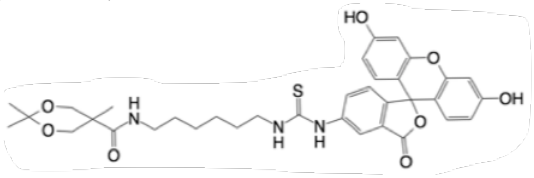

Figure 37. Molecular structure of FITC-HMDA-BMPAP

FITC-HMDA-BMPAP (Figure 37) obtained by the second method (using oxalyl chloride) was confirmed by FT-IR (Figure 38) and MALDI-TOF-MS (Figure 39). A comparison with FITC-HMDA FT-IR was done, where the change in functional groups could not be easily seen, due to the overlapping of the hydroxyl and amine signals around 3300 cm^{-1}. On the other hand, the peculiar shape (a broad rounded signal with

a small double sharp shoulder) observed at 3300 cm^{-1} in the spectrum of FITC-HMDA-BMPAP can be attributed to an amide.

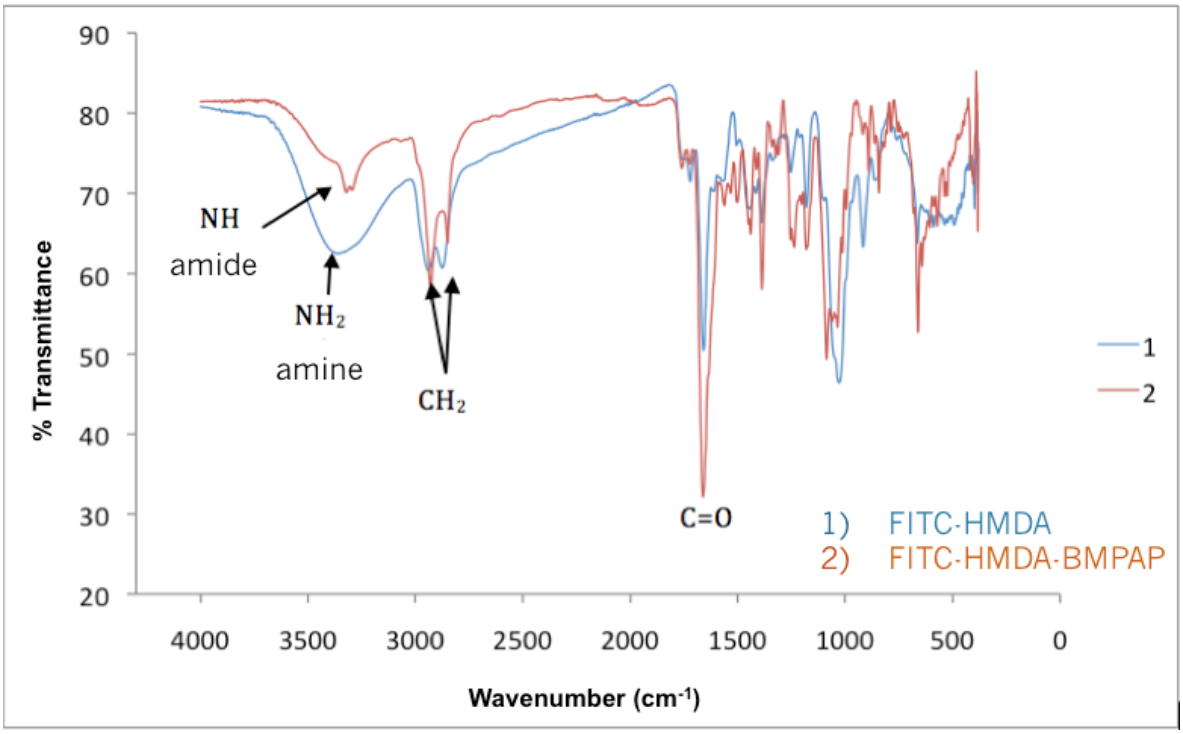

Figure 38. FT-IR of FITC-HMDA-BMPAP compared to FITC-HMDA. 1) FITC-HMDA. 2) FITC-HMDA-BMPAP.

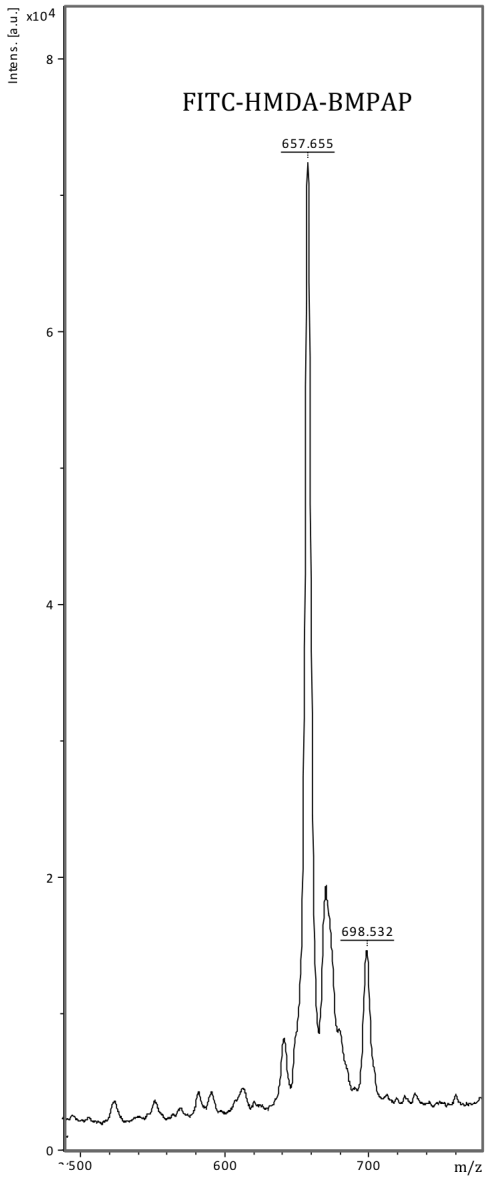

Figure 39. MALDI-TOF-MS of FITC-HMDA-BMPAP. MF: $C_{35}H_{39}N_3O_8S$ Exact mass: 661.246

FITC-HMDA-BMPAP was confirmed by MALDI-TOF-MS (mass 657). The difference in mass can be attributed to the deprotonation of hydroxyl and amino groups. Peaks with highest intensity are attributed to the sodium ion adducts [M + Na^+]. The cationization by sodium is due to arbitrary sodium impurities in the samples, frequently present by this type of analysis.[65] As a result, an adduct with Na^+ was shown at mass 698.

The deprotection of the acetonide group of BMPAP (Figure 40), from FITC-HMDA-BMPAP structure, was confirmed by FT-IR (Figure 41). Where we can observe the presence of hydroxyls in the spectrum of FITC-HMDA-BMPA in comparison with the spectrum of FITC-HMDA-BMPAP that is protected by acetonide, showing only an amine signal.

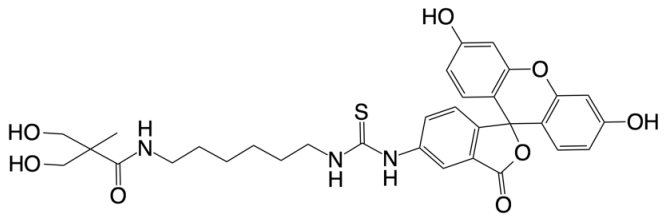

Figure 40. Molecular structure of FITC-HMDA-BMPA
Molecular formula: $C_{32}H_{135}N_3O_8S$ Exact mass: 621.214

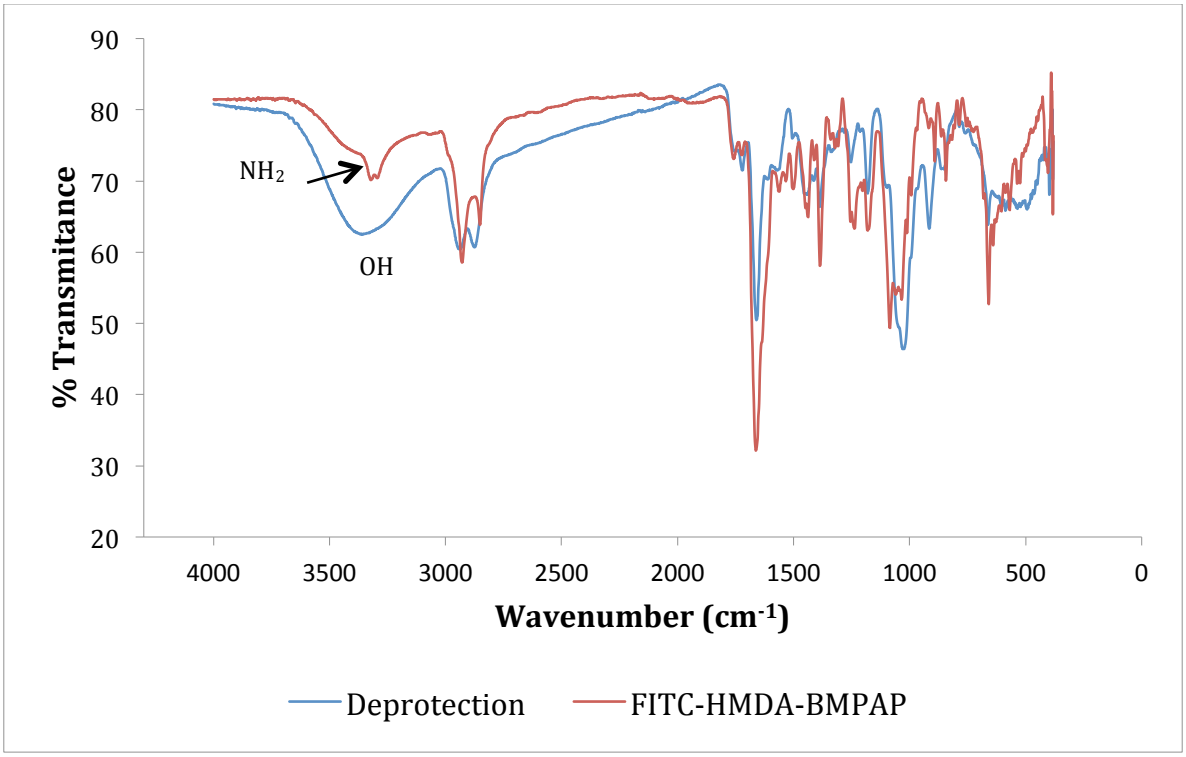

Figure 41. FT-IR comparison between FITC-HMDA-BMPAP and the deprotection of its hydroxyl groups (FITC-HMDA-BMPA)

In general, compounds with FITC were difficult to dissolve and purify. Increasing the amount of FITC, a continuous decrease in dendrons or dendrimers solubiity occurrs. The use of pH buffer has a fundamental role on precipitation.[66] Using buffer $NaHCO_3$-Na_2CO_3 (0.1 M, pH 9), helped reduce signficantly precipitation in comparison to using THF as solvent during the reaction. Several methods of purification were tried including ultrafiltration and dialysis cassettes. But the most effective method was alternating centrifugation of the sample with buffer pH 9, then decanting and passing the decantation liquid to a Sephadex G-15 column, and repeating the same procedure until a clear solution was observed. However, since a lot of steps and sample manipulation were involved, the yield decreased significantly. Also, in order to prepare the samples for characterization, the solvent had to be removed and make a change (e.g. for NMR, deuterated solvent), and once the product was dried, it was very difficult to dissolve again. Low solubilization in ethanol, methanol, acetone, water, even DMF and DMSO was observed for FITC-HMDA and FITC-HMDA-BMPAP, which

complicated the sample preparation and analysis by NMR, HPLC-MS and MALDI-TOF-MS. Sample preparation for characterization takes a long time. In order to enhace solubilization, a sample pre-treatment is needed; which can be by leaving the sample in dissolution under stirring during two to three days. Then, ultrasonicate it for 1 h at 40°C (low temperature led to precipitation) and/or vortexing it to help dissolve it completely. A filtration step should be carried out to avoid interferences in the analysis.

4.5. Pristimerin succinate modification

Pristimerin and other drugs with a terminal hydroxyl can be modified with succinic anhydride, DMAP, and pyridine, to obtain a carboxyl terminal that can be used in multiple synthesis (Figure 42). Pristimerin succinate was analyzed by MALDI-TOF-MS (Figure 43) (mass 569.9). The difference with the experimental mass could be attributed to protonation in the succinate part of the molecule.

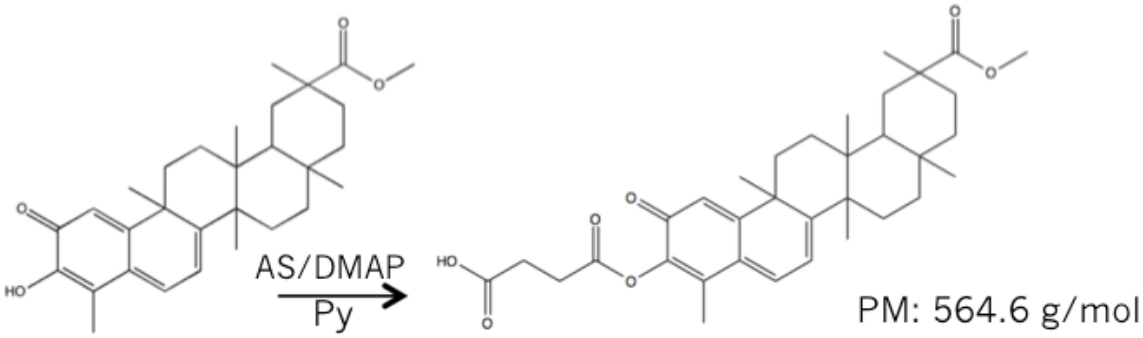

Figure 42. Chemical modification of pristimerin hydroxyl to a carboxyl group: (Pristimerin-COOH).

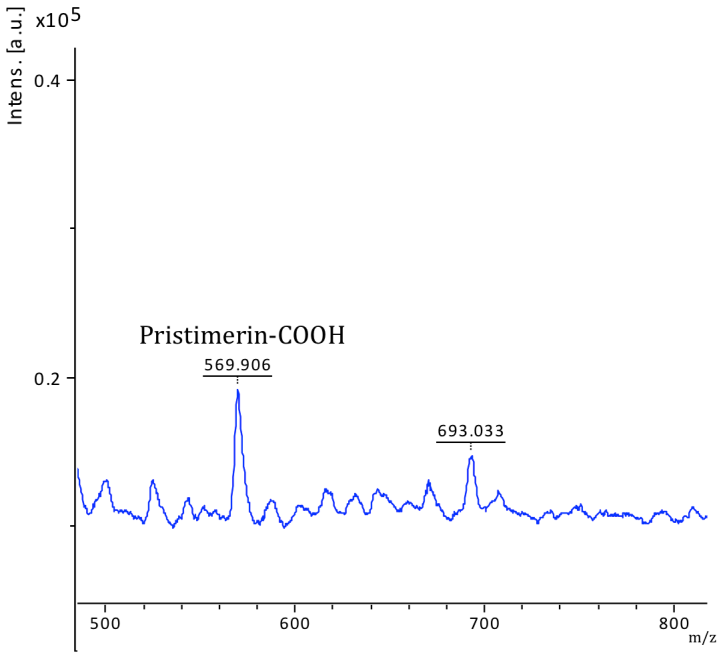

Figure 43. MALDI-TOF-MS of Pristimerin-COOH. MF: $C_{34}H_{44}O_7$. Exact mass: 564.6

5. Conclusions and recommendations

- In this work, we show the synthesis, purification strategies, and characterization of several compounds that are key building blocks for the synthesis of site-specific dendrimers. They are the most important molecules in the synthetic pathway because the dendritic architecture comes from their condensation in the next steps. In this way, this work is contributing to the advancement in the obtention of the final conjugates.
- EB-AS was obtained as an alternative for branching molecules with a broad application in the synthesis of polyester dendrimers, and its synthesis is simple, its yield is high (80%) and highly soluble in organic solvents like DCM.
- The synthesis of C1-PEG3350 was done with a yield of 72%. The compound was confirmed by MALDI-TOF-MS, with a spectrum very characteristic of PEGylated compounds.
- C1-PEG3350, in combination with poorly-soluble folic acid, helped to enhance the solubility of the building block in aqueous solution, methanol and DMF.
- Also, PEG3350-C1 has a potential application as a dendron for multiple applications, since it has two arms with two free carboxylic groups that can be used in combination with other drugs and a benzyl group protecting its other carboxyl, which can be deprotected when needed by hydrogenation, for its application as a dendrimer building block.
- Ultrafiltration (5 kDa) in aqueous solution was a faster and more efficient purification method for PEGylated compounds (C1-PEG3350,, yield 82%) than column chromatography with silica gel (yield 43%).
- The syntheses of FITC building blocks, FITC-HMDA, FITC-HMDA-BMPAP were done.
- Folic acid building blocks (FA-PEG3350-C1 and FA-TEG-NH_2, showed higher purification yields when using dialysis cassettes (7 kDa) and PBS buffer, in comparison to SEC with Sephadex in $NaHCO_3$, or ultrafiltration (5 kDa) in water.
- Column chromatography with silica gel represented a good alternative for simple purifications of low molecular weight compounds, such as EB-AS, CI-TEG and pristimerin succinate, that were soluble in inorganic compounds (hexane: ethyl acetate 1:5, ethanol:DCM 1:2, and hexane:acetone 7:3, respectively), since there is no risk of damaging a dialysis membrane, is a cost effective method and purification yields were above 72%.
- FITC building blocks (FITC-HMDA, FITC-HMDA-BMPAP, and FITC-HMDA-BMPA) were more soluble in a buffer solution $NaHCO_3$-Na_2CO_3 (0.1 M, pH 9) and Phenomenex C18-E cartridge was a faster purification method than silica gel columns.
- C1-TEG dendron was obtained by a simple and faster synthesis (24 h) than C1-PEG3350 (48 h). Thus, C1-TEG does not help to enhance the solubility of other compounds (e.g. in combination with folic acid, FA-TEG-C1), in contrary of CI-PEG3350 that can help increase the solubility of poorly-soluble compounds like folic acid (FA-PEG3350-C1). Therefore, C1-PEG3350 can be synthesized with

poorly-soluble compounds and C1-TEG can also be used as a dendron but with other compounds of similar solubility.

- Therefore, PEG3350 is a better linker of folic acid than TEG., due its solubility.

The availability of folic acid residue to interact with its corresponding receptor at a cellular level, has been a discussion topic in academia and research groups for several years. Therefore, a theoretical study about the ligand-receptor binding functionality of dendrimers is described in Chapter 2, and it represents a very pertinent contribution for the clarification of this topic.

CHAPTER 2

Structural analysis of binding functionality of folic acid-PEG dendrimers against folate receptor

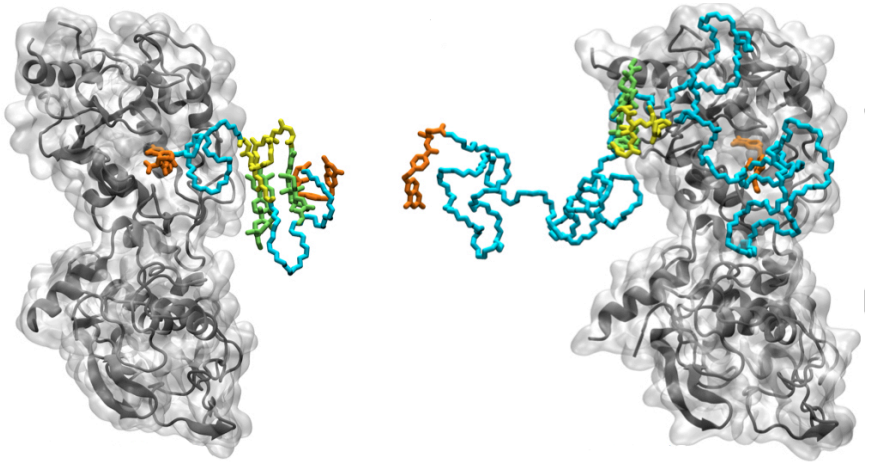

CHAPTER 2. Structural analysis of binding functionality of folic acid-PEG dendrimers against folate receptor

Diana Sampogna-Mireles, Ingrid D. Araya-Durán, Valeria Márquez-Miranda, Jesús A. Valencia-Gallegos, Fernando D. González-Nilo*

Published in: ***Journal of Molecular Graphics and Modelling*** (2017)

Abstract

Dendrimers functionalized with folic acid (FA) are drug delivery systems that can selectively target cancer cells with folate receptors (FR-α) overexpression. Incorporation of polyethylene glycol (PEG) can enhance dendrimers solubility and pharmacokinetics, but ligand-receptor binding must not be affected. In this work we characterized, at atomic level, ligand-receptor binding functionality of conventional site-specific dendrimers conjugated with FA with PEG 750 or PEG 3350 as a linker. After Molecular Dynamics simulation, we observed that both PEGs did not interfere over ligand-receptor binding functionality. The folate fragment from both dendrimers remained exposed to the solvent before approaching selectively to FR-α. PEG 3350 provided better solubility and protection from enzymatic degradation to the dendrimer than PEG 750. Also, FA-PEG3350 dendrimer showed a slightly better interaction with FR-α than FA-PEG750 dendrimer. Therefore, theoretical evidence supports that both dendrimers are suitable as drug delivery systems for cancer therapies. However, experimental corroboration is required. The content of this chapter was published in the Journal of Molecular Graphics and Modelling in 2017 (DOI: 10.1016/j.jmgm.2017.01.004).[67]

1. Introduction

Cancer therapies used nowadays lack of selectivity to cancer cells, which leads to diverse secondary effects.[2] As a result, there is a critical need to develop new therapies and drug delivery systems that reduce local and systemic toxicity.[68] Dendrimers are well known carriers that have been used as drug delivery systems.[69] Polyamidoamine (PAMAM) dendrimers have been widely studied for biomedical applications.[10] However, they have potential toxicological effects, especially at higher generations (≥G7).[70,71] Therefore, a more favorable strategy consists in the use of dendrimers based on polyester units, like biodegradable 2,2-bis(hydroxymethyl)propionic acid (bis-MPA), due it can help reduce cytotoxicity, shows very good biocompatibility and can be easily prepared in large quantities.[72–76]

In addition, dendrimers can selectively target cancer cells incorporating folic acid on their surface and reducing, as a result, normal cells toxicity and secondary effects in comparison with free drug.[23,25,27] Folic acid is stable, inexpensive, and non-immunogenic compared with monoclonal antibodies, has a very high affinity for its cell-surface receptor (K_d ~1 nM) and it moves into the cell cytoplasm, which favors an

efficient intracellular delivery of anticancer agents.[77] Although expressed at very low levels in most tissues, folate receptors, especially FR-α, are overexpressed in numerous cancers such as nasopharyngeal epidermoid carcinoma, cervical, uterine, endometrial, renal, and pancreatic carcinoma.[78] Although folic acid-conjugated dendrimers can present low water solubility,[79] this problem can be overcome by the incorporation of polyethylene glycol (PEG) to the drug delivery system. In addition, PEG can also increase lifetime in bloodstream, drug loading capacity, improves kinetic stability, reduces enzymatic degradation, conjugates aggregation and toxicity, and decreases drug release.[31,69,80–83] Also, it might change hydrophobicity of several compounds, making them hydrophilic.[84] The increase in PEG chain length leads to a decrease of the hydrogen bonding degree and an appreciable growth of molecular mobility and stability.[85,86] Docking analyses indicate that the binding affinity to a receptor depends on PEG chain length and PEGylation site.[87] Folic acid conjugated to PEG linker has been used in biodegradable nanoparticles,[77] on G3 PAMAM dendrimers for boron neutron capture therapy (BNCT)[31] and conjugated with α-cyclodextrin as a siRNA delivery carrier.[88] Also, a FA-PEG degradable amphiphilic dendrimer with a poly(L-lactide) core and six polyester dendrons based on bis-MPA was successfully synthesized to be used as a nanoscale carrier for cancer cell-targeted drug delivery.[89] However, a concern of using PEG as a linker of folic acid ligand in site-specific dendrimers is that it must not affect ligand-receptor binding.[87] Also, FA-PEG complexes may lead to agglomeration due to hydrophobicity of folic acid.[90] Hence, folic acid must remain solvent exposed and capable to bind to their receptors. Kim et al.[91] and Yang et al.,[92] suggested based on experimental observations, the longer PEG chain lengths conjugated to PAMAM dendrimers increases cytotoxicity probably due to the formation of intermolecular aggregates. However, Lee and Larson[93] demonstrated by Molecular Dynamics (MD) that neither short nor long PEG chain lengths (PEG 550 and PEG 5000) induce aggregations of G3 PAMAM-PEG dendrimers (without FA). Although MD and computer simulation are scientific tools that have been exploited during the last 50 years to optimize experimental work by providing valuable insight to analyze and optimize ligand-receptor behavior,[6,94] no MD studies have been reported regarding FA conjugated to PEGylated dendrimers.

With regard to PEG chain lengths, PEG 750 did not improve blood circulation of liposomes,[95,96] but it could be an interesting linker alternative since it has shown reduced cytotoxicity of PAMAM dendrimers[91] and improved solubility of micelles.[92] Additionally, it has been observed that when using PEG of intermediate chain-lengths (e.g. PEG 2000, PEG 3350), leaded to better drug encapsulation, extended blood circulation and a major improvement on target binding of liposomes in comparison to long-chain length PEG (e.g. PEG 5000).[95–97] Therefore, PEG 750 and PEG 3350 are interesting linker alternatives for dendrimers. Meanwhile, additional evidence is required to confirm which PEG chain length is better to incorporate to folate conjugates, but the results depend on the complete drug delivery system.

The aim of this work is to study by full-atom molecular dynamics (MD) ligand-receptor binding functionality of conventional site-specific dendrimers, conjugated with PEG (750 and 3350 Da) as a linker of folic acid ligand; and evaluate their

interaction with folate receptor (FR-α), for the development of future cancer therapies.

2. Theoretical methods

2.1 Dendrimer structure and molecular modeling

The structure proposed is a site-specific polyester dendrimer that consists in an ethylene glycol nucleus, bis-MPA as branching unit, polyethylene glycol spacer (PEG 750 or PEG 3350) to facilitate motility and solubility, folic acid as targeting molecule, and a triterpenoid as an anticancer drug. Although the whole dendrimer structure was considered for calculations, this study is focused on the interaction between the folic acid-PEG (ligand-spacer) part of the dendrimer against folate receptor and the effects of PEG in ligand-receptor binding.

The two molecular models of site specific dendrimers were built according to previous home-made scripts with the only variation of PEG chain lengths (MW: 750 and 3350 Da), using Gaussian View 5.0.9 software for the structure construction, and VMD (Visual Molecular Dynamics 1.9.2) as a molecular visualization tool.[98–102] Figure 1 shows the chemical structure of the dendrimers in two dimensions (2D). Although a specific triterpenoid anticancer molecule was considered for calculations, several drugs can be incorporated to the dendrimer scaffold.

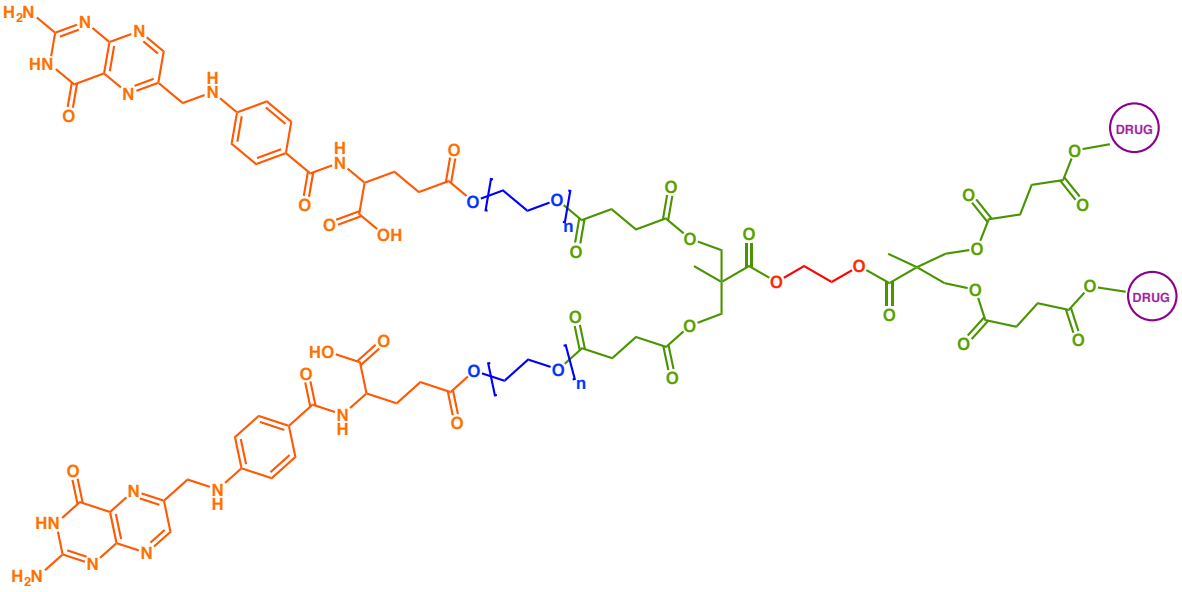

Figure 1. 2D Chemical structure of dendrimer with PEG 750 or PEG 3350. Where orange represents folic acid, PEG is in blue, bis-MPA branching unit in green, ethylene glycol nucleus in red, and the anticancer drug in purple.

Both dendrimer structures were divided into several fragments in order to facilitate the parametrization, calculations and subsequent analysis. The fragments were parameterized using CHARMM General force field (Cgenff)[103] and PARAMCHEM[104] platform generating two dendrimer models.

2.2 Systems preparation and construction

After building the dendrimers, seven molecular systems were placed in TIP3P water boxes,[105] at 300 K, 1 atm, pH 7.0, and 150 nM of NaCl to simulate physiological conditions. Two systems correspond to the dendrimers conjugated with PEG 750 (FA-PEG750) and with PEG 3350 (FA-PEG3350); another two systems correspond to dendrimer-folate receptor complexes with PEG 750 and with PEG 3350; a system consisting of a folic acid molecule in contact with folate receptor complex (FA-FRα); and the receptor (FR-α) alone.

The crystal structure of human folic acid receptor (FR-α) was obtained from Protein Data Bank; PDB ID: 4LRH,[6] and two chains were considered to facilitate calculations. As described by Chen et al.[6] the section of folate receptor, which recognizes folate, is located in a fragment exposed to the extracellular side of the cells. Thus, doing a molecular simulation of the full receptor is not required, since our focus is not the characterization of the folate triggering signal cascade inside cells. Moreover, the folate binding site in the same receptor has been characterized by molecular dynamics simulations in previous studies without considering the membrane-bound section.[106]

The molecular docking was carried out in AutoDock 4.2 software[100] considering as the center of the grid the binding pocket of the folic acid as reported in the crystallographic structure. A 100 x 100 x 100 grid points box and spacing of 0.375 Å was chosen. Folic acid was then docked into the grid to contrast its position against those contained in the crystallographic data. Then, the PEG fragment of each dendrimer was added to the γ-carboxylic group of folic acid to obtain the full 3D structure of the dendrimer.

2.3 Molecular dynamics simulations

All molecular dynamics (MD) simulations were performed using Nanoscale Molecular Dynamics (NAMD) computational package.[107] A constant temperature and constant pressure (NPT) ensemble (isothermal-isobaric ensemble) under periodic boundary conditions (T=300 K; P=1 atm) was considered for all systems.

In a first stage, each dendrimer (only in contact with water) was minimized until reach convergence. For the rest of the systems, a minimization stage was carried out. After that, molecular simulations were performed during 100 ns for FA alone and FR-α alone, and 200 ns for FA-FRα system, FA-PEG750 dendrimer, FA-PEG3350 dendrimer, and for the dendrimers in contact with FR-α.

The folate receptor amino acids considered for visualization purposes correspond to those present between the distance of 2 Å from FR-α protein to folic acid molecule or the folate part of the dendrimers structure, where receptor internalization is most likely to occur.

All of the calculations were obtained from MD trajectory results, for the dendrimers alone and for dendrimer-folate receptor systems with PEG 750 and PEG 3350.

SASA analysis were obtained for the dendrimers alone in water (FA-PEG750) and FA-PEG3350) and in contact with folate receptor FR-α considering 200 ns. Also, SASA of folic acid molecule alone in water, with 100 ns of simulation, was calculated as a reference. Only one folate receptor was considered to facilitate calculations. The results were graphed as percent of SASA against time (ns) of MD trajectory.

The radius of gyration (Rg) was obtained for both dendrimers with PEG 750 and with PEG 3350 in water and ions, and in contact with folate receptor FR-α, in physiological conditions; and it was graphed as a function of the trajectory time (ns). The complete time of simulation for the dendrimers alone and in contact with FR-α was of 200 ns. Also, a mean Rg value was calculated for each system considering the last 50 ns of the simulation, where it remained more stable.

Charge and nature of FR-α aminoacids involved in binding of FA were obtained at 7 Å from FA-PEG750 and FA-PEG3350 dendrimers and from folic acid molecule as comparison, considering the last 30 ns of MD simulation. Also, the frequency of interaction (%) of each FR-α aminoacid for both dendrimers with PEG 750 and PEG 3350 were graphed and classified according to their negative and positive charge, and as hydrophobic or hydrophilic, and were compared with FA crystal in contact with FR-α at the beginning of simulation.

The percentages of contact with folate receptor protein, for each segment of the dendrimers (folic acid, PEG, core, bis-MPA, and pristimerin), were calculated in order to probe that the folic acid ligand part of the dendrimer has greater contact with the receptor.

Also, an analysis of π stacking interactions was done between folate fragment from FA-PEG750 and FA-PEG3350 dendrimers and FR-α aminoacids.

The number of hydrogen bonds between the folate receptor and the folic acid fragment of the dendrimer with PEG 750 and with PEG 3350, and of the complete dendrimers with PEG 750 and with PEG 3350, were monitored through the whole trajectory. Hydrogen bonds occupancy was also obtained for both dendrimers, with PEG 750 and with PEG 3350.

Folic acid self-diffusion coefficients were calculated alone in water, considering the last 4 ns of simulation, and were compared with folic acid dendrimers with PEG 750 and PEG 3350. The data obtained were graphed as mean squared displacements (MSD, nm^2) against time of simulation (ns). Mean values were obtained for each dendrimer and folic acid.

3. Results and discussion

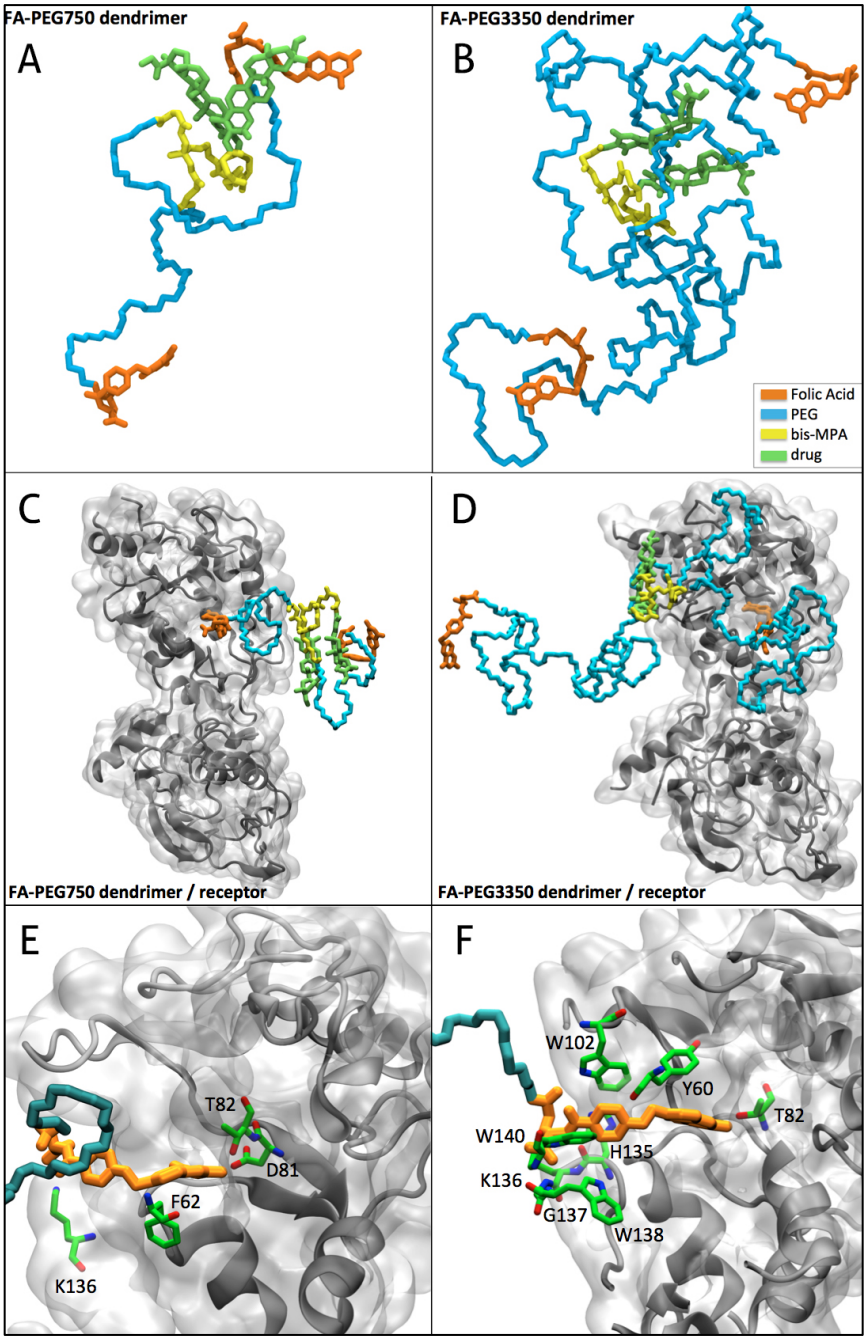

Figure 2. 3D chemical structures of dendrimers with PEG 750 (A) and with PEG 3350 (B) and snapshots of dendrimer-receptor systems with PEG 750 (C) and PEG 3350 (D) at the end of simulation (70 ns) with their zoom (E and F) of the interaction between FA fragment and FR-α. FR-α protein is represented in new cartoon in gray and the dendrimers in sticks. Amino acids at 2 Å of FA are represented in green sticks (E and F).

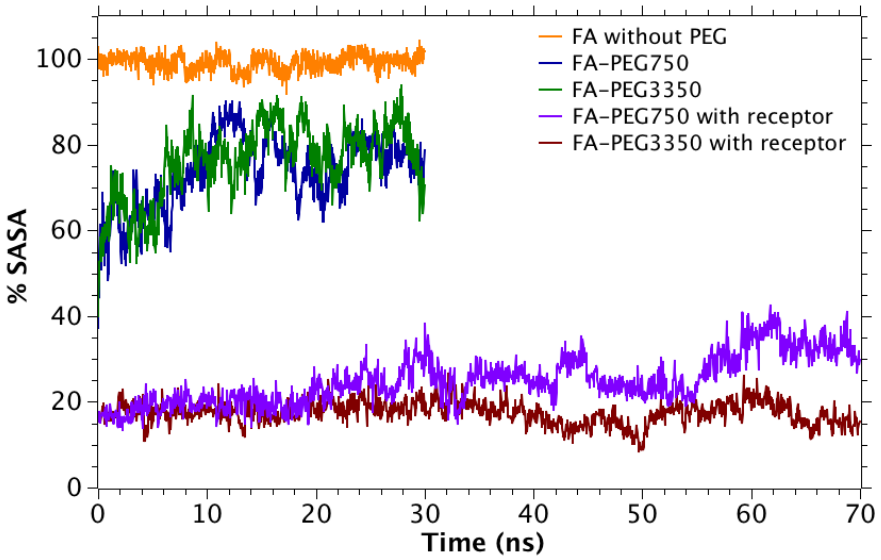

Figure 3. SASA of folic acid (FA) of systems with FA-PEG750 and FA-PEG3350 alone and in contact with FR–α.

3D molecular representations of the dendrimers with PEG 750 and PEG 3350 in contact with water (Figure 2A and B, respectively) and in contact with FR-α (Figure 2C-F), showed that PEG chain remains flexible and provides a steric shielding effect on the rest of the dendrimer, as reported before in other works.[87,108] Therefore, PEG 3350 can provide more solubility and protection from enzymatic degradation to the rest of the dendrimer than PEG 750.[31,84] Also, the dendrimers in contact with water showed that their folic acid fragment remained exposed to the solvent, without being covered by PEG. This observation was also confirmed with SASA results (Figure 3), where both dendrimers in water resulted between 25% and 90% accessible to the solvent, whereas FA molecule was 100% accessible. Therefore, both dendrimers are able to reach the folate receptor. The variation of their SASA values were expected, due the dendrimers alone with water are able to move more freely and are more exposed to the solvent. Thus, the dendrimer with longer chain length (PEG 3350) showed more variation during the trajectory and it behaved with more motility and stretching than the dendrimer with PEG 750. Meanwhile, when both dendrimers were in contact with the folate receptor, they remained more stable than dendrimers alone. Less than 40% of SASA was observed during the whole trajectory of dendrimer-receptor systems. The variation observed between SASA of dendrimers-receptor systems during the first 110 ns of trajectory can be caused by the lack of stability of the dendrimers with the receptor. Once both dendrimer-receptor systems reached stability, no significant difference was observed between FA-PEG750 and FA-PEG3350 dendrimers during the rest of the trajectory. As a result, we can infer that both dendrimers in presence of FR-α were able to strongly interact with the folate receptor during the whole trajectory. Therefore, we can assume that the folate fragment from both dendrimers was protected inside the receptor.

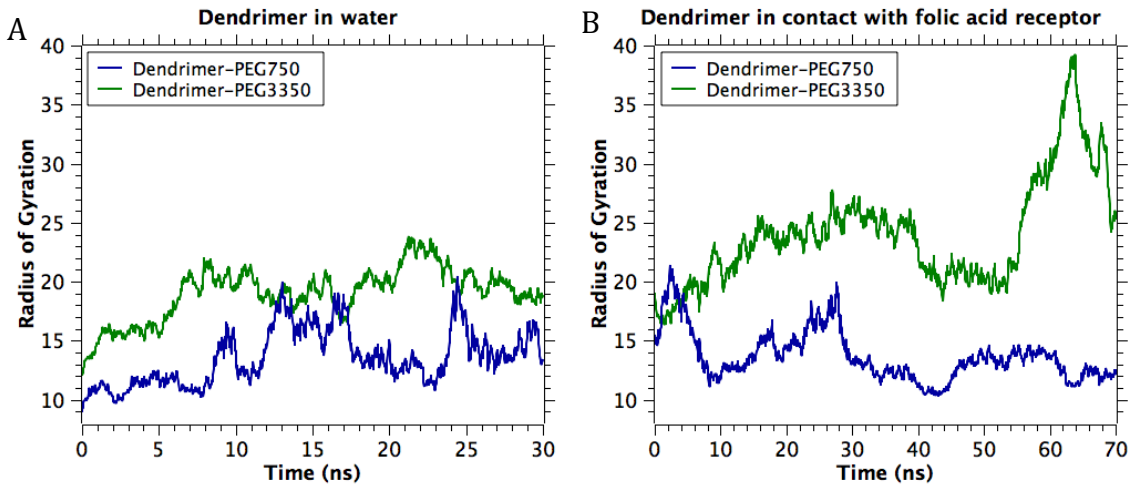

Figure 4. Radius of gyration comparison between dendrimers A) in water, and B) in contact with FR-α.

In addition, these results were in accordance with the single key-lock binding mechanism corroborated by Van Dongen et al. They evaluated the interaction of single and multivalent conjugation of FA in G5-Ac-FAn dendrimers and their binding mechanism to surface FBP (folate binding protein), and corroborated that the mechanism of interaction is 2-fold: an initial, reversible, FA concentration dependent key-lock, tight-binding interaction between the conjugate and protein, followed by irreversible interaction between the dendrimer and protein surfaces. Which means, that even if we have multiple receptors or folate groups in the dendrimer, only one of them will bind and "lock" to a single receptor,[63] but increasing the number of folate units will also increase the probability of binding to the receptor, leading to a more efficient conjugate.

Both dendrimers kept their conformation in contact with water during the whole trajectory. The radius of gyration (Rg) of FA-PEG3350 dendrimer (20.5 Å) was higher than FA-PEG750 dendrimer (14.2 Å) (Figure 4A). Also, FA-PEG750 dendrimer, in contact with folate receptor (Figure 4B), had a lower Rg mean value (12.8 Å) than FA-PEG3350 dendrimer (22.6 Å). The increment in Rg of FA-PEG3350 dendrimer can be due to the fact that it possesses a larger chain length, and as a result, more contact area that can interact with folate receptor aminoacids. In addition, the radius of gyration of both dendrimers in contact with the receptor (Figure 4B) remained in equilibrium after 150 ns, where no significant variation was observed. Therefore, after this time the dendrimers remained stable in contact with the receptor. Meanwhile, the dendrimer alone in water (Figure 4A) had more degrees of freedom and moved freely during the whole trajectory. As a result, PEG with higher molecular weight (PEG 3350) had also a higher radius of gyration than the PEG with lower molecular weight (PEG 750). Therefore, it can have a greater interaction with the folate receptor. These findings corroborate the results previously obtained by SASA analysis.

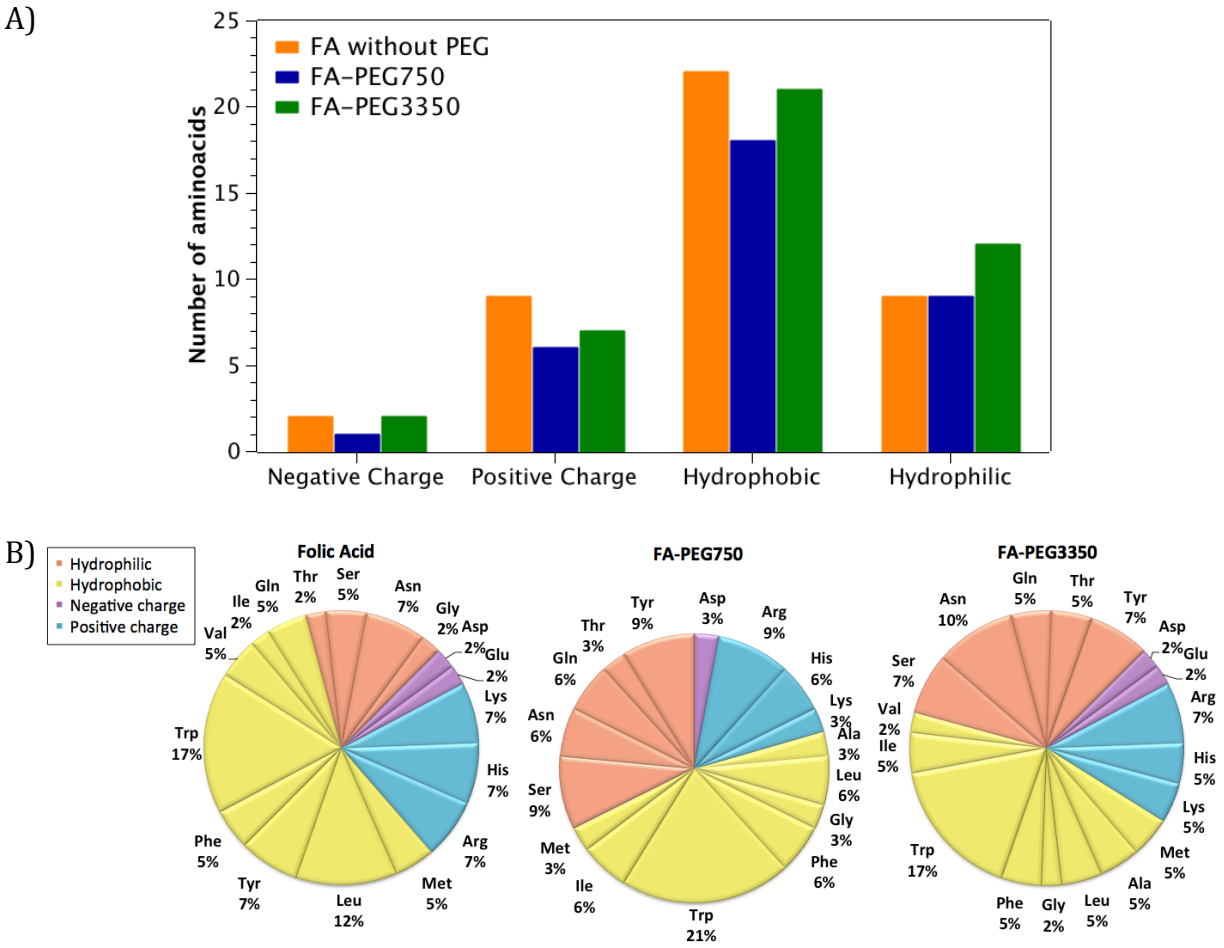

Figure 5. A) Charge and polarity distributions of FR-α amino acids at 7 Å from folic acid alone and from FA-PEG dendrimers and their B) interaction frequency.

Hydrophobic amino acids tend to be located in the interior of the protein hydrophobic pocket. However, nonpolar intermolecular interactions between host and guest lead to protein conformational changes, exposing the hydrophobic amino acids to the surface.[86]

In the present study, most of the folate receptor amino acids involved with dendrimer binding were hydrophobic (Figure 5A). FA-PEG3350 dendrimer presented slightly more interaction with hydrophobic aminoacids than FA-PEG750 dendrimer and folic acid alone. This makes sense because the longer FA-PEG3350 chain length allows more exposition of FA residue to the aqueous solvent, and therefore, to the active site of the receptor. In fact, tryptophan (Trp) (Figure 5B) was the FR-α aminoacid with the highest interaction with the folate fragment of both dendrimers (17% and 18% of the time simulation for FA-PEG750 and FA-PEG3350 dendrimers, respectively). Also, these results were in accordance to those published by Maziarz et al. that reported that tryptophan and tyrosine residues may contribute to the affinity of ligand binding, and also alanine, valine, and glutamic acid act synergistically to produce the distinguishing ligand binding characteristics of FR-α compared with FR-β.[109]

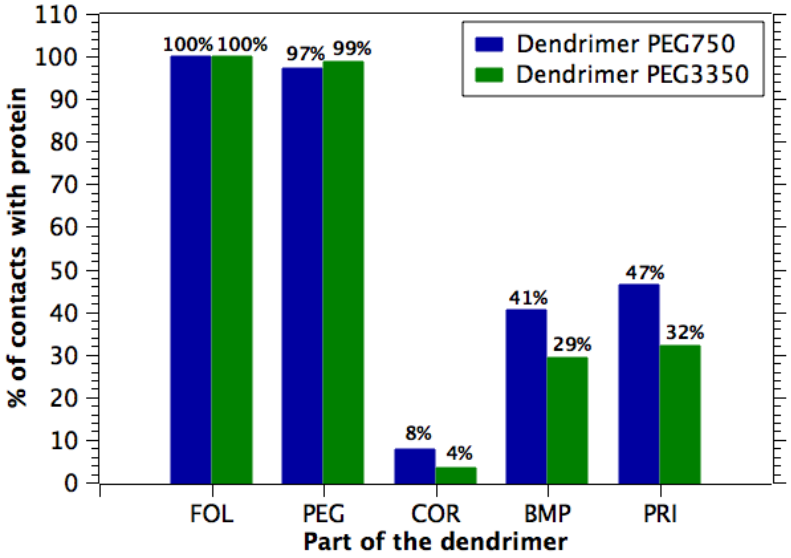

Figure 6. Percent of contact with receptor for each dendrimer fragment (FOL: folic acid, PEG: polyethylene glycol 750 or 3350, COR: core of ethylene glycol, BMP: bis-MPA, PRI: anticancer drug).

These results were in agreement with those reported by Wu et al. Long-chain PEG is more capable of interacting with proteins in aqueous solution. PEG-protein interactions induce conformational charges to relatively open structures with increased hydrophobic cavities, provide multiple binding sites of proteins to PEG, and facilitate the formation of PEG-protein complexes.[82]

In contrast, short chain PEG showed little tendency to interact with proteins due to its lack of capability to form multiple binding sites.[82] Meanwhile, there is no evidence corresponding to which length is optimal for polymer-protein complex.[86]

Also, an important positive charge contribution was observed for FR-α amino acids, such as Arg, His and Lys, that interact with both dendrimers. This observation can be considered significant because folic acid has a negative charge conferred by its carboxylate group, while the rest of the dendrimer has neutral formal charge. Therefore, the negative folic acid fragment of both dendrimers will directly bind to the positive aminoacids of the receptor.

It was also confirmed that the folate and PEG fragments from both dendrimers with PEG 750 and 3350 Da had more contact with folate receptor (Figure 6). In addition, PEG protects and avoids the anticancer drug (DRG) from directly interacting with the receptor. The dendrimer with PEG 3350 showed a greater protection effect than the one with PEG 750, as it was expected. A similar protection effect occurs with the rest of the dendrimer with bis-MPA (BMP) and the dendrimers core (COR) with the least contact with the receptor. However, it was expected that the dendrimer with longer chain length had more contact with the receptor as reported by Wu et al.[82] In this case, no significant difference was obtained between the contacts with PEG 750 or with PEG

3350. Previous reports have shown that PEG with high molecular weight could change the microenvironment and conformation of proteins, and such changes are likely to change the activity of PEGylated proteins.[82]

There are two forces that influence in solubility increment: the decreased planar stack force and the presence of intermolecular hydrogen bonds.[84] The dendrimer with PEG 750 showed a sandwich π-stacking interaction between the folate section of the dendrimer and Tyr60 or Trp171 from the receptor. This sandwich configuration (face-centered parallel stack) has low stability, is preferred in organic solvents and the interaction is strengthened as the difference in aromatic electron density between two rings increases.[110,111] Also, a more stable and isoenergetic T-shaped π-stacking interaction between pterin group of folic acid and hydrophobic Trp64 or His135 has been observed during the molecular dynamics simulation of the dendrimer with PEG 750. Meanwhile, the dendrimer with PEG 3350 showed a sandwich π-stacking interaction between pteridine ring of folic acid and Trp 171 from the folate receptor, and a T-shaped π-stacking interaction between benzoic group of folic acid and positively charged His135.

The analysis of ligand-receptor interactions of folic acid and crystal structure of FR-α reference showed eight H-bonds that retain the folic acid inside the binding pocket. The main amino acids involved in this binding are Asp81, Trp 102, Arg103, Arg106, Trp140, His135 and Gly137. The side chains of the first five amino acids directly interact with folic acid, and the last two with the backbone part of the amino acid. On the other hand, π-π stacking interactions over the pterin ring were observed, formed by His135 and Trp171 amino acids. As it was expected, when we evaluated the interactions of the complete dendrimers against the folate receptor, we observed several variations in comparison with the FA-FRα crystal reference. Which means that the dendrimers have an effect over the interactions with the aminoacids of the receptor evaluated at 200 ns of MD.

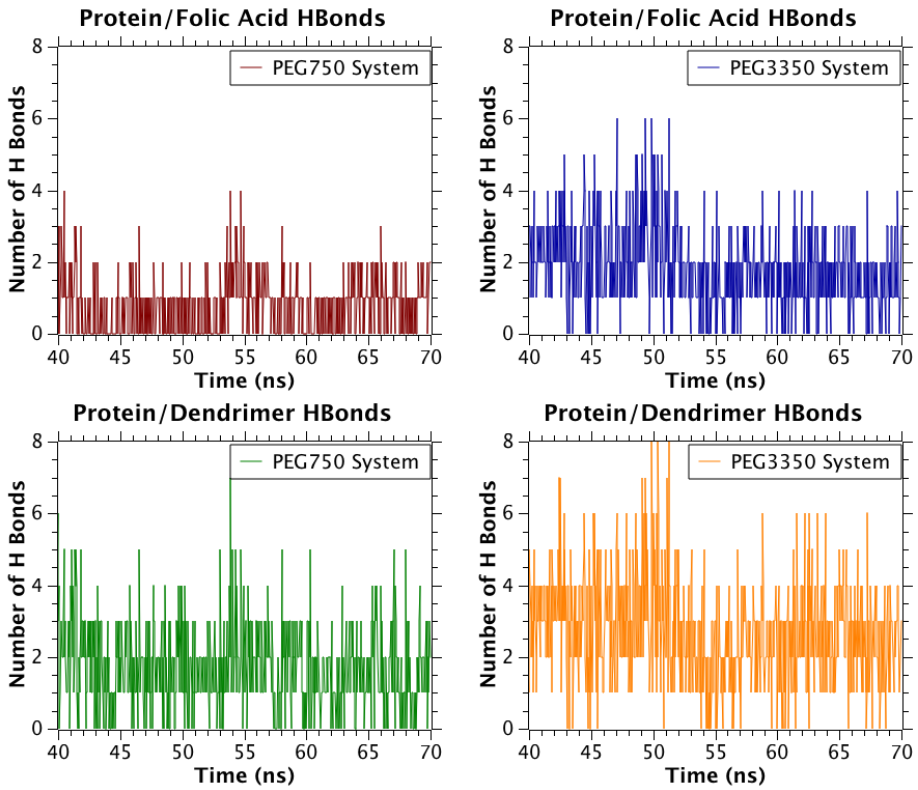

Figure 7. Number of hydrogen bonds formed between dendrimers and folate receptor.

In addition, we can assume that the folate fragment from the dendrimer with PEG750 remains inside of the receptor, as we can observe a low number of hydrogen bonds (Figure 7) very close or equal to zero through the whole trajectory. Also, when the whole dendrimer with PEG750 was in contact with the FR-α, it showed the presence of H-bonds and as a result, some interaction with the receptor. Meanwhile, the dendrimer with PEG3350 presented slightly more H-bonds than the dendrimer with PEG750.

As a result, we can imply that FA-PEG3350 dendrimer has a slightly better interaction and stability with the receptor than FA-PEG750 dendrimer. However, the dendrimer with PEG750 is also an interesting vehicle for further experimentation.

In addition, histidine (HIS135) was the amino acid with higher percent of hydrogen bonds occupancy between the receptor and the folic acid fragment from both dendrimers with PEG750 and PEG3350. According to Müller et al., histidine residues can help improve stability.[90]

Finally, FA-PEG3350 dendrimer showed the least diffusion coefficient (MSD) (Figure 8) along the molecular dynamics trajectory with a mean value of 1.34×10^3 nm^2/ns in comparison with FA-PEG750 dendrimer and folic acid itself, which presented MSD mean values of 4.35×10^3 nm^2/ns and 2.068×10^4 nm^2/ns respectively.

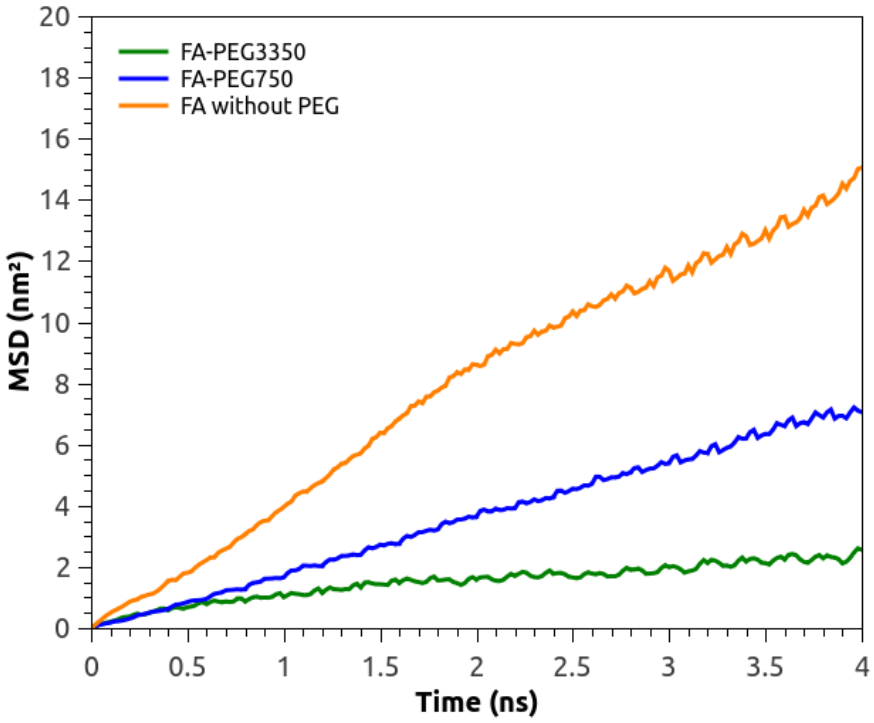

Figure 8. Self-diffusion coefficients of FA-PEG750 and FA-PEG3350 dendrimers.

As a result, PEG 3350 has a better chance to interact with folate receptor FR-α, being a better alternative in conjugation with folic acid for drug delivery systems.

As reported before by Schmidtke et al.,[112] when a ligand and a receptor interact via H-bonds shielded from water by surrounding hydrophobic regions, as in the case, the resulting complex tends to be more kinetically stable than if the hydrogen bonds were less shielded. However, the difficulty with which water diffuses into and away from the hydrophobic sites-appears to create a kinetic barrier to ligand binding and unbinding. In other words, low diffusion could affect the kinetic properties of the dendrimers.

4. Conclusions

This molecular dynamics study validated that PEG chain lengths (750 and 3350 Da) did not interfere over ligand-receptor binding functionality. Although kinetic binding may be affected, especially for the FA-PEG3350 dendrimer, the folate fragment from both dendrimers remained exposed to the solvent before approaching to folate receptor, so it could selectively direct the dendrimer towards FR-α, where interaction and internalization would be able to occur. As a result, theoretical evidence supports that the proposed PEG-folic acid dendrimers represent a new viable alternative as drug delivery systems for cancer therapies. Nevertheless, experimental corroboration is required to verify if PEG fragment length of this dendrimer allows an adequate diffusion in water and does not affect its application in cancer therapy.

Therefore, in vitro and in vivo experimental corroboration is necessary by isothermal titration calorimetry, fluorescence microscopy to probe the effectivity of the dendrimer against cell death and to corroborate dendrimer-receptor binding. Flow cytometry and MTT assays can also help to determine cell viability and cytotoxicity of FA-PEG systems.

5. Acknowledgements

This research is financially supported by Fraunhofer Chile Research Foundation, Consejo Nacional de Ciencia y Tecnología (CONACYT), and the research funds for the universities Center of Bioinformatics and Molecular Biology (Universidad Andrés Bello, Santiago, Chile), and Centro de Biotecnología FEMSA, (Tecnológico de Monterrey, México). F.G.N, V.M.M and I.A.D thanks to RED CYTED 214RT0482. V.M.M. thanks Conicyt for a PhD Scholarship and CONICYT + PAI/ "Concurso Nacional Tesis de Doctorado en la Empresa" 2014 (781413007). D.G.N., V.M., and I.A. thank for support of Fraunhofer Chile Research, Innova-Chile CORFO (FCR-CSB 09CEII-6991) and Anillo Científico ACT1107. The Centro Interdisciplinario de Neurociencia de Valparaíso (CINV) is a Millennium Institute supported by the Millennium Scientific Initiative of the Ministerio de Economía, Fomento y Turismo.

CHAPTER 3

Optimization of Dual Asymmetric Centrifugation for liposomes preparation

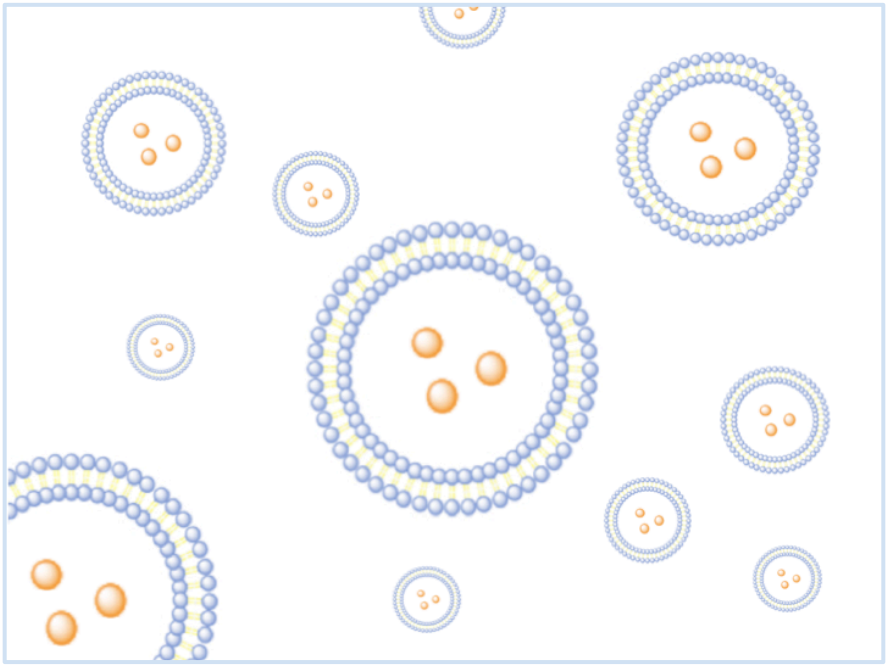

CHAPTER 3 - Optimization of Dual Asymmetric Centrifugation for liposomes preparation

Abstract

Liposomes are the most mature drug carriers for passive and active targeting used in oncology and other disease treatments. In early drug development of liposomes loaded with New Chemical Entities (NCEs), a limited amount of drug is available. Dual Asymmetric Centrifugation (DAC) is a novel, fast, simple, and reproducible method for liposomal formulation screening that facilitates the preparation of liposomes of small diameter (<120 nm) in a small scale, with high lipid concentration and high encapsulation efficiency (EE). In this work we optimized the parameters of DAC to reduce liposomes size to 70-80 nm with high encapsulation efficiency, and determine the best method for liposomes purification.

1. Introduction

1.1 Liposomes

Liposomes overcome the limitations of conventional chemotherapy by improving the bioavailability and stability of the drug molecules and minimizing side effects by site-specific targeted delivery of the drugs. They have revolutionized cancer therapy by their broad clinical applications. So far, liposomes have established themselves in nanocarriers-based drug delivery systems due to the successful clinical applications of liposomal formulations in anti-cancer therapy. [113]

They were the first nanotechnology-based drug delivery systems approved for clinical applications. Some of them are already in the market and many more are undergoing research and clinical trials. Nowadays, they are extensively used for drug delivery as they meet all the requirements of a good delivery vehicle. Liposomes are spherical vesicles in which an inner aqueous volume is surrounded by one or more phospholipid bilayers. They can encapsulate both hydrophilic and lipophilic drugs, are biodegradable, biocompatible, and stable in colloidal solutions. Liposomes protect the drug from degradation and reduce drug-related nonspecific toxicity and can be produced and formulated easily for the target specific delivery.[113]

A liposomal preparation suitable for *in vivo* application is typically characterized by (i) its average size in the double to lower triple-digit nanometer range, (ii) a size distribution which is not too broad (polydispersity index (PI) below 0.6) and (iii) in most cases neutral surfaces. The entrapment of a drug in liposomes offers two major advantages: protection of the drug and a resulting prolongation of its circulation time, as well as accumulation in tumor tissue due to the enhanced permeability and retention effect (EPR-effect).[114]

1.2 Liposomes applications in cancer.

A number of different liposomal formulations of anti-cancer agents have been shown

to deliver the drug at the site of solid tumors with minimum toxicity as compared to free drug. Currently, there are many products in the market and in clinical development for use as anti-cancer drug delivery vehicles. Doxil, a PEGylated liposomal formulation, is the first liposomal product that was approved by the FDA for the treatment f kaposi's sarcoma in AIDS patients. It is a PEGylated liposomal formulation encapsulating anticancer drug doxorubicin, which is also active against refractory ovarian cancer, breast cancer, multiple myeloma. DaunoXome is the liposomal formulation of daunorubicin approved by the FDA for the treatment of AIDS related kaposi's sarcoma. Myocet, is a non-PEGylated liposomal formulation of doxorubicin, which in combination with cyclophosphamide was approved for the treatment of metastatic breast cancer.[113]

1.3 Particle size importance.

Size and size distribution (polydispersity) of the formulated nanoliposomes are of particular importance in their characterization. Maintaining a constant size and/or size distribution for a prolonged period of time is an indication of liposome stability.[115]

Also, the size of liposomes can affect in the success of drug delivery to the desired place, according to its application. For example, nanoparticles of < 200 nm in diameter and those with positive surface charge are known to preferentially accumulate and reside in the tumor mass for longer duration than either neutral or negatively charged nanoparticles.[116,117]

In addition, to increase the solubility of poorly soluble compounds one of the suitable technologies is to reduce their particle size, thus increasing the effective particle surface area, which leads to a higher rate of dissolution and an oversaturation effect.[118]

1.4 Liposomes classification.

Liposomes can be classified on the basis of size and number of phospholipid membrane layers (Figure 1).[113]

Multilamellar vesicles (MLV): These liposomes are composed of a number of concentric phospholipid bilayer membrane separated by aqueous phase. These are big in size and may be up to 5 mm.

Large unilamellar vesicles (LUV): These are also composed of a single lipid bilayer surrounding aqueous compartment. Their size is in the range of 100-250 nm.

Small unilamellar vesicles (SUV): These liposomes are composed of aqueous compartment enclosed by a single lipid bilayer. The size of these liposomes may be in the range of 20-100 nm.

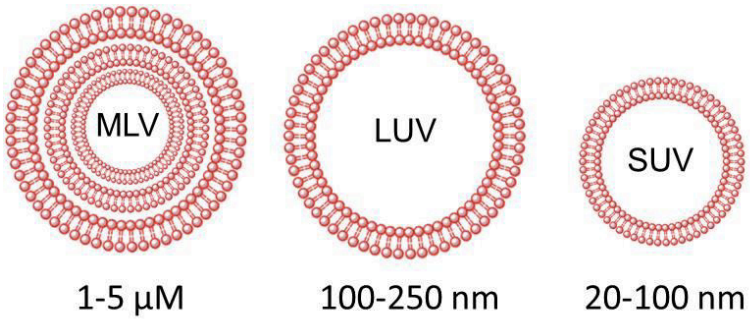

Figure 1. Liposomes classification based on the lamellarity.

1.5 Components of liposomes.

Depending upon the component used, liposomes can be neutral, negative, or positively charged. The charge on the surface of liposomes plays an important role for the fate and application of the liposomes. The major components of liposomes are phospholipids and cholesterol, major constituents of natural bio-membranes.[113]

Phospholipids. The most common phospholipids (Figure 2) used for liposomes preparation are natural (egg or soy) or synthetic phosphatidylcholine (PC). The synthetic phospholipids provide more stability than the natural phospholipids because the last ones contain substantial levels of polyunsaturated fatty acids that affects the stability. The molar percentage of phospholipids varies from 55 to 100% of total liposomal components.[113]

1,2-dipalmitoyl-*sn*-glycero-3-phosphocholine (DPPC) can be typically used as a primary lipid of temperature sensitive liposomes. DPPC liposomes become leaky to small water-soluble molecules at a gel-to-liquid crystalline phase transition (41°C). Adding small amount of DPPC as a co-lipid to the liposomal membrane can help in adjusting the desired transition temperature.[116]

Negatively charged lipids such as phosphatidylserine (PS) are preferentially recognized by macrophages. Studies comparing phosphatidyl-choline (PC; neutral) and PS-composed liposomes have established that negative liposome formulations have enhanced macrophage internalization. 1,2-di-(9Z-octadecenoyl)-*sn*-glycero-3-phospho-L-serine (DOPS) is an excellent substitute for the naturally occurring brain PS. It is more stable to oxidation and has been used in lipid mixtures to mimic platelet membranes for coagulation studies. Kelly et al. found a 5.3-fold increase in the association of negatively charged DOPS:Cholesterol liposomes with a macrophage cell model, differentiated THP-1 cells, compared to neutral DOPC:Cholesterol liposomes, an effect also seen *in vivo*.[119]

Cationic liposomes are associated with efficient cellular delivery of drug cargoes and routinely applied for *in vitro* gene delivery. Electrostatic interactions between positively charged liposomes and the negatively charged membranes and cell surface proteoglycans facilitate cell uptake. Unfortunately, cationic liposomes can cause cytotoxicity limiting their safety for clinical use. 1,2-Dioleoyl-sn-glycero-3-

phosphocholine (DOPC) is a synthetic phosphocholine that forms liposomes in aqueous media, alone or in combination with other lipids. N-[1-(2,3-dioleoyloxy)propyl]-N,N,N-trimethylammonium chloride **(**DOTAP-Cl) is a cationic liposome-forming compound for transfection of DNA, RNA and other negatively charged molecules into eukaryotic cells. Mixing DOTAP with DNA results in spontaneously formed stable complexes that can be directly added to cell culture medium. These complexes fuse with the cell membrane and release DNA into the cytoplasm. The cells are transfected efficiently without cytotoxic effects. When DNA is mixed with cationic liposomes (CLs) composed of mixtures of cationic DOTAP and neutral DOPC lipids, the resulting CL–DNA complex consists of a multilamellar structure comprising DNA monolayers sandwiched between lipid bilayers.[119,120]

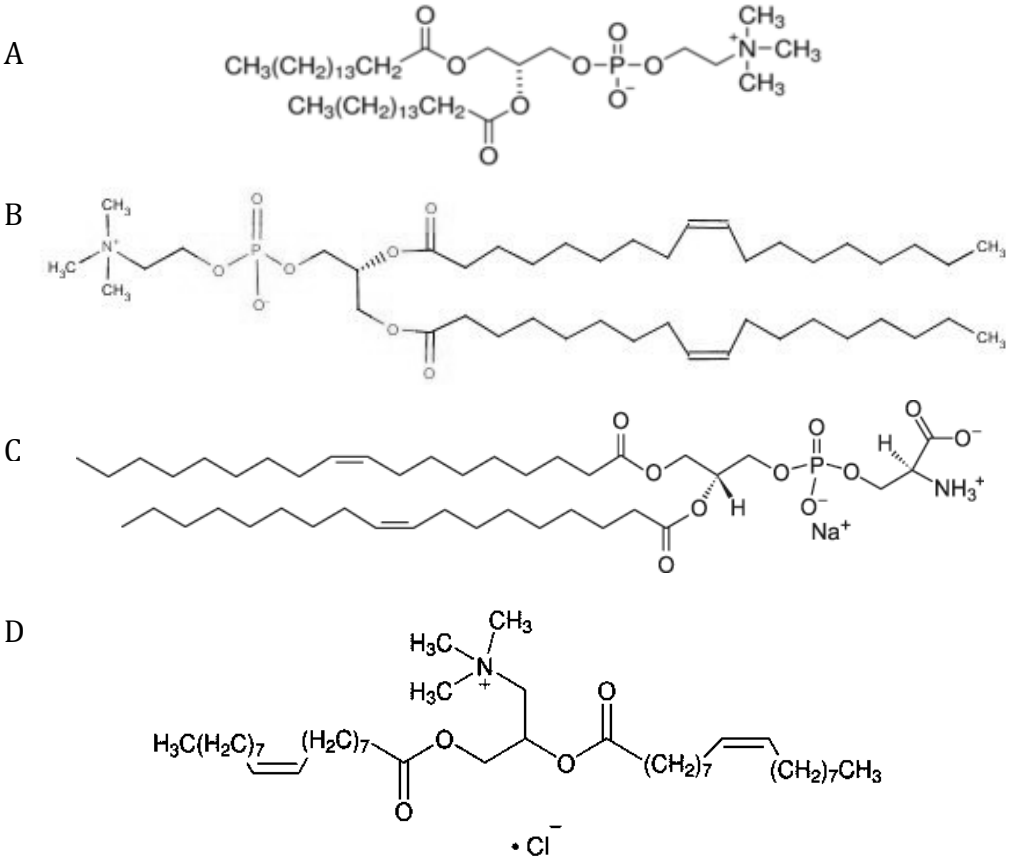

Figure 2. Chemical structure of A. DPPC, B. DOPC, C. DOPS, and C. DOTAP.Cl lipids.

The type, molar percentage and packing orientation of phospholipids determine the ultimate shape and size of the liposomes. The orientation of phospholipids in liposome bilayer depends upon the length of lipid molecules and the size of head groups.

The phase transition temperature is defined as the temperature at which the lipid physical state converts from an ordered gel phase to a disordered liquid crystalline phase. The conversion of phases depends on hydrocarbon chain length, degree of saturation, charge, and head group species. Therefore, the phase transition

temperature of phospholipids is an important criterion to choose phospholipid for the preparation of liposomes.

The use of phospholipids with higher phase transition temperatures generates bilayers, which are more stable. This decreases the possibility for premature leakage of encapsulated components. On the other hand, if the phase transition temperature of the selected phospholipids is too high, denaturation of the encapsulated drugs may occur during the sizing, or loading processes. Therefore, a good balance must be met to guarantee that the selected lipids have phase transition temperatures that prevent premature leakage of components but enable processing to occur at temperatures that are harmless to all liposomal components.[113]

Cholesterol. The rotational freedom because of flip-flop movements in phospholipids generates liposomes of leaky properties. Cholesterol is the main component added in the liposomal formulations to stabilize the bilayer of liposomes. Depending upon the rigidity and fluidity of the bilayer, the molar percentage of cholesterol varies from 30-45% of total liposomes components. It provides membrane fluidity, elasticity, permeability and stability to liposomes. Due to hydrophobic properties, cholesterol resides in the interior portion of lipid bilayers and serves to fill the gap created because of imperfect packing of phospholipid molecules. The packing of cholesterol within phospholipid bilayers prevents the flip-flop of membrane components and the movement across the membranes. Cholesterol also provides the rigidity to liposomes as it prevents the phase transition of lipid bilayers, and thus reduces the leakage of encapsulated drugs. Also, it can help protect the lipid bilayer from hydrolytic degradation.[113]

PEG. PEG is another commonly used liposome component typically incorporated to increase the blood circulation times because of its stealth properties and broad applications.[113]

DSPE. The 1,2-distearoyl-s*n*-glycero-3-phosphoethanolamine (DSPE) is an example of a functional phospholipid used to conjugate other polymers like PEG.[113]

1.6 Liposomes preparation methods.

Liposomes can be made by different liposome preparation techniques. Some conventional methods include extrusion, thin-film hydration (Bangham), reversed phase evaporation, solvent injection, ultrasound treatment, detergent dialysis, and high pressure homogenization (HPH). Some newer techniques include supercritical anti-solvent (SAS), supercritical reverse-phase evaporation, membrane contactors, cross-flow filtration detergent depletion, freeze drying double emulsion, and dual asymmetric centrifugation (DAC).[114]

Industrial scale production of liposomes mainly uses high-pressure homogenizers and filter extruders, that allow to prepare small and homogeneous liposomes. HPH also allows the preparation of highly concentrated (300 to 600 mg/g), semisolid phospholipid dispersions (also called vesicular phospholipid gels or VPGs), and small unilamellar vesicles (SUVs) from powdered lipid(s) and aqueous drug solution.[121]

One approach to produce small drug particles is to mill an aqueous suspension containing the poorly soluble drug, polymer(s) and surfactant(s) for stabilization by avoiding agglomeration. This process uses milling beads (wet ball- or pearl milling), having as an advantage that no organic solvents are needed and low batch to batch variations. There are several FDA approved products on the market which have been produced by this technique including Rapamune® (Sirolimus, Wyeth), TriCor® (Fenofibrate, Abbott) and Megace® ES (Megestrol acetate, Par Pharmaceuticals).[118]

Frequently, a buffer solution with high content of sugar (e.g. His-Suc) is used in liposomes preparation. The roles of sugars, like sucrose, include the stabilization of membrane by lowering lipid phase transition temperature and the prevention of liposome aggregation and fusion. It has been demonstrated that sugar molecules directly interact with membranes by forming hydrogen bonds with the polar headgroups of phospholipids. Because sugars are at high concentrations before drying, dry liposomes inevitably exist in a sugar glass matrix. As water is removed during freeze-drying, sucrose solution is increasingly concentrated. It is possible that the glass matrix prevents liposome fusion and protects liposomes from the mechanical damage of ice crystals during freeze-drying. Solute leakage from dry liposomes is extremely slow at temperatures below the glass transition temperature; however, it increases exponentially as temperature increases to near or above the transition temperature, indicating that the glassy state had to be maintained for dry liposomes to retain trapped solutes. The kinetic stability is achieved by the extremely high viscosity of the glassy state.[122]

Although there are multiple methods for liposomes preparation, many new chemical entities, drugs or metabolites recently discovered are very expensive or there is a limited amount available for experiments. Therefore, there is a strong incentive for reducing the batch size of liposomal preparations, e.g. in screening for optimal lipid composition. At the same time, the typical demands in drug development must be considered, including sterility, analytics, and validation issues. Most of the techniques mentioned above for liposomes preparation are time consuming, require experienced lab personal, are difficult to scale-up, and fail to offer a suitable combination of features such as sterility, small batch sizes, and high entrapment efficiencies. [114,123]

One of the most used methods for liposomes preparation is the dry film hydration method, attributed to little demand in terms of equipment and training needed, and it is easy to use. Other methods for liposome manufacturing applied in pharmaceutical companies are the fluidic method, microfluidics and high pressure homogenization (HPH). A comparison between these methods and DAC was previously done. Microfluidics needs a very time consuming setup and microfluidic chips tend to break very fast. Meanwhile, HPH is a large scale method (more than 250 mL). The only advantage of the fluidic method in comparison to DAC is its ability to generate homogenous unilamellar liposomes below 100 nm. The film method has no single advantage over DAC; DAC uses >70x less drug, entraps >60 % drug vs >20%, produces liposomes with higher homogeneity and needs 10x less lab handling time. These results prove that for lab scale formulation screening, DAC is the best option.[124]

1.7 Dual Asymmetric Centrifugation (DAC).

DAC is a new technique described by Massing et al.[121] in 2008; which principally allows to prepare very small batches of sterile liposomes with high entrapment efficiencies for water soluble compounds.[114] Also, DAC has multiple advantages in comparison to conventional techniques for liposomes preparation. DAC is an easy, fast process, temperature can be controlled, it is very gentle with sensitive substances without changing their crystal structure, batch sizes are very small (100-1000 mg), 40 sample vials can be processed in parallel.[118,125] In addition, the shear forces generated by DAC are much lower than those generated by HPH, which might be advantageous when sensitive compounds are entrapped within liposomes.[121]

Liposome formation by DAC is facilitated by a kind of homogenization of highly concentrated lipid dispersions in a vial. DAC differs from normal centrifugation by an additional rotation of the samples during centrifugation, resulting in a very fast and powerful movement of the samples inside the vials. DAC-homogenization takes place when the concentrated, viscous lipid dispersion – in combination with milling beads – is centrifuged around a central axis (axis 1) while the vial itself turns around its own vertical axis (axis 2). While the viscous lipid dispersion is accelerated away from axis 1 due to centripetal forces (outwards direction), the material is moved inwards due to friction of the material to the wall of the constantly turning vial. Both overlaying movements of the viscous lipid dispersions result in its homogenization and in the formation of a highly viscous liposome formulation.[114,118,121]

DAC has been known since the 1970s as a convenient technology for the rapid mixing of viscous components and is widely used to rapidly mix two or more component composites. Since mixing by DAC is astoundingly fast, the DAC-technology is also named “speed-mix”-technology and the DAC-apparatus “Speedmixer”.[121]

Figure 3 shows an schematic drawing of DAC principle with the main rotating arm and the vial holder at its distal end. The main rotation arm of the DAC forms an angle of about 40º with the rotation plane. At this angle, the rotating arm forces the content of the vial into the corner between the bottom and the vial wall. The DAC allows a maximum speed of 3540 rpm, and reaches a maximum acceleration of the sample of about 911 x g. The vial holder rotates in the opposite direction with approximately one fourth of the rotating arm’s frequency.[121]

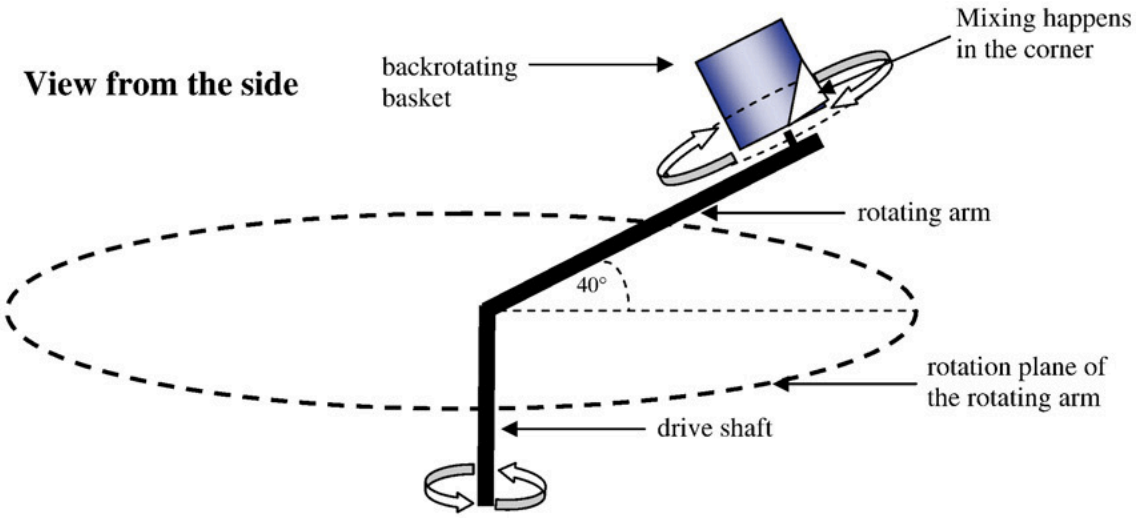

Figure 3. Dual asymmetric centrifugation principle (Massing et al. 2008)

This unique combination of two very fast movements of a viscous sample material should result in constant and strong shear forces within the material, therefore, it might also be used for homogenization purposes and thus for the production of liposomes, which are often made by the homogenization of a phospholipid/water blend using different homogenization machines.[121]

The DAC apparatus is a bench top machine, cheaper than most alternative lab-scale machines such as high-pressure homogenization or filter extrusion and can readily be used in any research lab without the need of much extra space.

1.8 Applications of DAC

The suitability and versatility of DAC for liposomes production has already been demonstrated in some studies.[114,121,123,126–128] Since the technique provides a closed system and eliminates the need of organic solvents, it has several advantages compared to other available production methods.[121,129] DAC is suitable for entrapping sensitive compounds within liposomes. Furthermore, since the process is fast and can be performed aseptically within sealed sterile containers, it might be possible to even entrap compounds which are short-lived (e.g. isotopes) or chemically instable (e.g. alkylants) in a bedside preparation.[121]

Concentrated vesicular phospholipid gels (VPGs) are formed as intermediate product, making it especially suitable for obtaining high liposome content in secondary vehicles such as creams, lotions or hydrogels.[123,130] Tenambergen et al., 2013, prepared fat emulsions with a droplet size distribution in the submicron range with DAC. Compared to the HPH, preparation time and effort were lower.[125] In 2016, Ingebrigtsen et al., 2016, developed a reproducible method using DAC for the production of homogenous liposomes-in-hydrogel formulations for topical application, with a higher lipid and drug content than what have previously been possible with the conventional film hydration and hand-mixing methodology.[123]

Hagedorn et al. 2017, used DAC for an effective and rapid nanomilling of active pharmaceutical ingredients (API) of low solubility. Their results showed that DAC-nanomilling experiments are highly comparable to the results obtained by common agitator mills, resulting in same or smaller particle sizes, and drug concentrations up to 40%. Hence, DAC-milling can be assumed as predictive for milling in a larger scale.[118] Recently, Ingebrigtsen et al. demonstrated the suitability of DAC for the co-encapsulation of benzoyl peroxide (BPO) and chloramphenicol (CAM) in liposomes.[130]

In addition, tenfold smaller sample sizes could be used compared to the film hydration method – even less when compared to other formulation methods. This resulted in 70 times reduction in amount of drug substances per screened formulation. As consequence, early phase development of liposomal drugs in pharmaceutical companies can directly profit from this technology. Besides needing around seventy times less drug, DAC substantially helps increase overall efficiency by enabling broader and deeper screenings at reduced lab time and costs.[121] As a result, this method is ideal for the screening of suitable polymer/surfactant combinations,[118] and as a model for screening active pharmaceutical ingredients in pharmaceutical preformulation development.[125]

Very few publications involving optimization of DAC are currently available. In 2011, Adrian et al. published an optimization of the preparation of targeted liposomes for efficient siRNA delivery to neuroblastoma, by combining DAC method and sterol-based post-insertion technique (SPIT) to couple anti-GD2 antibody for selective interaction with neuroblastoma cells. The size of liposomes ranged from 190 to 240 nm and the encapsulation efficiency was up to 50%.[126] Recently, Hagedorn et al. used fenofibrate to investigate DAC-nanomilling for formulation screening by applying a DoE-approach. They varied mixing speed (1000 to 2000 rpm), beads weight (700 mg to 1.3 g), and milling time (30 min to 2 h).[118]

1.9 Encapsulation of drugs into liposomes.

Drug encapsulation into the liposomes can occur by passive or active loading.

Passive loading. The passive loading occur during the vesicle formation process. Hydrophilic drugs are loaded within the internal core of the liposomes by mixing with the hydrating buffer used to hydrate the thin lipid film during the formation of liposomes. Lipophilic drugs are mixed with other liposome components during the preparation of thin dry film of lipids and ultimately loaded into lipid bilayers. The unentrapped drug molecules are removed from liposome suspension by dialysis, or gel-filtration chromatography.[113]

Active loading. Certain weakly acidic, or alkaline drug molecules are loaded into preformed liposomes by active loading, or remote loading method. This process is driven by an electrochemical potential created by the pH, or ion gradients established across the lipid bilayer of the liposomes. The pH, or ion gradients are created during the liposomes preparation by using a buffer or specified pH and ion concentration. The external pH of liposomes is then exchanged with another buffer of different pH, or

ion concentration through dialysis, or size exclusion chromatography. After crating the pH gradient across the liposomes membranes, drug is loaded by mixing with liposomes typically at a temperature above the phase transition temperature of the lipids to ensure the fluidity and efficient transport across the bilayer. The drug molecules interact with the ions within liposomes and get charged. The charged drug molecules are not capable to come out and remain entrapped within liposome core. A commercial example of active loading by pH gradient is Doxil® liposomal doxorubicin.[113]

The **encapsulation efficiency** depends on lipid concentration, liposome size, lipid mix, etc. The encapsulation efficiency of water-soluble compounds, which do not interact with the lipid bilayer, is relatively low if loaded by passive method and proportional to the aqueous volume enclosed in the liposomes. Large vesicles will have higher encapsulation efficiency than small vesicles. While the drug that interacts with lipid bilayer, such as lipophilic compound, normally have better encapsulation rate.[113]

Therefore, several strategies have been developed to improve the encapsulation efficiency by linking lipophilic chain to drug molecule to increase its lipophilicity and better partition into the lipid bilayer. The choice of lipid composition is also critical for better loading efficiently by this method. For example, to load highly negatively charged nucleotide compounds, such as antisense or siRNA, selection of cationic lipid will greatly improve the encapsulation efficiency due to enhanced drug/lipid interaction.

1.10 Liposomes purification

Purification remains a significant hurdle in the development of liposomal products. Irrespective of which production method is adopted, non-entrapped contaminant molecules, small molecule drugs or proteins must be removed from the final liposome product. Separation is typically achieved by filtration or ultra-centrifugation, which can be challenging for the large-scale purification. Other possible routes for removal of non-encapsulated material include dialysis, gel-permeation chromatography, ion-exchange chromatography, and size exclusion chromatography.[131–133] There are different kinds of commercial systems for each kind of purification procedure, but between the different methods there can be variations in reproducible results, efficiency, time and cost.

2. Objectives

- To reduce liposomes size less than 100 nm using DAC, for further specific applications.
- To determine the best method for liposomes purification.
- To study the effect of preparation parameters over the encapsulation efficiency.

3. Materials and methods

3.1 Materials

DPPC, PEG2000-DSPE, DOPS, DOTAP-Cl, and DOPC lipids (Lipoid GmbH, Switzerland); tert-butanol, ethanol, cholesterol, calcein, Triton-X100, Phosphate Buffer Saline (PBS), histidine and sucrose, were acquired from Sigma-Aldrich (Switzerland). Histidine-sucrose (His-Suc) buffer was prepared in the lab using 1.5 g of histidine and 90 g of sucrose, volumetrically adjusted to 1 L of distilled water, and pH 6.5. Calcein buffer solutions 1 mM and 5 mM were prepared in His-Suc buffer or in PBS buffer, and the pH was adjusted to 6.5 in every case.

3.2 Liposomes preparation

For all formulations, the lipid mix was completely dissolved by ultrasound at 40°C, froze and lyophilized in a freeze-drier Alpha 1-2 LD-plus for 24 hours. Calcein dye was used as a model of hydrophilic drug. Calcein 5 mM was encapsulated by passive loading during the formation of liposomes.

In this work, four different kinds of liposomes (neutral PEGylated, neutral without PEG, anionic, and cationic) were prepared.

Neutral-PEGylated liposomes. The lipid mix composition for neutral PEGylated liposomes consists of 18.9 mg of cholesterol, 61.5 mg of DPPC, and 19.5 mg of PEG2000-DSPE, for a total of 100 mg of lipids dissolved in 1 mL of tert-butanol by ultrasound at 45°C.

Neutral non-PEGylated liposomes. The lipid mix consists of 23.6 mg of cholesterol and 76.4 mg of DPPC dissolved in 1 mL of tert-butanol by ultrasound at 45°C.

Anionic liposomes. The lipid mix consists of 41.11 mg of DPPC, 8.64 mg of DOPS, and 12.89 mg of cholesterol, dissolved in 1 mL of tert-butanol by ultrasound at 45°C.

Cationic liposomes. The lipid mix consists of 54.2 mg of DOTAP-Cl, 30.7 mg of DOPC, and 15.1 mg of cholesterol, dissolved in 1 mL of tert-butanol by ultrasound at 45°C.

Once the lipid mixes were prepared, the vials were froze for 2 h and then lyophilized in a freeze drier (Alpha 1-2 LD) for 24 h. The pellets were stored in the freezer in case they were not immediately used.

3.3 Dual Asymmetric Centrifugation (DAC)

Beads weight was selected according to literature; increasing the weight from 50 to 600 mg resulted in a mean reduction of liposome size.[124] Therefore, 600 mg of Yttrium Stabilized Zirconia (YTZ®) grinding beads (1.0 mm or 1.5 mm) were added to each vial of lyophilized lipid mix to favor homogenization, increase the shear stress, to help reduce particle size allowing to work with high lipid loads. Each formulation was diluted with calcein solution 5 mM, pH 6.5 only during the first centrifugation run to favor encapsulation at high viscosity. Then, a second centrifugation run is done, in this

case adding buffer (without calcein). The DAC experiments are performed in a bench top centrifuge Zentrimix 380R (Hettich Zentrifugen).

3.4 Size optimization

3.4.1 Influence of beads size and buffer volume

The optimization of DAC methodology was performed to decrease liposomes size, maintaining constant lipid weight, beads weight, speed and time of centrifugation, and temperature (Table 1), according to the procedure commonly used for liposomes preparation at the pharmaceutical company. The variables, evaluated at first, were volume of calcein solution (150 μL, 200 μL and 250 μL) during the first centrifugation step and beads size (1.0 mm and 1.5 mm). Each experiment was done by triplicate.

Table 1. Constant DAC parameters for beads size and buffer volume evaluation.

Lipid weight	100 mg	
Beads weight	600 mg	
Beads size	Variable	
DAC	**1st Run**	**2nd Run**
His-Suc buffer volume	Variable	800 μL
Speed	2350 rpm	1250 rpm
Time	30 min	2 min
Temperature	40°C	40°C

3.4.2 Influence of time of centrifugation and type of buffer

The effects of the first centrifugation time (15 min, 30 min, and 60 min) and type of buffer (His-Suc and PBS, pH 6.5) were evaluated, using as constant parameters those with the better results for beads size and buffer volume (Table 2).

Table 2. Constant DAC parameters for time of centrifugation and type of buffer evaluation.

Lipid weight	100 mg	
1.5 mm Beads	600 mg	
DAC	**1st Run**	**2nd Run**
Type of Buffer	Variable	Variable
Buffer volume	200 μL	800 μL
Speed	2350 rpm	1250 rpm
Time	Variable	2 min
Temperature	40°C	40°C

3.5 Particle size and PDI determination

A particle size analyzer Beckman Coulter DelsaNanoC was used to determine particle size and PDI. 10 μL of sample was placed in cell with 990 μL of the buffer used for preparation. The DelsaNanoC uses photon correlation spectroscopy (PCS), which determines particle size by measuring the rate of fluctuations in laser light intensity scattered by particles as they diffuse through a fluid, for size analysis measurements.

3.6 Liposomes purification

The objective of liposomes purification is to remove free calcein from the liposomes to obtain purified liposomes with calcein encapsulated. The four different types of liposomes (neutral, PEGylated neutral, anionic, and cationic) were purified by three different purification systems. Two purification systems based in size exclusion chromatography (SEC) were evaluated including Zeba-Spin desalting columns (7 kDa MWCO 0.5 mL Thermo Scientific, Sweden), and Sephadex Micro-Spin G-25 columns (Illustra-GE Healthcare, 0.5 mL). Also, dialysis purification was tested using Spectra/Por® Float-A-Lyzer® G2 (100 kDa, 1 mL).

Zeba-Spin columns manufacturer procedure:

1. Place the column into a collection tube on top of a wash plate and centrifuge to remove the storage solution.
2. Discard flow-through and replace the column back into the collection device.
3. Add wash buffer on top of the resin. Centrifuge device and discard flow-through. Repeat this step two additional times.

Note: After each spin, the resin should appear white and free of liquid. If liquid is present, make sure you are using the correct centrifugation speed and time. Incomplete centrifugation may result in poor sample recovery or sample dilution.

4. Blot the bottom of the column to remove excess liquid. Transfer device to a new collection tube.
5. Apply sample on top of the resin. If needed, add a stacker as soon as the sample has entered the resin. Adding a stacker is optional but recommended for dilute protein solutions or small sample volumes to ensure maximum sample recovery.
6. Centrifuge and retain flow-through that contains sample. Discard spin column.

Table 3. Centrifugation conditions for 0.5 mL Zeba-Spin columns.

Sample volume range (μL)	30-130
Wash buffer volume	300 μL
Sample volume (μL)*	< 70
Optional stacker volume (μL)*	15
Centrifuge speed (x g)	1500
Centrifugation time (min)	
Storage solution removal	1
Wash 1	1
Wash 2	1
Wash 3	1
Sample recovery	2

*When using the indicated sample volumes, use a stacker to achieve the higher recovery. The stacker is a volume of wash/equilibration buffer applied after the added sample has completely entered the desalting resin bed.

Manufacturer protocol for Sephadex Micro-Spin G-25 columns:

1- Column Preparation
a. Re-suspend the resin in the column by vortex.
b. Loosen the cap one-quarter turn and twist off the bottom closure.
c. Place the column in the supplied collection tube for support.
d. Spin for 1 minute at 735 x g.

Note: Use columns immediately after preparation to avoid drying out of the resin. If the column resin appears dry, displaced or cracked after the first spin, this is usually indicative of over-centrifugation (too fast or too long). Re-hydrate the column with 250 μL of double distilled water, vortex and re-centrifuge, checking the settings. Spin speed can be reduced by 20% if necessary.

Do not use the pulse button on the microcentrifuge as this may over-ride the speed setting.

e. Proceed immediately to step 2 below.
2. Sample application
a) Place the column into a fresh DNAse-free 1.5 mL microcentrifuge tube.
b) Slowly apply appropriate volume of sample to the top-center of the resin, being careful not to disturb the resin bed (see Table 2 below).

Table 4. Loading volumes for different sample types

Sample type	Loading volume (μL)
Oligonucleotides following de-protection in Ammonia	100-150
Oligonucleotide labeling reaction	25-50
De-salting or buffer exchange	50

Where sample volume exceeds that shown in table, use multiple columns, or consider use of NAP/5 Columns. Where sample volume is less than the minimum shown in the table, dilute the sample to improve product recovery (note concentration will be reduced).

Note: The resin will have come away from the column slightly to form a pillar. It is essential that the sample being purified is applied slowly and is not allowed to run down the sides of the resin bed. Avoid touching the resin bed with the pipette tip.

4. Elution

a. Spin for 2 minutes at 735 x g. Because of centrifuge settings we used 700 x g.

The purified sample is collected in the bottom of the 1.5 mL centrifuge tube.

The **dialysis Float-A-Lyzer G2 manufacturer protocol** was slightly modified according to previous experience in the lab according to the following steps.

1. Pre-wetting the membrane: To most effectively wet the membrane, remove glycerin and achieve maximum membrane permeability, the Float-A-Lyzer G2

device should be soaked first in 10% ethanol inside and outside of the Float-A-Lyzer.
2. Flush the device thoroughly with DI water inside and outside of the device for 15-20 minutes.
3. After pre-wetting, the Float-A-Lyzer G2 is conditioned overnight by rinsing inside and outside the membrane with buffer that will be used later with the sample. In this case Histidine-sucrose buffer pH 6.5 was used.
4. Using a pipette carefully load the sample inside and at the bottom of the membrane.
5. Float the Float-A-Lyzer vertically in the dialysate reservoir containing a stir bar and adjust the stirring rate to form a gentle rotating current. Be careful not to create a strong vortex that can pull the device down and interfere with the stir bar.
6. Dialyze the samples at room temperature during 30 h approx. with buffer changes after 2 h, 4 h, 7h, 24 h and 30 h. Before changing the buffer take some sample from the external reservoir for further analysis (fluorescence, HPLC, etc.).
7. After dialysis, open screw-on cap, and retrieve total sample volume by slowly aspirating while inserting pipette toward bottom of membrane. Make sure to retrieve every drop of sample.
8. Dispense sample in appropriate receptacle and discard used Float-A-Lyzer G2.

3.7 Fluorescence analysis and liposomes concentration

In order to analyze the calcein encapsulated, the previously purified liposomes were treated with Triton-X100 (1:1), and were vortexed to release the calcein and determine their fluorescence.

Calcein-encapsulated liposomes and free calcein concentration were indirectly determined by fluorescence using an Infinite 200Pro plate reader. Data was obtained by Tecan i-control 1.10.4.0 software. The reading was performed at 485-520 nm, Corning® low volume 384 well flat bottom black polystyrol plates. A calibration curve of calcein buffer was used to calculate final concentration of calcein that was encapsulated by Lambert-Beer law.

3.8 % Liposomes recovery

The four types of liposomes (neutral, PEGylated-neutral, anionic, and cationic) obtained after purification, were quantitatively analyzed by HPLC-MS and compared against the lipids used for their preparation.

3.9 Encapsulation efficiency (EE)

To determine the encapsulation efficiency, we used PEGylated-neutral liposomes in calcein buffer 1 mM, pH6, centrifuged by DAC with the best parameters previously determined for the first centrifugation run. During the second DAC run, the effects of buffer volume and centrifugation speed were analyzed. The liposomes were purified

by dialysis, the His-Suc buffer was changed and sample was taken from the external dialysis solution at 2h, 4h, 7h, 24h, and 30h of dialysis. After purification, the samples were treated with Triton-X100 1:1 and vortexed to analyze encapsulated calcein, and free calcein from the external solution was also analyzed by fluorescence to indirectly determine the encapsulation efficiency. Encapsulation efficiency was calculated according to the following equations:

$$C1V1 = C2V2;\ C2 = CIVI/V2$$

$$C2V2 = C3V3;\ C3 = C2V2/V3$$

Where C1: Calcein buffer concentration (1mM)

V1: Volume of calcein buffer (200 μL)

C2: Calcein buffer concentration after dilution during 2nd DAC run

V2: Total volume of calcein buffer, considering the buffer added during 2nd DAC. It is the volume of liposomes used for dialysis purification.

C3: Theoretical final concentration in the external dialysis solution.

V3: Volume in the external dialysis solution (100 mL).

$$\%Calcein\ concentration = \frac{Concentration\ at\ each\ time}{C3}$$

$$Total\ Free\ Calcein\ Concentration\ =\ Summatory\ of\ \%Calcein\ for\ each\ time$$

Indirect % EE = 100 – Total Free Calcein Concentration

Mean % EE = Average between 3 EE Replicas

3.10 Zeta potential

The samples were diluted 1:100 (v/v) in PBS buffer pH 6.5. For the measurements the Zetasizer Nano ZS (Malvern Instruments) was used. Every sample passed five measurement cycles at 25°C.

3.11 Storage stability

To investigate the long time stability, the liposomes were stored at 2°C. Directly after preparation and after 3 months the droplet size distribution was determined by dynamic light scattering (DLS). The samples were shaken gently before the measurement to achieve a homogeneous dispersion. Additionally, the zeta potential of the liposomes was determined after 3 months.

3.12 Statistics

The Tukey Test for multiple comparisons was used to evaluate the results using Minitab 18.

4. Results

4.1 Size optimization

Liposomes size was firstly evaluated by using different beads sizes (1.5 and 1.0 mm) and different buffer volumes (150, 200 and 250 μL) during the first DAC run (Table 5).

Table 5. Variable parameters during first DAC run.

Sample	Buffer (μL)	Beads size (mm)
A1	150	1.5
A2	200	1.5
A3	250	1.5
B1	150	1
B2	200	1
B3	250	1

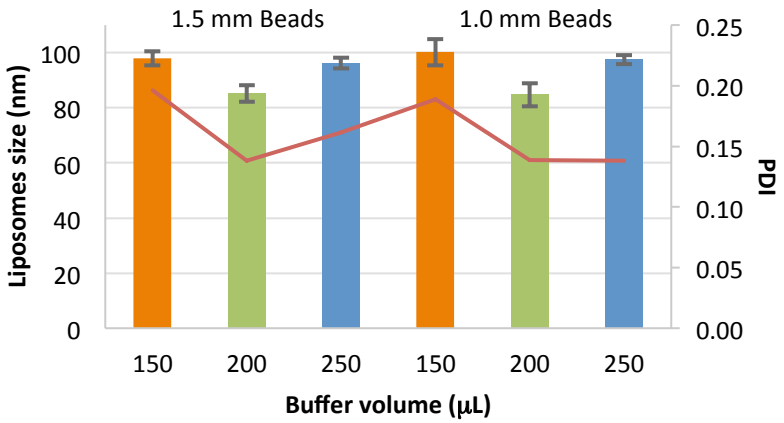

Figure 4. Effect of beads size and buffer volume on liposomes size during first centrifugation run. The red line corresponds to the PDI values.

The use of different beads sizes (1.0 mm and 1.5 mm) did not affect liposomes size. Also, some tests were made with 0.5 mm beads and a combination of 1.5 and 0.5 mm beads, and no effect was observed either. These results are in accordance to the ones previously reported by Massing et al.[121] In the other hand, buffer volume plays a significant role over liposomes size (Figure 4). Liposomes of 80 nm were achieved using 200 μL of calcein buffer during the first run at PDI<0.2.

The PDI was used as an indicator for nanoparticle stability and uniformity of formation. The PDI value reflects the nanoparticle size distribution; samples with a wider range of particle sizes have higher PDI values, while samples consisting of evenly sized particles have lower PDI values. In this case, the obtention of PDI lower than 0.2 (closer to zero) indicates the presence of more monodisperse liposomes and greater particle stability.[134]

The influence of time during the first centrifugation (15 min, 30 min, and 60 min) and type of buffer (Histidine-Sucrose and PBS, pH 6.5) was evaluated using 200 μL of buffer during the first run, since it was the volume that led to a smaller liposome size., Time of centrifugation was not a significant variable between 15 min and 30 min, which agrees with Massing et al. discussion: "20 to 30 min is necessary to get small liposomes with only minimal size differences between the batches".[121] In this work we were able to reduce DAC time to 15 min with reproducible results and low PDI (<0.15). In addition, at 60 min liposomes size increased, most likely because of particle aggregation. This result is also in accordance to previous publications.[124]

Meanwhile, type of buffer affected liposomes size, otherwise the results reported by Akschuti in 2005, where he discussed that Histidine buffer (pH 6.5) and PBS (pH 7.4) had no influence on liposome size.[124] Using PBS buffer helped to reduce liposomes size to 70 nm, which can be achieved at 15 min of centrifugation, and with a PDI<0.15. Most likely, the favorable effect of PBS buffer can be attributed to its lower viscosity, in comparison to His-Suc buffer, which has a very high viscosity because of the high proportion of sucrose that it contains (1:9).

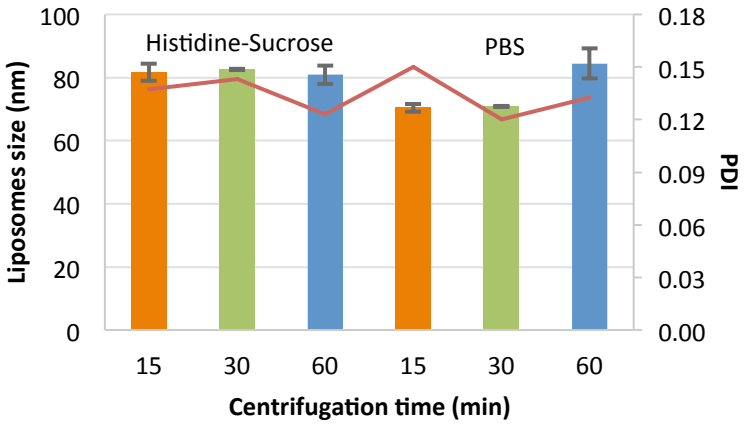

Figure 5. Effect of buffer type and DAC time on liposomes size during first centrifugation run. The red line corresponds to the PDI values.

4.2 Purification efficiency of calcein using Sephadex columns, Zeba-Spin columns and Dialysis Float-A-Lyzers.

The calibration curve obtained for calcein buffer 1 mM was used to calculate the purification efficiency for each experiment.

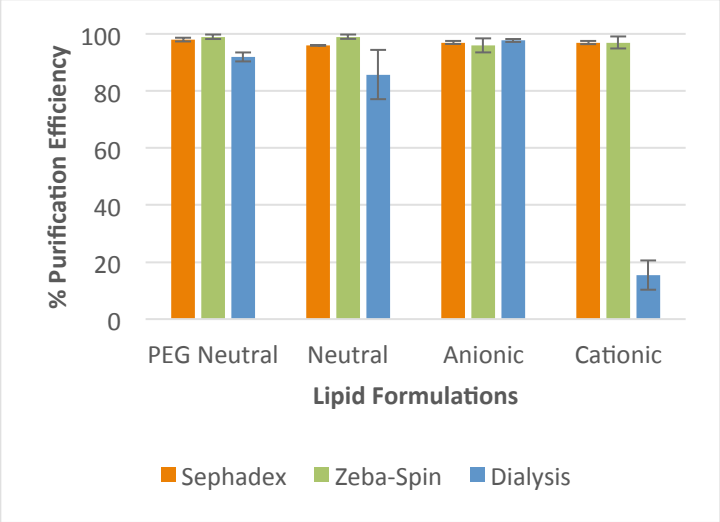

Figure 6. Purification efficiency of calcein using Sephadex, Zeba-Spin and Dialysis.

Table 6. % Liposomes Recovery

	Sephadex	Zeba-Spin	Dialysis
PEG Neutral	0	0	93.08
Neutral	0	0	87.1
Anionic	0	0	96.4
Cationic	0	0.52	100

Dialysis Float-A-Lyzers showed the best results for free calcein removal (Figure 7) and highest recovery of calcein-encapsulated liposomes with negative and neutral charge (Table 6). However, in this case they were inefficient for cationic liposomes, most likely due to ionic interactions between the negatively charged dye and positively charged liposomal surface. The use of another pH buffer is recommended for cationic liposomes.

After using Sephadex and Zeba-Spin columns, both the free calcein and the liposomes were retained in the column. Although both columns seemed to lead to high purification efficiencies (Figure 7), the retention effect might be due to low elution volume, recommended by the manufacturer. When we analyzed the corresponding fractions by HPLC-MS, we found out that the columns did not show any liposomes recovery (Table 6). Therefore, following the manufacturer procedure for both columns, the free calcein and the liposomes remained in the column.

Additional tests were made with Zeba-Spin and Micro-Spin columns. A comparison of the purification of PEGylated neutral liposomes with calcein encapsulated against free calcein buffer 1 mM was done for both purification systems. Centrifugation parameters were followed according to manufacturer's protocol. But in this case, after sample centrifugation, 50 μL of His-Suc buffer was added to the column and centrifuged, repeating this step until a clear solution was observed.

Calcein-encapsulated liposomes were purified with Zeba-Spin columns, (Figure 7) obtaining 9 fractions. A colored solution was visually observed between fractions 2 and 7. This purification procedure took 22 min.

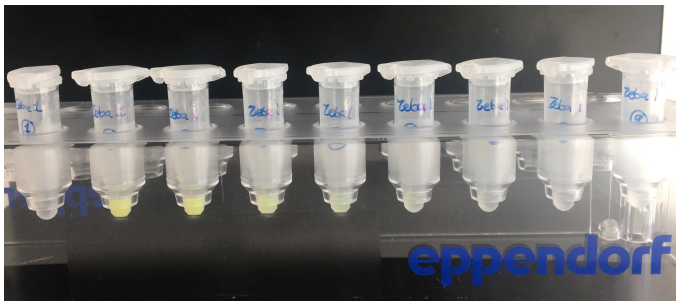

Figure 7. Calcein-encapsulated liposomes purified by Zeba-Spin columns.

Free calcein buffer 1 mM was passed through the Zeba-Spin columns (Figure 8), and 11 fractions were obtained. A colored solution was observed in fractions 1 to 9. This procedure took in total 26 min.

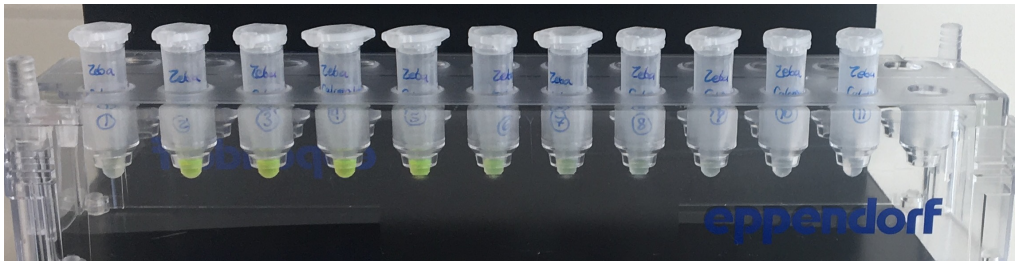

Figure 8. Free calcein buffer 1 mM purified by Zeba-Spin columns.

Calcein-encapsulated liposomes were purified with Sephadex Micro-Spin columns (Figure 9), obtaining 11 fractions. A colored solution was visually observed between fractions 3 and 9. This purification procedure took 23 min.

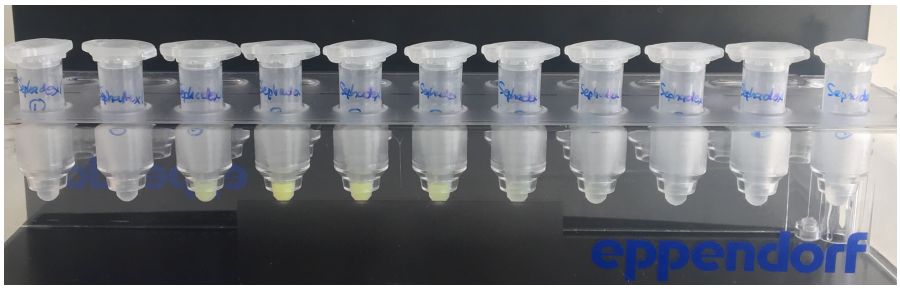

Figure 9. Calcein-encapsulated liposomes purified by Micro-Spin columns.

Free calcein buffer 1 mM was passed through the Sephadex Micro-Spin columns (Figure 10), and 14 fractions were obtained. A colored solution was observed in fractions 2 to 12. This procedure took in total 29 min.

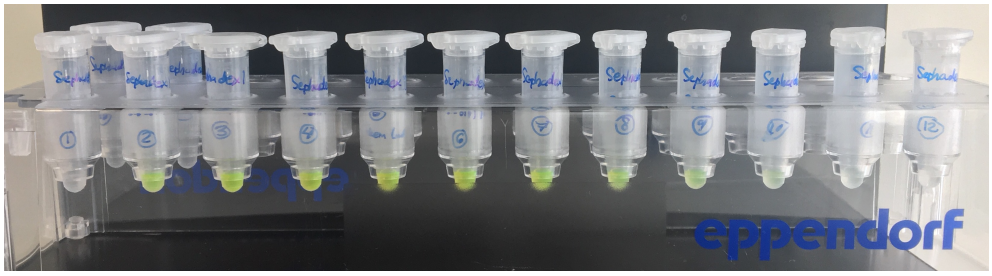

Figure 10. Free calcein buffer 1 mM purified by Micro-Spin columns.

The efficiency of purification for both types of columns was evaluated by comparing the concentration of free calcein against the concentration of liposomes-encapsulated calcein for each fraction (Figure 11).

Three repetitions (columns) were done for each sample. We calculated the summatory of the fractions concentrations for each column, and this was considered the Total Concentration for each column.

Theoretical Concentration. The average of the Total Concentrations for the 3 repetitions, represents the 100% of calcein eluted.

Experimental Concentration. The average of the 3 repetitions was calculated for each fraction concentration.

$$\%\ Calcein\ Elution = \frac{Experimental\ Concentration}{Theoretical\ Concentration} x\ 100$$

These calculations were repeated for the 4 cases (free calcein from Zeba-Spin column, calcein-encapsulated from Zeba-Spin column, free calcein from Sephadex column, and calcein-encapsulated from Sephadex column).

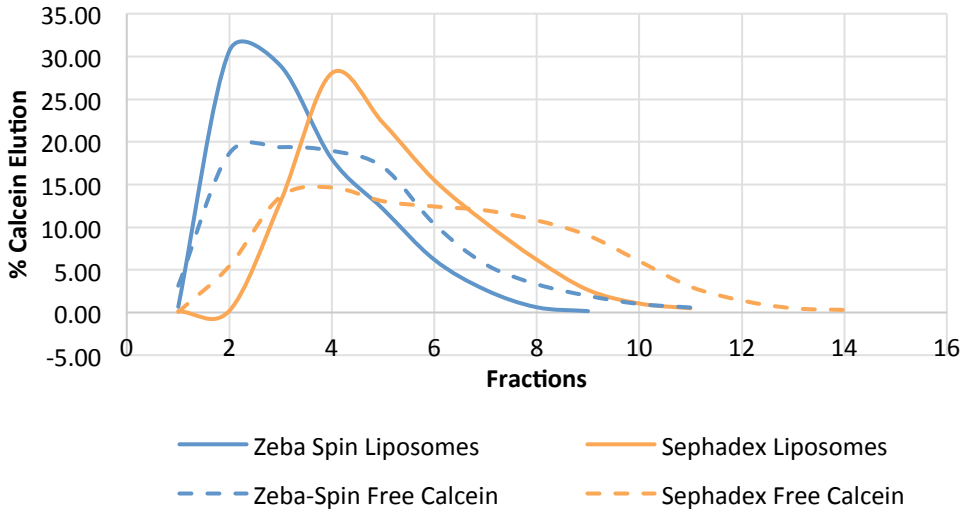

Figure 11. Purification of calcein-encapsulated liposomes and free calcein buffer by Zeba-Spin and Micro-Spin columns. %Calcein elution represents either the free calcein or calcein-encapsulated from liposomes that was eluted in each fraction.

Free calcein dye was not retained in the Zeba-Spin or Sephadex Micro-Spin columns, it was obtained in the same fractions as the liposomes. Therefore, Zeba-Spin columns and Sephadex Micro-Spin columns are not recommended for liposomes purification following the manufacturer's protocol. Dialysis Float-A-Lyzers is the best option for negative and neutral liposomes purifications during the screening process.

4.3 Effect of second DAC parameters on Encapsulation Efficiency

PEGylated-neutral liposomes, were centrifuged by DAC with the best parameters previously determined for the first centrifugation run (Table 7). The variable parameters during the DAC were buffer volume and speed of centrifugation during the second DAC run (Table 8).

Table 7. Constant parameters used during the first DAC run.

Lipid weight	100 mg	
Beads weight	600 mg	
DAC	**1st Run**	**2nd Run**
Buffer volume	200 µL	Variable
Speed	2350 rpm	Variable
Time	15 min	2 min
Temperature	40°C	40°C

Table 8. Variable parameters and results of second DAC run

Sample	Buffer	Speed (rpm)	Size (nm)	PDI	% EE	STD of EE
A	**400 µL**	1250	94.0	0.153	56.3	0.906
B	**800 µL**	1250	89.9	0.130	52.0	3.250
C	**1200 µL**	1250	91.1	0.129	**71.4***	2.404*
D	800 µL	**600**	90.8	0.112	57.9	2.175
E	800 µL	**1250**	89.8	0.118	59.2	0.806
F	800 µL	**2350**	93.5	0.142	61.8	3.116

* Significant increment of %EE according to Tukey test for experiment C.

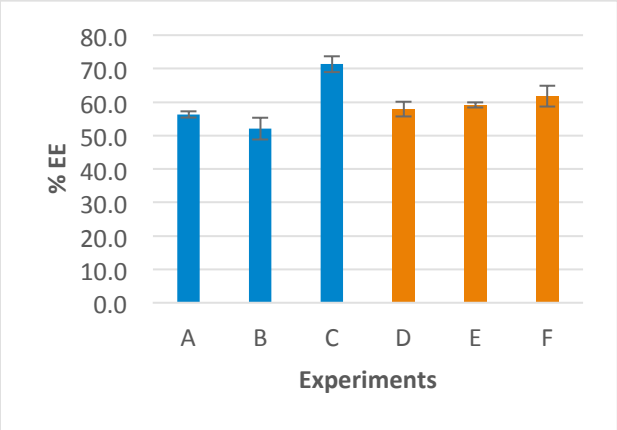

Figure 12. Comparison between the effect of buffer volume and the effect of DAC speed on Encapsulation Efficiency.

Figure 13 shows the statistical results obtained from the average of three replicas for two independent analysis: buffer volume (blue), and speed of centrifugation (orange)

during the second DAC stage. Experiments A-C varied buffer volume during second DAC run, and speed remained constant at 1250 rpm. A. 400 μL buffer, B. 800 μL buffer, C. 1200 μL buffer. Experiments D-F varied speed of centrifugation during second run and buffer remained constant at 800 μL. D. 600 rpm, E. 1250 rpm. F. 2350 rpm.

According to Tukey test, there was a significant difference between Experiment C) and the rest of the experiments, and no significant difference between the others. Therefore, the speed of centrifugation was not a significant variable for encapsulation efficiency. Even though other publications showed that accelerating speed from 1000 rpm to 2500 rpm decreased liposome size, and speed reduction led to bigger liposome sizes and broader size distributions.[121,124] Meanwhile, increasing the volume of buffer to 1.2 mL helped to obtain a higher encapsulation efficiency of 71 % (Table 8, Figure 13). The increment in particle size to around 90 nm can be attributed to the fact that we used lipid mixtures that were in storage for about 1 month. It is recommended to use freshly prepared lipid mixes to reduce particle size, as in the case of previous experiments.

DLS and zeta potential measurements allowed to determine that all of the liposomes were stable over three months and no significant difference was observed between their size at 0 and 3 months of storage; which confirms that DAC is a preparation technique that favors the obtention of stable liposomes, as reported before in other publications.[125]

5. Conclusions

DAC parameters were successfully optimized for liposomes preparation with application in screening phase of drug research and development.
The type of buffer and volume were the most effective parameters for reducing liposomes size.
Liposomes of 70 nm were obtained by using 200 μL of PBS buffer after only 15 min during the first centrifugation run.
Dialysis Float-A-Lyzer was the best purification system for neutral and anionic liposomes.
Zeba Spin columns and Micro Spin columns are not suitable for liposomes purification.
The information and strategies obtained from the different purification methods, are not exclusive to liposomes, but applicable to a wide variety of drug delivery systems.
The highest encapsulation efficiency (71%) was accomplished by diluting the lipid mix with a higher buffer volume (1200 μL) during the second DAC run.
The four different liposomes prepared for this work (neutral, PEGylated-neutral, anionic, and cationic) were stable over 3 months of storage at 2°C.
The preparation of liposomes by DAC allowed us to reduce liposomes size, with high drug load concentration and high encapsulation efficiency.

6. Acknowledgements

Global Scientific Capabilities Centre of Excellence in Global Drug Development, Novartis Pharma and the Global Health Office in Novartis Institutes for BioMedical Research, Basel, Switzerland.

General Conclusions

This work focus on two alternatives of controlled drug delivery systems, dendrimers and liposomes, with potential use as carriers of highly active drugs like pristimerin.

We reported the synthesis, purification strategies, and characterization of several compounds as key building blocks for the synthesis of site-specific dendrimers formed by 2,2-bis (hydroxymethyl) propanoic acid (bis-MPA) as a branching molecule, pristimerin as an anticancer drug model; folic acid (FA) to provide selectivity to folate receptors overexpressed in cancer cells; and fluorescein isothiocyanate (FITC), as a fluorescent dye, for future evaluation as cancer treatment.. They represent the most important molecules in the synthetic pathway, since the dendritic architecture comes from the condensation in the next steps. In this way, this work contributes to the advancement in the obtention of the final conjugates.

EB-AS was obtained as an alternative for a branching molecule or dendron with a broad application in the synthesis of polyester dendrimers; its synthesis is simple, and its yield high (80%).

PEGylated compounds, such as C1-PEG3350, were synthesized. C1-PEG3350, in combination with poorly-soluble folic acid, helped to enhance the solubility of the building block in aqueous solution, methanol and DMF. It represents a potential alternative to use as a dendron for multiple applications, since it has two arms with two free carboxylic groups that can be used in combination with other drugs and a benzyl group protecting its other carboxyl, which can be deprotected when needed by hydrogenation, for its application as a dendrimer building block.

Also, the purification of PEGylated compounds was favored by Ultrafiltration (5 kDa) in aqueous solution with a faster and more efficient purification than column chromatography with silica gel.

The syntheses of FITC building blocks, FITC-HMDA, FITC-HMDA-BMPAP were carried out, and the products were more soluble in buffer solution $NaHCO_3$-Na_2CO_3 (0.1 M, pH 9) and Phenomenex C18-E cartridge was a faster purification method than silica gel columns.

Folic acid building blocks (FA-PEG3350-C1 and FA-TEG-NH_2), showed higher purification yields when using dialysis cassettes (7 kDa) and PBS buffer, in comparison to SEC with Sephadex in $NaHCO_3$, or ultrafiltration (5 kDa) in water.

Column chromatography with silica gel represented a good alternative for simple purifications of low molecular weight compounds, such as EB-AS, CI-TEG and pristimerin succinate, that were soluble in inorganic compounds (hexane: ethyl acetate 1:5, ethanol:DCM 1:2, and hexane:acetone 7:3, respectively), since there is no

risk of damaging a dialysis membrane, is a cost effective method and purification yields were above 72%.

C1-PEG3350 can be synthesized with poorly-soluble compounds, like folic acid, enhancing their solubility. Meanwhile, C1-TEG difficulted the synthesis with folic acid, and is not a viable option to use with compounds of low solubility or complex chemical structure. Anyway, C1-TEG can also be used as a dendron but with other compounds of similar solubility. In this way, PEG3350 is a better linker of folic acid than TEG., due its solubility.

The molecular dynamics study validated that PEG chain lengths (750 and 3350 Da) do not interfere over ligand-receptor binding functionality of the proposed dendrimers with folic acid. The folate fragment from both dendrimers remained exposed to the solvent before approaching to folate receptor, so it could selectively direct the dendrimer towards FR-α, where interaction and internalization would be able to occur. In addition, the dendrimer with PEG 3350 may have more interaction with FR-α receptor than the dendrimer with PEG 750. As a result, theoretical evidence supports that the proposed PEG-folic acid dendrimers represent a new viable alternative as drug delivery systems for cancer therapies.

Meanwhile, the determination of the optimal parameters for the preparation of encapsulated liposomes by Dual Asymmetric Centrifugation (DAC) was carried out as part of a new technology applied in pharmaceutical industry.

The results showed that the volume and type of buffer had a signficant effect over the size of liposomes during the first centrifugation stage. Also, buffer volume had a significant effect over encapsulation efficiency during the second centrifugation stage.

As a result, according to the best results obtained from DAC parameters optimization, we were able to prepare liposomes of 70 nm, with high encapsulation efficiency (71%) using 200 μL of PBS buffer during the first centrifugation, and 1.2 mL of buffer during the second centrifugation.

A comparison was made between three purification systems commonly used for liposomes preparation and other drug delivery systems, such as dendrimers. These purification systems were Zeba-Spin columns, Sephadex Micro-Spin columns, and dialysis Float-A-Lyzers.

Dialysis Float-A-Lyzers (100 kDa) was the best system to remove free drug (in this case, calcein) and for the obtention of highly pure liposomes (> 87%) with calcein encapsulated.

Meanwhile, Zeba-Spin and Micro-Spin columns were not useful for liposomes purification, being unable to separate the liposomes from free drug.

Therefore, dialysis represents a great alternative for the purification of PEGylated compounds, folic acid conjugates, and drug delivery systems, as we probed with FA-PEG3350-C1 (73%).

DAC is an affordable, easy, and fast method that can be applied for the encapsulation of highly active drugs, like pristimerin.

Over all, site-specific dendrimers demand a meticulous control on their structure during synthesis. Their preparation is time consuming and analytically complex. Meanwhile, theoretical evidence supports their potential to selectively carry drugs and interact with cancer cell receptors.

Liposomes are a faster, easier and versatile alternative as drug delivery carriers of highly toxic drugs.

Appendix A

Abbreviations and acronyms

2D	two dimensions
3D	tridimensional
5-mTHF	N5-methyltetrahydrofolate
Å	Angstroms
AIDS	Acquired Immunodeficiency Syndrome
API	active pharmaceutical ingredients
AS	succinic anhydride
atm	atmosphere
ATR	Attenuated Total Reflectance
bis-MPA	2,2-bis (hydroxymethyl) propanoic acid
BMP	bis-MPA
BMPA	bis-(2,2-hydroxymethyl)propanoic acid
BMPAP	protection of hydroxyl groups of bis-(2,2,-hydroxymethyl)propanoic acid
BNCT	boron neutron capture therapy
BPO	benzoyl peroxide
CAM	chloramphenicol
$CDCl_3$	deuterated chloroform
CDI	carbonyldiimidazole
CIQA	Centro de Investigación en Química Aplicada
CLs	cationic liposomes
cm	centimeters
COR	core
Da	Daltons
DAC	Dual Asymmetric Centrifugation
DCC	dicyclohexyl carbadoiimide
DCM	dichloromethane
DCU	dicyclohexylurea
DHP	dihydropyran
DI	deionized
DLS	Dynamic Light Scattering
DMAP	dimethylaminopyridine
DMF	dimethylformamide
DMF-d7	deuterated dimethylformamide
DMP	dimethoxypropane
DMSO	dimethylsulfoxide
DNA	Desoxyribonucleic acid
DoE-approach	Design of experiments
DOPC	1,2-Dioleoyl-sn-glycero-3-phosphocholine
DOPS	1,2-di-(9Z-octadecenoyl)-sn-glycero-3-phospho-L-serine

DOTAP-Cl	N-[1-(2,3-dioleoyloxy)propyl]-N,N,N-trimethylammonium chloride
DOX	doxorubicin
DPPC	1,2-dipalmitoyl-sn-glycero-3-phosphocholine
DPTS	1,4-Dimethylpyridinium p-toluenesulfonate
DRG	anticancer drug
DSPE	1,2-distearoyl-sn-glycero-3-phosphoethanolamine
e.g.	for example
EA	ethyl acetate
EB	benzyl 3-hydroxy-2-(hydroxymethyl)-2-methylpropanoate -
EB-AS	benzyl ester of bis-MPA succinylate
EE	Encapsualtion efficiency
EPR	Enhanced Permeability and Retention effect
et al.	and others
etc.	etcetera
FA	folic acid
FA-NHS	Activated folic acid
FBP	folate binding protein
FDA	Food and Drug Administration
FITC	fluorescein isothiocyanate
FMOC	9-fluorenyl- methyloxycarbonyl
FOL	folic acid
FP_{exp}	experimental fusion point
FP_{theo}	theoretical fusion point
FR	folate receptor
FR-α	folate receptor alpha
FRβ	folate receptor beta
FRγ	folate receptor gamma
FT-IR	Fourier Transform Infrared spectroscopy
g	grams
G-3	three generations
G1	one generation
GPC	gel permeation chromatography
h	hours
HCl	hydrochloric acid
His-Suc	Histidine-sucrose
HMDA	1,6-hexamethylene diamine
HPH	high pressure homogenization
HPLC	High Performance Liquid Chromatography
IC50	half maximal inhibitory concentration
ID	identification
K	Kelvin
KB	epithelial human cancer
KCl	potassium chloride
Kd	dispersion coefficient
kDa	kilodalton

Km	Michaelis constant
KOH	potassium hydroxide
kV	kilovolts
L	liter
lab	laboratory
LUV	Large unilamellar vesicles
m/z	mass/charge
MALDI-TOF-MS	Matrix Assisted Laser Desorption/Ionization-Mass Spectrometry
MD	molecular dynamics
MDA-MB-231	human breast cancer cells
mg	milligrams
MgSO4	magnesium sulfate
MHz	megahertz
min	minutes
mL	milliliters
MLV	Multilamellar vesicles
μM	micromolar
mm	millimeters
mM	millimolar
mmol	millimoles
Mn	molecular number
MSD	mean squared displacements
MTT	cell viability and proliferation assay
MW	molecular weight
MWCO	molecular weight cut-off
N	normal
Na_2CO_3	sodium carbonate
NaCl	sodium chloride
$NaHCO_3$-Na_2CO_3	sodium bicarbonate-sodium carbonate
NAMD	Nanoscale Molecular Dynamics
NCEs	New Chemical Entities
NF –Kβ	nuclear factor
NH2-TEG-NH2	diamino triethylene glycol
NHS	N-hydroxysuccinimide
nm	nanometers
nM	nanomolar
NMR	Nuclear Magnetic Resonance
NPT	isothermal-isobaric
ns	nanoseconds
PAMAM	Polyamidoamine
PBS	phosphate buffer saline
PC	phosphatidylcholine
PCS	photon correlation spectroscopy
Pd/C	palladium/carbon
PDB	Protein Data Bank
PDI	polydispersity index

PEG	Polyethylene glycol
PEGylated	with polyethylene glycol
PF theo	theoretical fusion point
pH	potential of hydrogen
PI	Polydispersity Index
Prsitimerin-COOH	pristimerin succinate modification
PS	phosphatidylserine
psi	pounds per square inch
Py	pyridine
Rg	radius of gyration
RNA	Ribonucleic acid
rpm	revolutions per minute
SAS	supercritical anti-solvent
SASA	Solvent Accessible Surface Area
SEC	size exclusion chromatography
siRNA	small interfering ribonucleic acid
SPIT	sterol-based post-insertion technique
SUV	Small unilamellar vesicles
TEA	triethylamine
TEG	triethylene glycol
TES	triethylsilane
THF	tetrahydrofuran
TLC	Thin Layer Chromatography
TMS	tetramethylsilane
Trp	tryptophan
UNAB	Universidad Andrés Bello
UV	ultraviolet
VMD	Visual Molecular Dynamics
VPGs	vesicular phospholipid gels
WHO	World Health Organization
x g	gravities
XTT	2,3-Bis-(2-Methoxy-4-Nitro-5-Sulfophenyl)-2H-Tetrazolium-5-Carboxanilide

References

(1) Geografía, I. N. de E. y. Estadísticas a propósito del día mundial contra el cáncer http://www.inegi.org.mx/saladeprensa/aproposito/2017/cancer2017_Nal.pdf (accessed Oct 10, 2017).

(2) Murray, R. K.; Jacob, M.; Varghese, J. *Harper's Illustrated Biochemistry*; McGraw-Hill Publishers, New York, N.Y., 2012.

(3) Cho, K.; Wang, X.; Nie, S.; Chen, Z.; Shin, D. M. Therapeutic Nanoparticles for Drug Delivery in Cancer. *Clinical Cancer Research*. 2008, pp 1310–1316.

(4) FDA approved drug products 2012. www. accesdata.fda.gov/scripts/cder/drugsatfda/index.cfm (accessed Nov 28, 2012).

(5) Agarwal, A.; Asthana, A.; Gupta, U.; Jain, N. K. Tumour and Dendrimers: A Review on Drug Delivery Aspects. *J. Pharm. Pharmacol.* **2008**, *60*, 671–688.

(6) Chen, C.; Ke, J.; Zhou, X. E.; Yi, W.; Brunzelle, J. S.; Li, J.; Yong, E.-L.; Xu, H. E.; Melcher, K. Structural Basis for Molecular Recognition of Folic Acid by Folate Receptors. *Nature* **2013**, *500* (7463), 486–489.

(7) Lu, Y.; Low, P. S. Folate-Mediated Delivery of Macromolecular Anticancer Therapeutic Agents. *Adv. Drug Deliv. Rev.* **2002**, *54* (5), 675–693.

(8) Hilgenbrink, A. R.; Low, P. S. Folate Receptor-Mediated Drug Targeting: From Therapeutics to Diagnostics. *J. Pharm. Sci.* **2005**, *94* (10), 2135–2146.

(9) Hourani, R. Design and Synthesis of Dendrimers for Multipurpose Tasks, Mc. Gill University, 2009.

(10) Duncan, R.; Izzo, L. Dendrimer Biocompatibility and Toxicity. *Advanced Drug Delivery Reviews*. 2005, pp 2215–2237.

(11) Bharali, D. J.; Khalil, M.; Gurbuz, M.; Simone, T. M.; Mousa, S. A. Nanoparticles and Cancer Therapy: A Concise Review with Emphasis on Dendrimers. *Int. J. Nanomedicine* **2009**, *4*, 1–7.

(12) Svenson, S.; Tomalia, D. A. Dendrimers in Biomedical Applications - Reflections on the Field. *Advanced Drug Delivery Reviews*. 2005, pp 2106–2129.

(13) Malik, N.; Evagorou, E. G.; Duncan, R. Dendrimer-Platinate: A Novel Approach to Cancer Chemotherapy. *Anticancer Drugs*. 1999, pp 767–776.

(14) Padilla De Jesús, O. L.; Ihre, H. R.; Gagne, L.; Fréchet, J. M. J.; Szoka, F. C. Polyester Dendritic Systems for Drug Delivery Applications: In Vitro and In Vivo Evaluation. *Bioconjug. Chem.* **2002**, *13* (3), 453–461.

(15) Tekade, R. K.; Kumar, P. V.; Jain, N. K. Dendrimers in Oncology: An Expanding Horizon. *Chem. Rev.* **2009**, *109*, 49–87.

(16) Allen, T. M.; Cullis, P. R. Liposomal Drug Delivery Systems: From Concept to Clinical Applications. *Advanced Drug Delivery Reviews*. 2013, pp 36–48.

(17) Gatter, K.; Brown, G.; Trowbridge, I.; Woolston, R.; Mason, D. Transferrin Receptors in Human Tissues: Their Distribution and Possible Clinical Relevance. *J. Clin. Pathol.* **1983**, *36* (5), 539–545.

(18) Gomes, J. P. M.; Cardoso, C. R. P.; Varanda, E. A.; Molina, J. M.; Fernandez, M. F.; Olea, N.; Carlos, I. Z.; Vilegas, W. Antitumoral, Mutagenic and (Anti)estrogenic Activities of Tingenone and Pristimerin. *Brazilian J. Pharmacogn.* **2011**, *21* (6), 963–971.

(19) Dubé, D.; Francis, M.; Leroux, J. C.; Winnik, F. M. Preparation and Tumor Cell Uptake of poly(N-Isopropylacrylamide) Folate Conjugates. *Bioconjug. Chem.* **2002**, *13* (3), 685–692.

(20) Kono, K.; Liu, M.; Fréchet, J. M. J. Design of Dendritic Macromolecules Containing Folate or Methotrexate Residues. *Bioconjug. Chem.* **1999**, *10* (6), 1115–1121.

(21) Cao, W.; Zhou, J.; Wang, Y.; Zhu, L. Synthesis and in Vitro Cancer Cell Targeting of Folate-Functionalized Biodegradable Amphiphilic Dendrimer-like Star Polymers. *Biomacromolecules* **2010**, *11* (12), 3680–3687.

(22) Yoo, H. S.; Park, T. G. Folate-Receptor-Targeted Delivery of Doxorubicin Nano-Aggregates Stabilized by Doxorubicin-PEG-Folate Conjugate. *J. Control. Release* **2004**, *100* (2), 247–256.

(23) Moon, W. K.; Lin, Y.; O'Loughlin, T.; Tang, Y.; Kim, D. E.; Weissleder, R.; Tung, C. H. Enhanced Tumor Detection Using a Folate Receptor-Targeted near-Infrared Fluorochrome Conjugate. *Bioconjug. Chem.* **2003**, *14* (3), 539–545.

(24) Wang, S.; Lee, R. J.; Mathias, C. J.; Green, M. a; Low, P. S. Synthesis, Purification, and Tumor Cell Uptake of 67Ga-Deferoxamine--Folate, a Potential Radiopharmaceutical for Tumor Imaging. *Bioconjug. Chem.* **1996**, *7* (1), 56–62.

(25) Hermanson, G. T. Bioconjugation Techniques. *Acad. Press* **2008**, *10*, 0123705010.

(26) Quintana, A.; Raczka, E.; Piehler, L.; Lee, I.; Myc, A.; Majoros, I.; Patri, A. K.; Thomas, T.; Mulé, J.; Baker, J. R. Design and Function of a Dendrimer-Based Therapeutic Nanodevice Targeted to Tumor Cells through the Folate Receptor. *Pharm. Res.* **2002**, *19* (9), 1310–1316.

(27) Majoros, I. J.; Myc, A.; Thomas, T.; Mehta, C. B.; Baker, J. R. PAMAM Dendrimer-Based Multifunctional Conjugate for Cancer Therapy: Synthesis, Characterization, and Functionality. *Biomacromolecules* **2006**, *7* (2), 572–579.

(28) Hong, S.; Leroueil, P. R.; Majoros, I. J.; Orr, B. G.; Baker, J. R.; Banaszak Holl, M. M. The Binding Avidity of a Nanoparticle-Based Multivalent Targeted Drug

Delivery Platform. *Chem. Biol.* **2007**, *14* (1), 107–115.

(29) Kukowska-Latallo, J. F.; Candido, K. A.; Cao, Z.; Nigavekar, S. S.; Majoros, I. J.; Thomas, T. P.; Balogh, L. P.; Khan, M. K.; Baker, J. R. Nanoparticle Targeting of Anticancer Drug Improves Therapeutic Response in Animal Model of Human Epithelial Cancer. *Cancer Res.* **2005**, *65* (12), 5317–5324.

(30) Sun, C.; Sze, R.; Zhang, M. Folic Acid-PEG Conjugated Superparamagnetic Nanoparticles for Targeted Cellular Uptake and Detection by MRI. *J. Biomed. Mater. Res. Part A* **2006**, 550–557.

(31) Shukla, S.; Wu, G.; Chatterjee, M.; Yang, W.; Sekido, M.; Diop, L. A.; Müller, R.; Sudimack, J. J.; Lee, R. J.; Barth, R. F.; et al. Synthesis and Biological Evaluation of Folate Receptor-Targeted Boronated PAMAM Dendrimers as Potential Agents for Neutron Capture Therapy. *Bioconjug. Chem.* **2003**, *14* (1), 158–167.

(32) Sagwan, S.; Rao, D. V.; Sharma, R. A. Maytenus Emarginata (Willd.): A Promising Drug for Cancer Therapy. *Asian J. Pharm. Clin. Res.* **2011**, *4* (3), 8–12.

(33) Ramirez Apan, A. A. M. T.; Pérez-Castorena, A. L.; de Vivar, A. R. Anti-Inflammatory Constituents of Mortonia Greggii Gray. *Z. Naturforsch. C.* **2004**, *59* (3-4), 237–243.

(34) Salminen, A.; Lehtonen, M.; Suuronen, T.; Kaarniranta, K.; Huuskonen, J. Terpenoids: Natural Inhibitors of NF-kappaB Signaling with Anti-Inflammatory and Anticancer Potential. *Cell. Mol. Life Sci.* **2008**, *65* (19), 2979–2999.

(35) Hill, M. Structure of Two Triterpenes. Application of Partially Relaxed Fourier Transform 13C Nuclear Magnetic Resonance. *J. Am. Chem. Soc.* **1973**, *95* (19), 6473–6475.

(36) Patri, A. K.; Kukowska-Latallo, J. F.; Baker, J. R. Targeted Drug Delivery with Dendrimers: Comparison of the Release Kinetics of Covalently Conjugated Drug and Non-Covalent Drug Inclusion Complex. *Adv. Drug Deliv. Rev.* **2005**, *57* (15), 2203–2214.

(37) Dinkova-Kostova, A. T.; Liby, K. T.; Stephenson, K. K.; Holtzclaw, W. D.; Gao, X.; Suh, N.; Williams, C.; Risingsong, R.; Honda, T.; Gribble, G. W.; et al. Extremely Potent Triterpenoid Inducers of the Phase 2 Response: Correlations of Protection against Oxidant and Inflammatory Stress. *Proc. Natl. Acad. Sci. U. S. A.* **2005**, *102* (12), 4584–4589.

(38) Rabi, T.; Bishayee, A. Terpenoids and Breast Cancer Chemoprevention. *Breast Cancer Res. Treat.* **2009**, *115* (2), 223–239.

(39) Wu, C.-C.; Chan, M.-L.; Chen, W.-Y.; Tsai, C.-Y.; Chang, F.-R.; Wu, Y.-C. Pristimerin Induces Caspase-Dependent Apoptosis in MDA-MB-231 Cells via Direct Effects on Mitochondria. *Mol. Cancer Ther.* **2005**, *4* (8), 1277–1285.

(40) Yang, H.; Landis-Piwowar, K. R.; Lu, D.; Yuan, P.; Li, L.; Reddy, G. P.-V.; Yuan, X.; Dou, Q. P. Pristimerin Induces Apoptosis by Targeting the Proteasome in Prostate Cancer Cells. *J. Cell. Biochem.* **2008**, *103* (1), 234–244.

(41) Valencia, J. Á.; Álvarez, M. M.; Martínez, V. J.; Micheli, B. J. M.; Pacheco, A.; Bonilla, J. Dendrones Y Dendrímeros Multifuncionales Altamente Cargados: El Concepto Troyano., ITESM, Campus Monterrey, 2010.

(42) Sampogna-Mireles, D.; Valencia, J. Á. Síntesis de Dendrímeros Multifuncionales Como Agentes Terapéuticos Potenciales., ITESM, Campus Monterrey, 2012.

(43) Byun, J. Y.; Kim, M. J.; Eum, D. Y.; Yoon, C. H.; Seo, W. D.; Park, K. H.; Hyun, J. W. Reactive Oxygen Species-Dependent Activation of Bax and Poly (ADP-Ribose) Polymerase-1is Required for Mitochondrial Cell Death Induced by Triterpenoid Pristimerin in Human Cervical Cancer Cells. *Mol. Pharmacol.* **2009**, *76* (4), 1–32.

(44) Eum, D. Y.; Byun, J. Y.; Yoon, C. H.; Seo, W. D.; Park, K. H.; Lee, J. H.; Chung, H. . Triterpenoid Pristimerin Synergizes with Taxol to Induce Cervical Cancer Cell Death through Reactive Oxygen Species-Mediated Mitochondrial Dysfunction. *Anticancer Drugs* **2011**, *22* (8), 763–773.

(45) Lu, Z.; Jin, Y.; Chen, C.; Li, J.; Cao, Q.; Pan, J. Pristimerin Induces Apoptosis in Imatinib-Resistant Chronic Myelogenous Leukemia Cells Harboring T315I Mutation by Blocking NF-kappaB Signaling and Depleting Bcr-Abl. *Mol. Cancer* **2010**, *9* (1), 112.

(46) Luo, D.-Q.; Wang, H.; Tian, X.; Shao, H.-J.; Liu, J.-K. Antifungal Properties of Pristimerin and Celastrol Isolated from Celastrus Hypoleucus. *Pest Manag. Sci.* **2005**, *61* (1), 85–90.

(47) Molina, J.; Fernandez, M. F.; Olea, N.; Carlos, I. Z.; Vilegas, W. Antitumoral, Mutagenic and (Anti)estrogenic Activities of Tingenone and Pristimerin. *J. Nat. Prod.* **2011**, 963–971.

(48) Nagase, M.; Oto, J.; Sugiyama, S.; Yube, K.; Takaishi, Y.; Sakato, N. Apoptosis Induction in HL-60 Cells and Inhibition of Topoisomerase II by Triterpene Celastrol. *Biosci. Biotechnol. Biochem.* **2003**, *67* (9), 1883–1887.

(49) Tiedemann, R. E.; Schmidt, J.; Keats, J. J.; Shi, C. X.; Yuan, X. Z.; Palmer, S. E.; Mao, X.; Schimmer, A. D.; Stewart, A. K. Identification of a Potent Natural Triterpenoid Inhibitor of Proteosome Chymotrypsin-like Activity and NF-kappaB with Antimyeloma Activity in Vitro and in Vivo. *Blood* **2009**, *113* (17), 4027–4037.

(50) López-Barrios, L. Evaluación Del Índice Quimiopreventivo de Fitoquímicos Aislados de Plantas Mexicanas En Células de Hepatoma Murino., ITESM, 2010.

(51) Cho, H. K.; Lone, S.; Kim, D. D.; Choi, J. H.; Choi, S. W.; Cho, J. H.; Kim, J. H.; Cheong, I. W. Synthesis and Characterization of Fluorescein Isothiocyanate (FITC)-Labeled PEO-PCL-PEO Triblock Copolymers for Topical Delivery. *Polymer*

(Guildf). **2009**, *50* (11), 2357–2364.

(52) Jullian, M.; Hernandez, A.; Maurras, A.; Puget, K.; Amblard, M.; Martinez, J.; Subra, G. N-Terminus FITC Labeling of Peptides on Solid Support: The Truth behind the Spacer. *Tetrahedron Lett.* **2009**, *50* (3), 260–263.

(53) Haraguchi, T.; Shimi, T.; Koujin, T.; Hashiguchi, N.; Hiraoka, Y. Spectral Imaging Fluorescence Microscopy. *Genes to Cells* **2002**, *7*, 881–887.

(54) Deka, C.; Lehnert, B. E.; Lehnert, N. M.; Jones, G. M.; Sklar, L. A.; Steinkamp, J. A. Analysis of Fluorescence Lifetime and Quenching of FITC-Conjugated Antibodies on Cells by Phase-Sensitive Flow Cytometry. *Cytometry* **1996**, *25*, 271–279.

(55) Staines, W.; Meister, B.; Melander, T.; Nagy, J.; Hökfelt, T. Three-Color Immunofluorescence Histochemistry Allowing Triple Labeling within a Single Section. *J. Histochem. Cytochem.* **1998**, *36* (2), 145–151.

(56) Beckton; Dickinson. *Introduction to Flow Cytometry: A Learning Guide*; 2000; Vol. 11.

(57) Mandal, P. K.; McMurray, J. S. Pd - C-Induced Catalytic Transfer Hydrogenation with Triethylsilane. *J. Org. Chem.* **2007**, *72*, 6599–6601.

(58) Li, R.; Wu, R.; Zhao, L.; Hu, Z.; Guo, S.; Pan, X.; Zou, H. Folate and Iron Difunctionalized Multiwall Carbon Nanotubes as Dual-Targeted Drug Nanocarrier to Cancer Cells. *Carbon N. Y.* **2011**, *49* (5), 1797–1805.

(59) Lafrance, D.; Bowles, P.; Leeman, K.; Rafka, R. Mild Decarboxylative Activation of Malonic Acid Derivatives by 1,1'-Carbonyldiimidazole. *Org. Lett.* **2011**, *13* (9), 2322–2325.

(60) de la Re, B. Proceso de Extracción Y Modificaciones Químicas de Ácido Oleanólico de Phoradendro Tomentosum Y Su Uso Para Tratar Cáncer, Instituto Tecnológico y de Estudios Superiores de Monterrey, 2010.

(61) Aronov, O.; Horowitz, A. T.; Gabizon, A.; Gibson, D. Folate-Targeted PEG as a Potential Carrier for Carboplatin Analogs. Synthesis and in Vitro Studies. *Bioconjug. Chem.* **2003**, *14* (3), 563–574.

(62) Chen, Q.; Li, K.; Wen, S.; Liu, H.; Peng, C.; Cai, H.; Shen, M.; Zhang, G.; Shi, X. Targeted CT / MR Dual Mode Imaging of Tumors Using Multifunctional Dendrimer-Entrapped Gold Nanoparticles. *Biomaterials* **2013**, *34* (21), 5200–5209.

(63) Van Dongen, M. A.; Silpe, J. E.; Dougherty, C. A.; Kanduluru, A. K.; Choi, S. K.; Orr, B. G.; Low, P. S.; Banaszak Holl, M. M. Avidity Mechanism of Dendrimer-Folic Acid Conjugates. *Mol. Pharm.* **2014**, *11* (5), 1696–1706.

(64) Myers, B. K.; Lapucha, J. E.; Grayson, S. M. Synthesis and MALDI-ToF Characterization of Dendronized Poly(ethylene Glycol)s. *Brazilian J. Pharm. Sci.* **2013**, *49* (SPL.ISS.), 45–55.

(65) Yu, D.; Vladimirov, N.; Fréchet, J. M. J. MALDI-TOF in the Characterizations of Dendritic - Linear Block Copolymers and Stars. *Macromolecules* **1999**, *32* (16), 5186–5192.

(66) Arnold, W.; von Mayersbach, H. Changes in the Solubility of Immunoglobulins after Fluorescent Labeling and Its Influence on Immunofluorescent Techniques. *J. Histochem. Cytochem.* **1972**, *20* (12), 975–985.

(67) Sampogna-Mireles, D.; Araya-Durán, I. D.; Márquez-Miranda, V.; Valencia-Gallegos, J. A.; González-Nilo, F. D. Structural Analysis of Binding Functionality of Folic Acid-PEG Dendrimers against Folate Receptor. *J. Mol. Graph. Model.* **2017**, *72*, 201–208.

(68) Cohen, M. S.; Cai, S.; Xie, Y.; Forrest, M. L. A Novel Intralymphatic Nanocarrier Delivery System for Cisplatin Therapy in Breast Cancer with Improved Tumor Efficacy and Lower Systemic Toxicity in Vivo. *Am. J. Surg.* **2009**, *198* (6), 781–786.

(69) Peer, D.; Karp, J. M.; Hong, S.; Farokhzad, O. C.; Margalit, R.; Langer, R. Nanocarriers as an Emerging Platform for Cancer Therapy. *Nat. Nanotechnol.* **2007**, *2* (12), 751–760.

(70) King Heiden, T. C.; Dengler, E.; Kao, W. J.; Heideman, W.; Peterson, R. E. Developmental Toxicity of Low Generation PAMAM Dendrimers in Zebrafish. *Toxicol. Appl. Pharmacol.* **2007**, *225* (1), 70–79.

(71) Jones, D. E.; Ghandehari, H.; Facelli, Julio, C. Predicting Cytotoxicity of PAMAM Dendrimers Using Molecular Descriptors. *Beilstein J. Nanotechnol.* **2015**, *6*, 1886–1896.

(72) Gillies, E. R.; Fréchet, J. M. J. Designing Macromolecules for Therapeutic Applications: Polyester Dendrimer-Poly(ethylene Oxide) "bow-Tie" hybrids with Tunable Molecular Weight and Architecture. *J. Am. Chem. Soc.* **2002**, *124* (47), 14137–14146.

(73) Mintzer, M. a; Grinstaff, M. W. Biomedical Applications of Dendrimers: A Tutorial. *Chem. Soc. Rev.* **2011**, *40* (1), 173–190.

(74) Ihre, H.; Hult, A.; Fréchet, J. M. J.; Gitsov, I. Double-Stage Convergent Approach for the Synthesis of Functionalized Dendritic Aliphatic Polyesters Based on 2,2-Bis(hydroxymethyl)propionic Acid. *Macromolecules* **1998**, *31* (13), 4061–4068.

(75) Ihre, H.; Hult, A.; Söderlind, E. Synthesis, Characterization, and 1H NMR Self-Diffusion Studies of Dendritic Aliphatic Polyesters Based on 2,2-Bis(hydroxymethyl)propionic Acid and 1,1,1-Tris(hydroxyphenyl)ethane. *J. Am.*

Chem. Soc. **1996**, *118* (27), 6388–6395.

(76) Twibanire, J. D. amour K.; Grindley, T. B. Polyester Dendrimers. *Polymers*. 2012, pp 794–879.

(77) Stella, B.; Arpicco, S.; Peracchia, M. T.; Desmaële, D.; Hoebeke, J.; Renoir, M.; D'Angelo, J.; Cattel, L.; Couvreur, P. Design of Folic Acid-Conjugated Nanoparticles for Drug Targeting. *J. Pharm. Sci.* **2000**, *89* (11), 1452–1464.

(78) Kelemen, L. E. The Role of Folate Receptor ?? In Cancer Development, Progression and Treatment: Cause, Consequence or Innocent Bystander? *International Journal of Cancer*. 2006, pp 243–250.

(79) Patri, A. K.; Kukowska-Latallo, J. F.; Baker, J. R. Targeted Drug Delivery with Dendrimers: Comparison of the Release Kinetics of Covalently Conjugated Drug and Non-Covalent Drug Inclusion Complex. *Advanced Drug Delivery Reviews*. 2005, pp 2203–2214.

(80) Gianella, A.; Mieszawska, A. J.; Hoeben, F. J. M.; Janssen, H. M.; Jarzyna, P. a; Cormode, D. P.; Costa, K. D.; Rao, S.; Farokhzad, O. C.; Langer, R.; et al. Synthesis and in Vitro Evaluation of a Multifunctional and Surface-Switchable Nanoemulsion Platform. *Chem. Commun. (Camb).* **2013**, *49*, 9392–9394.

(81) Boas, U.; Heegaard, P. M. H. Dendrimers in Drug Research. *Chem. Soc. Rev.* **2004**, *33* (1), 43–63.

(82) Wu, J.; Zhao, C.; Lin, W.; Hu, R.; Wang, Q.; Chen, H.; Li, L.; Chen, S.; Zheng, J. Binding Characteristics between Polyethylene Glycol (PEG) and Proteins in Aqueous Solution. *J. Mater. Chem. B* **2014**, *2*, 2983–2992.

(83) Bhadra, D.; Bhadra, S.; Jain, S.; Jain, N. K. A PEGylated Dendritic Nanoparticulate Carrier of Fluorouracil. *Int. J. Pharm.* **2003**, *257* (1-2), 111–124.

(84) Li, D.; Li, P.; Lin, H.; Jiang, Z.; Guo, L.; Li, B. A Novel Chlorin-PEG-Folate Conjugate with Higher Water Solubility, Lower Cytotoxicity, Better Tumor Targeting and Photodynamic Activity. *J. Photochem. Photobiol. B Biol.* **2013**, *127*, 28–37.

(85) Vartapetian, R. S.; Khozina, E. V; Kärger, J.; Geschke, D.; Rittig, F.; Feldstein, M. M.; Chalykh, A. E. Molecular Dynamics in poly(N-Vinylpyrrolidone)-Poly(ethylene Glycol) Blends Investigated by the Pulsed-Field Gradient NMR Method: Effects of Aging, Hydration and PEG Chain Length. *Macromol. Chem. Phys.* **2001**, *202* (12), 2648–2656.

(86) Bekale, L.; Agudelo, D.; Tajmir-Riahi, H. a. The Role of Polymer Size and Hydrophobic End-Group in PEG-Protein Interaction. *Colloids Surf. B. Biointerfaces* **2015**, *130*, 141–148.

(87) Mu, Q.; Hu, T.; Yu, J. Molecular Insight into the Steric Shielding Effect of PEG on the Conjugated Staphylokinase: Biochemical Characterization and Molecular

Dynamics Simulation. *PLoS One* **2013**, *8* (7), 1–10.

(88) Arima, H.; Yoshimatsu, A.; Ikeda, H.; Ohyama, A.; Motoyama, K.; Higashi, T.; Tsuchiya, A.; Niidome, T.; Katayama, Y.; Hattori, K.; et al. Folate-PEG-Appended Dendrimer Conjugate with α-Cyclodextrin as a Novel Cancer Cell-Selective siRNA Delivery Carrier. *Mol. Pharm.* **2012**, *9* (9), 2591–2604.

(89) Cao, W.; Zhou, J.; Mann, A.; Wang, Y.; Zhu, L. Folate-Functionalized Unimolecular Micelles Based on a Degradable Amphiphilic Dendrimer-like Star Polymer for Cancer Cell-Targeted Drug Delivery. *Biomacromolecules* **2011**, *12* (7), 2697–2707.

(90) Müller, K.; Kessel, E.; Klein, P. M.; Höhn, M.; Wagner, E. Post-PEGylation of Si-RNA Lipo-Oligoamino Amide Polyplexes Using Tetra-Glutamylated Folic Acid as Ligand for Receptor-Targeted Delivery. *Mol. Pharm.* **2016**, *13*, 2332–2346.

(91) Kim, Y.; Klutz, A. M.; Jacobson, K. A. Systematic Investigation of Polyamidoamine Dendrimers Surface-Modified with Poly(ethylene Glycol) for Drug Delivery Applications: Synthesis, Characterization, and Evaluation of Cytotoxicity. *Bioconjug. Chem.* **2008**, *19* (8), 1660–1672.

(92) Yang, H.; Morris, J. J.; Lopina, S. T. Polyethylene Glycol-Polyamidoamine Dendritic Micelle as Solubility Enhancer and the Effect of the Length of Polyethylene Glycol Arms on the Solubility of Pyrene in Water. *J. Colloid Interface Sci.* **2004**, *273* (1), 148–154.

(93) Lee, H.; Larson, R. G. Molecular Dynamics Study of the Structure and Interparticle Interactions of Polyethylene Glycol-Conjugated PAMAM Dendrimers. *J. Phys. Chem. B* **2009**, *113* (40), 13202–13207.

(94) Mangoni, M.; Roccatano, D.; Di Nola, A. Docking of Flexible Ligands to Flexible Receptors in Solution by Molecular Dynamics Simulation. *Proteins Struct. Funct. Genet.* **1999**, *35* (2), 153–162.

(95) Perche, F.; Torchilin, V. P. Recent Trends in Multifunctional Liposomal Nanocarriers for Enhanced Tumor Targeting. *J. Drug Deliv.* **2013**, *2013*, 705265.

(96) Mori, A.; Klibanov, A. L.; Torchilin, V. P.; Huang, L. Influence of the Steric Barrier Activity of Amphipathic Poly(ethyleneglycol) and Ganglioside GM1 on the Circulation Time of Liposomes and on the Target Binding of Immunoliposomes in Vivo. *FEBS Lett.* **1991**, *284* (2), 263–266.

(97) Gabizon, A.; Shmeeda, H.; Horowitz, A. T.; Zalipsky, S. Tumor Cell Targeting of Liposome-Entrapped Drugs with Phospholipid-Anchored Folic Acid-PEG Conjugates. *Advanced Drug Delivery Reviews*. 2004, pp 1177–1192.

(98) Márquez-Miranda, V.; Camarada, M. B.; Araya-Durán, I.; Varas-Concha, I.; Almonacid, D. E.; González-Nilo, F. D. Biomimetics: From Bioinformatics to Rational Design of Dendrimers as Gene Carriers. *PLoS One* **2015**, *10* (9).

(99) Camarada, M. B.; Márquez-Miranda, V.; Araya-Durán, I.; Yévenes, A.; González-Nilo, F. D. PAMAM G4 Dendrimers as Inhibitors of the Iron Storage Properties of Human L-Chain Ferritin. *PCCP* **2015**, *17*, 19001–19011.

(100) Leiva, A.; Fuentes, I.; Bossel, E.; Urzúa, M.; Méndez, M.; Pino, M.; Radic, D.; Márquez, V.; González-Nilo, F. D. Block Copolymers in the Synthesis of Gold Nanoparticles. Two New Approaches: Copolymer Aggregates as Reductants and Stabilizers and Simultaneous Formation of Copolymer Aggregates and Gold Nanoparticles. *J. Polym. Sci. Part A* **2014**, *52* (21), 3069–3079.

(101) Vergara-Jaque, A.; Comer, J.; Monsalve, L.; Gonz??lez-Nilo, F. D.; Sandoval, C. Computationally Efficient Methodology for Atomic-Level Characterization of Dendrimer-Drug Complexes: A Comparison of Amine- and Acetyl-Terminated PAMAM. *J. Phys. Chem. B* **2013**, *117* (22), 6801–6813.

(102) Avila-Salas, F.; Sandoval, C.; Caballero, J.; Gui??ez-Molinos, S.; Santos, L. S.; Cachau, R. E.; Gonz??lez-Nilo, F. D. Study of Interaction Energies between the PAMAM Dendrimer and Nonsteroidal Anti-Inflammatory Drug Using a Distributed Computational Strategy and Experimental Analysis by ESI-MS/MS. *J. Phys. Chem. B* **2012**, *116* (7), 2031–2039.

(103) Vanommeslaeghe, K.; Hatcher, E.; Acharya, C.; Kundu, S.; Zhong, S.; Shim, J.; Darian, E.; Guvench, O.; Lopes, P.; Vorobyov, I.; et al. CHARMM General Force Field: A Force Field for Drug-like Molecules Compatible with the CHARMM All-Atom Additive Biological Force Fields. *J. Comput. Chem.* **2010**, *31* (4), 671–690.

(104) ParamChem http://cgenff.paramchem.org.

(105) Jorgensen, W. L.; Chandrasekhar, J.; Madura, J. D.; Impey, R. W.; Klein, M. L. Comparison of Simple Potential Functions for Simulating Liquid Water. *J. Chem. Phys.* **1983**, *79* (2), 926.

(106) Della-Longa, S.; Arcovito, A. Intermediate States in the Binding Process of Folic Acid to Folate Receptor α: Insights by Molecular Dynamics and Metadynamics. *J. Comput. Aided. Mol. Des.* **2015**, *29* (1), 23–35.

(107) Phillips, J. C.; Braun, R.; Wang, W.; Gumbart, J.; Tajkhorshid, E.; Villa, E.; Chipot, C.; Skeel, R. D.; Kalé, L.; Schulten, K.; et al. Scalable Molecular Dynamics with NAMD. *Journal of Computational Chemistry*. 2005, pp 1781–1802.

(108) Pawar, S. K.; Vavia, P. Efficacy Interactions of PEG-DOX-N-Acetyl Glucosamine Prodrug Conjugate for Anticancer Therapy. *Eur. J. Pharm. Biopharm.* **2015**, *97*, 454–463.

(109) Maziarz, K. M.; Monaco, H. L.; Shen, F.; Ratnam, M. Complete Mapping of Divergent Amino Acids Responsible for Differential Ligand Binding of Folate Receptors α and β. *J. Biol. Chem.* **1999**, *274* (16), 11086–11091.

(110) Sinnokrot, M. O.; Valeev, E. F.; Sherrill, C. D. Estimates of the Ab Initio Limit for

π-π Interactions: The Benzene Dimer. *J. Am. Chem. Soc.* **2002**, *124* (36), 10887–10893.

(111) Martinez, C. R.; Iverson, B. L. Rethinking the Term "pi-Stacking." *Chem. Sci.* **2012**, *3* (7), 2191.

(112) Schmidtke, P.; Luque, F. J.; Murray, J. B.; Barril, X. Shielded Hydrogen Bonds as Structural Determinants of Binding Kinetics: Application in Drug Design. *J. Am. Chem. Soc.* **2011**, *133* (46), 18903–18910.

(113) Pandey, H.; Rani, R.; Agarwal, V. Liposome and Their Applications in Cancer Therapy Human & Animal Health. *Arch. Biol. Technol. v. Arch. Biol. Technol. v* **2016**, *59*, 1–10.

(114) Hirsch, M.; Ziroli, V.; Helm, M.; Massing, U. Preparation of Small Amounts of Sterile siRNA-Liposomes with High Entrapping Efficiency by Dual Asymmetric Centrifugation (DAC). *J. Control. Release* **2009**, *135* (1), 80–88.

(115) Weissing, V. *Liposomes - Methods and Protocols*; Walker, J. M., Ed.; Springer New York Dordrecht Heidelberg London: Glendale, AZ, 2010; Vol. 1.

(116) Ganta, S.; Devalapally, H.; Shahiwala, A.; Amiji, M. A Review of Stimuli-Responsive Nanocarriers for Drug and Gene Delivery. *J. Control. Release* **2008**, *126* (3), 187–204.

(117) Verma, D. D.; Verma, S.; Blume, G.; Fahr, A. Particle Size of Liposomes Influences Dermal Delivery of Substances into Skin. *Int. J. Pharm.* **2003**, *258* (1-2), 141–151.

(118) Hagedorn, M.; Bögershausen, A.; Rischer, M.; Schubert, R.; Massing, U. Dual Centrifugation – A New Technique for Nanomilling of Poorly Soluble Drugs and Formulation Screening by an DoE-Approach. *Int. J. Pharm.* **2017**, *530* (1-2), 79–88.

(119) Kelly, C.; Jefferies, C.; Cryan, S.-A. Targeted Liposomal Drug Delivery to Monocytes and Macrophages. *J. Drug Deliv.* **2011**, *2011*, 1–11.

(120) Safinya, C. R. Structures of Lipid-DNA Complexes: Supramolecular Assembly and Gene Delivery. *Curr. Opin. Struct. Biol.* **2001**, *11* (4), 440–448.

(121) Massing, U.; Cicko, S.; Ziroli, V. Dual Asymmetric Centrifugation (DAC)-A New Technique for Liposome Preparation. *J. Control. Release* **2008**, *125* (1), 16–24.

(122) Sun, W. Q.; Leopold, A. C.; Crowe, L. M.; Crowe, J. H. Stability of Dry Liposomes in Sugar Glasses. *Biophys. J.* **1996**, *70* (4), 1769–1776.

(123) Ingebrigtsen, S. G.; Škalko-Basnet, N.; Holsæter, A. M. Development and Optimization of a New Processing Approach for Manufacturing Topical Liposomes-in-Hydrogel Drug Formulations by Dual Asymmetric Centrifugation.

Drug Dev. Ind. Pharm. **2016**, *9045* (February), 1–33.

(124) Akschuti, D. Liposomal Nanomedicine – Qualification of a New Technology as a Screening Tool for Liposomal Formulations. **2015**.

(125) Tenambergen, F.; Maruiama, C. H.; Mäder, K. Dual Asymmetric Centrifugation as an Alternative Preparation Method for Parenteral Fat Emulsions in Preformulation Development. *Int. J. Pharm.* **2013**, *447* (1-2), 31–37.

(126) Adrian, J. E.; Wolf, A.; Steinbach, A.; Rössler, J.; Süss, R. Targeted Delivery To Neuroblastoma of Novel siRNA-Anti-GD2-Liposomes Prepared by Dual Asymmetric Centrifugation and Sterol-Based Post-Insertion Method. *Pharm. Res.* **2011**, *28* (9), 2261–2272.

(127) Parmentier, J.; Hofhaus, G.; Thomas, S.; Cuesta, L. C.; Gropp, F.; Schr??der, R.; Hartmann, K.; Fricker, G. Improved Oral Bioavailability of Human Growth Hormone by a Combination of Liposomes Containing Bio-Enhancers and Tetraether Lipids and Omeprazole. *J. Pharm. Sci.* **2014**, *103* (12), 3985–3993.

(128) Tian, W.; Schulze, S.; Brandl, M.; Winter, G. Vesicular Phospholipid Gel-Based Depot Formulations for Pharmaceutical Proteins: Development and in Vitro Evaluation. *J. Control. Release* **2010**, *142* (3), 319–325.

(129) Wagner, A.; Vorauer-Uhl, K. Liposome Technology for Industrial Purposes. *J. Drug Deliv.* **2011**, *2011*, 1–9.

(130) Ingebrigtsen, S. G.; Škalko-Basnet, N.; de Albuquerque Cavalcanti Jacobsen, C.; Holsæter, A. M. Successful Co-Encapsulation of Benzoyl Peroxide and Chloramphenicol in Liposomes by a Novel Manufacturing Method - Dual Asymmetric Centrifugation. *Eur. J. Pharm. Sci.* **2017**, *97*, 192–199.

(131) Dhule, S. S.; Penfornis, P.; Frazier, T.; Walker, R.; Feldman, J.; Tan, G.; He, J.; Alb, A.; John, V.; Pochampally, R. Curcumin-Loaded γ -Cyclodextrin Liposomal Nanoparticles as Delivery Vehicles for Osteosarcoma. *Nanomedicine Nanotechnology, Biol. Med.* **2012**, *8* (4), 440–451.

(132) Guichardon, P.; Moulin, P.; Tosini, F.; Cara, L.; Charbit, F. Comparative Study of Semi-Solid Liposome Purification by Different Separation Methods. *Sep. Purif. Technol.* **2005**, *41* (2), 123–131.

(133) Dimov, N.; Kastner, E.; Hussain, M.; Perrie, Y.; Szita, N. Formation and Purification of Tailored Liposomes for Drug Delivery Using a Module-Based Micro Continuous-Flow System. *Sci. Rep.* **2017**, *7* (12045), 1–13.

(134) Masarudin, M. J.; Cutts, S. M.; Evison, B. J.; Phillips, D. R.; Pigram, P. J. Factors Determining the Stability, Size Distribution, and Cellular Accumulation of Small, Monodisperse Chitosan Nanoparticles as Candidate Vectors for Anticancer Drug Delivery: Application to the Passive Encapsulation of [14C]-Doxorubicin. *Nanotechnol. Sci. Appl.* **2015**, *8*, 67–80.

Published paper

Journal of Molecular Graphics and Modelling 72 (2017) 201–208

Contents lists available at ScienceDirect

Journal of Molecular Graphics and Modelling

Journal homepage: www.elsevier.com/locate/JMGM

Topical Perspectives

Structural analysis of binding functionality of folic acid-PEG dendrimers against folate receptor

Diana Sampogna-Mireles[a], Ingrid D. Araya-Durán[b], Valeria Márquez-Miranda[b,c], Jesús A. Valencia-Gallegos[a], Fernando D. González-Nilo[b,c,d,*]

[a] Centro de Biotecnología FEMSA, Escuela de Ingeniería y Ciencias, Tecnológico de Monterrey, Av. Eugenio Garza Sada 2501 Sur, Col. Tecnológico, Monterrey, N.L, Mexico
[b] Universidad Andres Bello, Center for Bioinformatics and Integrative Biology (CBIB), Facultad de Ciencias Biológicas, Av. República 239, Santiago, Chile
[c] Fundación Fraunhofer Chile Research, M. Sanchez Fontecilla 310, Las Condes, Chile
[d] Centro Interdisciplinario de Neurociencia de Valparaíso, Facultad de Ciencias, Universidad de Valparaíso, Valparaíso, Chile

ARTICLE INFO

Article history:
Received 4 October 2016
Received in revised form
23 December 2016
Accepted 4 January 2017
Available online 6 January 2017

Keywords:
Dendrimer
PEG
Folic acid
Molecular dynamics
Folate receptor
Drug delivery system

ABSTRACT

Dendrimers functionalized with folic acid (FA) are drug delivery systems that can selectively target cancer cells with folate receptors (FR-α) overexpression. Incorporation of polyethylene glycol (PEG) can enhance dendrimers solubility and pharmacokinetics, but ligand-receptor binding must not be affected. In this work we characterized, at atomic level, the binding functionality of conventional site-specific dendrimers conjugated with FA with PEG 750 or PEG 3350 as a linker. After Molecular Dynamics simulation, we observed that both PEG's did not interfere over ligand-receptor binding functionality. Although binding kinetics could be notably affected, the folate fragment from both dendrimers remained exposed to the solvent before approaching selectively to FR-α. PEG 3350 provided better solubility and protection from enzymatic degradation to the dendrimer than PEG 750. Also, FA-PEG3350 dendrimer showed a slightly better interaction with FR-α than FA-PEG750 dendrimer. Therefore, theoretical evidence supports that both dendrimers are suitable as drug delivery systems for cancer therapies.

1. Introduction

Cancer therapies used nowadays lack of selectivity to cancer cells, which leads to diverse secondary effects [1]. As a result, there is a critical need to develop new therapies and drug delivery systems that reduce local and systemic toxicity [2]. Dendrimers are well known carriers that have been used as drug delivery systems. [3] Polyamidoamine (PAMAM) dendrimers have been widely studied for biomedical applications [4]. However, they have potential toxicological effects, especially at higher generations (≥G7) [5,6]. Therefore, a more favorable strategy consists in the use of dendrimers based on polyester units, like biodegradable 2,2-bis(hydroxymethyl)propionic acid (bis-MPA), due it can help reduce cytotoxicity, shows very good biocompatibility and can be easily prepared in large quantities [7–11].

In addition, dendrimers can selectively target cancer cells incorporating folic acid on their surface and reducing, as a result, normal cells toxicity and secondary effects in comparison with free drug [12–14]. Folic acid is stable, inexpensive, and non-immunogenic compared with monoclonal antibodies, has a very high affinity for its cell-surface receptor (K_d ~1 nM) and it moves into the cell cytoplasm, which favors an efficient intracellular delivery of anticancer agents [15]. Although expressed at very low levels in most tissues, folate receptors, especially FR-α, are overexpressed in numerous cancers such as nasopharyngeal epidermoid carcinoma, cervical, uterine, endometrial, renal, and pancreatic carcinoma [16]. Although folic acid-conjugated dendrimers can present low water solubility [17], this problem can be overcome by the incorporation of polyethylene glycol (PEG) to the drug delivery system. In addition, PEG can also increase lifetime in bloodstream, drug loading capacity, improves kinetic stability, reduces enzymatic degradation, conjugates aggregation and toxicity, and decreases drug release [3,18–22]. Also, it might change hydrophobicity of several compounds, making them hydrophilic [23]. The increase in PEG chain length leads to a decrease of the hydrogen bonding degree and an appreciable growth of molecular mobility and stability [24,25]. Docking analyses indicate that the binding affinity to

* Corresponding author at: Universidad Andres Bello, Center for Bioinformatics and Integrative Biology (CBIB), Facultad de Ciencias Biológicas, Av. República 239, Santiago, Chile.
E-mail addresses: valencia@itesm.mx (J.A. Valencia-Gallegos), fernando.gonzalez@unab.cl (F.D. González-Nilo).

http://dx.doi.org/10.1016/j.jmgm.2017.01.004
1093-3263/

DOI: 10.1016/j.jmgm.2017.01.004

Curriculum Vitae

Diana Sampogna-Mireles was born in Monterrey, México, on July 4, 1986. She earned the Industrial Chemistry Bachelor degree from the *Faculty of Chemical Sciences, Universidad Autónoma de Nuevo León*, Monterrey, in June 2008. She earned her Master of Science in Biotechnology from Instituto Tecnológico y de Estudios Superiores de Monterrey, Monterrey Campus in December 2012 with her dissertation "Synthesis of multifunctional dendrimers as potential therapeutic agents. Her Ph.D. in Biotechnology was earned from Instituto Tecnológico y de Estudios Superiores de Monterrey, Monterrey Campus in December 2017 with her dissertation "Controlled drug delivery strategies: Advances on the synthesis and molecular dynamics of dendrimers, and optimization of liposomes preparation by Dual Asymmetric Centrifugation".

She participated in Next Generation Scientist 2017, an international program organized by Novartis, Pharma in Basel (Switzerland), where she worked for three months (June-August 2017) on the project "Optimization of Dual Asymmetric Centrifugation for liposomes preparation".

She also made a five-months internship and collaboration with Center for Bioinformatics and Integrative Biology at University Andrés Bello in Santiago (Chile) in May 2015, obtaining a publication about "Structural analysis of binding functionality of folic acid-PEG dendrimers against folate receptor" in January 2017.

She worked in the Laboratory of Environmental Quality Center (LCCA) at Instituto Tecnológico y de Estudios Superiores de Monterrey, Monterrey Campus, as support professional on the environmental field from 2008 to 2010, where she obtained a signatary accreditation emitted by the Mexican Accreditation Entity (EMA) for the determination of organochlorine pesticides and polychlorinated biphenyls (PCB's) from residues. She was also responsible of the determination of humidity by Karl-Fischer and gravimetry; and determination of fatty acids by GC-FID.

During her Ph.D. she had three oral presentations in international and national symposiums: 1) 9th International Dendrimer Symposium – IDS9 in Montreal (Canada) in 2015 on her work "Molecular dynamics study of PEG chain lengths in site-specific dendrimers". 2) 43º Congreso de Investigación y Desarrollo, Tecnológico de Monterrey (Mexico) in 2013 on her work "Synthesis of dendrimers conjugated with pristimerin for their evaluation against cancer". 3) Congreso Internacional de Química e Ingeniería Verde, Universidad Autónoma de Nuevo León (Monterrey, Mexico) in 2012. She had three poster presentations during her Ph.D and master. One of them at Next Generation Scientist 2017 in Novartis Pharma (Basel, Switzerland). Another poster presentation in 251st American Chemical Society National Meeting (San Diego, CA, USA) in 2016, and in the 3rd International Symposium on Biological Applications of Dendrimers (Toledo, Spain) in 2012.

Her research interests are mainly on drug delivery systems, dendrimers, liposomes, and nanocarriers, and their evaluation as therapeutics, especially against cancer.

This document was typed in using Microsoft Word by Diana Sampogna-Mireles.